



F6200

YEARBOOK '84/85

RESEARCH INSTITUTE FOR TECHNICAL PHYSICS
OF THE HUNGARIAN ACADEMY OF SCIENCES

PUBLISHED BY THE

Research Institute for Technical Physics
of the Hungarian Academy of Sciences

POSTAL ADDRESS:

H-1325, Budapest, Újpest 1., P.O.B. 76.

RESPONSIBLE PUBLISHER:

Elemér NAGY, director

OLVASOTERMI PELDANY

EDITOR:

Ivan, C.SZEP

KÖZPONTI FIZIKAI KUTATÓ INTÉZET KÖNYVTÁRA

leltárba véve 190. 4. 17 sz. alatt.

Budapest, 19. 86. év VII. hó ... 1. ...

PUBLISHER'S READER:

Robert C. SOMMERFIELD

2015

2014

EDITORIAL BOARD:

Mrs. Éva NÉMETH
Marianna SZABO

ISSN - 0139-4363

Hozott anyagról sokszorosítva

8516089 MTA Sokszorosító, Budapest. F. v.: dr. Héczey Lászlóné

PREFACE

Dear Reader,

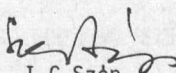
This issue of our biennial yearbook differs in some respects from previous volumes. Instead of review articles we have selected a number of invited papers summarizing those achievements of our colleagues which have already been appraised by the international scientific community in conferences or through publications. Some of the work was done in this country and some during shorter or longer stays in the scientific establishments of other countries - fine examples of friendly co-operation. Theoretical as well as practical problems are treated including highly sophisticated technology and methods of measurement. I hope the reader will be able to make an overall evaluation of the importance of our activities.

A brief survey of the work carried out in the respective divisions of RITPh is also given. One may notice that a new division, 'Microwave Devices' is reporting for the first time, which has been organized for practical purposes.

Interest for our activities, in our opinion, is testified by the number of visits paid to our institute by scientists from abroad; an incomplete selection is presented here together with a brief survey of our international relations.

A comprehensive bibliography of papers published by members of our Institute during 1984-1985, mostly in international publications, is given at the end. Reprints will be sent on request.

I hope you will find the contents worthy enough for you to make contact with the members of this Institute in any field of interest to you.


I.C. Szép
Ph.D., D. Eng. Sc.
Deputy Director

CONTENTS

PREFACE	III
I.C.Szép	

SELECTED PAPERS

ISOTHERMAL DLTS: EXAMPLES OF ITS APPLICATION	3
G.Ferenczi, J.Boda, T.Pavelka and M.Somogyi	
OPTICAL PROPERTIES OF SELECTED SEMICONDUCTOR COMPOUNDS	10
M.Gál	
TERNARY AND QUATERNARY A ^{III} B ^V ANTIMONIDES	20
E.Lendvay	
INVESTIGATION OF CLUSTER MODELS	28
J.Kertész	
FRACTAL STRUCTURE AND DYNAMICS IN AGGREGATION PHENOMENA	37
T.Vicsek	
NEW DEVELOPMENTS AND RESULTS IN SURFACE ANALYSIS	45
G.Gergely	
ENERGY DISPERSIVE X-RAY MICROANALYSIS AND FLUORESCENCE ANALYSIS	55
J.L.Lábár and I.Pozsgai	
GRAIN BOUNDARIES IN THIN METALLIC FILMS	64
G.Radnóczy and P.Barna	

INVESTIGATION OF EBIC DISLOCATION CONTRAST AS A FUNCTION OF SEM PARAMETERS	71
A.L.Tóth	
THE INFLUENCE OF THE TEST SAMPLES USED FOR CALCULATING COLOUR RENDERING INDICES	77
J.Schanda	
THERMAL DISSOCIATION OF InP COVERED WITH METALLIC CONTACT LAYERS	84
I.Mojzes, R.Verese gyházy, V.Malina	

REPORTS ON ACTIVITIES

INTRODUCTION	103
SEMICONDUCTOR RESEARCH DIVISION	105
E.Lendvay	
METAL RESEARCH DIVISION	109
L.Bartha	
STRUCTURE RESEARCH DIVISION	115
L.Zsoldos	
DIVISION OF OPTICS AND ELECTRONICS	119
J.Schanda	
DIVISION OF MICROWAVE DEVICES	125
I.Mojzes	
INTERNATIONAL RELATIONS	129
I.C.Szép	
LIST OF PUBLICATIONS	139

SELECTED PAPERS

ISOTHERMAL DLTS: EXAMPLES OF ITS APPLICATION

G. Ferenczi, J. Boda, T. Pavelka and M. Somogyi

This paper summarizes some recent results arrived at by a new version of Deep Level Transient Spectroscopy: Isothermal frequency scan DLTS. After a brief description of the technique its effectiveness is demonstrated:

- a) By the most accurate determination of the thermal activation energy ever reported
- b) By the introduction of Mercury-probe DLTS as a novel non-destructive wafer characterization technique.

INTRODUCTION

Since its introduction Deep Level Transient Spectroscopy¹ has become one of the most popular characterisation techniques for impurities, defects in semiconductor materials and devices, due to its unsurpassed sensitivity. DLTS monitors the thermally stimulated emission of captured carriers from defect energy levels by averaging and amplifying the capacitance or current transients caused by the emitted carriers. Since the fundamental physical process is thermally activated, DLTS measurements are generally carried out in the function of temperature using a preselected observation time window for averaging the capacitance decay (The averaging is done by a box-car integrator or by a lock-in amplifier²). This is not the only possibility however. In the ideal case the exponential decay of a capacitance transient can be calculated using:

$$C = C_0 + \Delta C_0 \exp [-t/\tau] \quad / 1/$$

where C_0 is the equilibrium capacitance of the sample at a given temperature and reverse bias, ΔC_0 is the capacitance change caused by the electrical (or optical) excitation and τ is the time constant of the thermal

emission process. In the case where the transients are averaged by the symmetrical square wave function of a broad band lock-in amplifier with a repetition time, P , the output signal $-S-$ of the lock-in is:

$$S(\tau, P) = \frac{\Delta C_0 \tau}{P} (1 - \exp[-P/2 \tau])^2 \quad /2/$$

where,

$$\tau^{-1} = N_c \sigma_n V_d \exp[-E_T/kT] \quad /3/$$

is the function of temperature (Notation:

N_c = free electron density of state

σ_n = electron capture cross section

V_d = electron thermal drift velocity

E_T = thermal activation energy)

As shown, S is the function of temperature and repetition time. The $S(\tau, P)$ function has an extreme of P at fixed temperature just as it has an extreme in temperature at a fixed repetition time. The latter case is the well known and generally used temperature scan DLTS as mentioned before. The first case represents the isothermal DLTS approach² which we call frequency scan DLTS. It should be noted however, that the temperature dependence is exponential, the frequency dependence is linear and hence a much wider range should be scanned in frequency than in temperature to cover the same activation energy interval. This electrical problem is solved in the DLS-82 system.

The frequency scan DLTS has some fundamental advantages over the temperature scan approach:

- The measurement is carried out at a constant temperature, i.e. thermal annealing does not take place during measurement as contrasted to the standard approach. This is an advantage in principle, if radiation damage centres or degradation phenomena has to be investigated. In these situations defect reactions occur within the temperature range of temperature scan

DLTS and hence the standard DLTS measurement modifies the defect structure under study.

- Frequency scan measurement is performed in complete thermal equilibrium; hence the accurate sample temperature can be better established.
- The frequency scanning is done electronically and for this reason it is much faster than temperature scanning especially for large samples (i.e. in case of large thermal mass).
- Frequency scan is suitable for wafer mapping i.e. a frequency scan DLTS system can be coupled to an automatic wafer mapping set-up to measure the lateral distribution of any defects.

In the following sections practical examples are given to demonstrate the use of the frequency scan DLTS technique.

THE ACCURACY OF THE ACTIVATION ENERGY MEASUREMENT

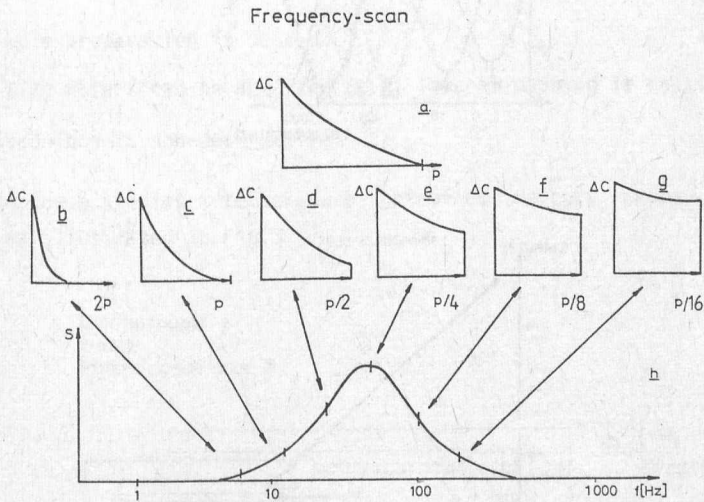


Fig.1

The principle of the frequency scan DLTS (eqn.2) can be better visualized using Fig.1. The transient seen on Fig.1/a is averaged with the symmetrical square wave weight function of the lock-in amplifier.

The length of the repetition period however is continuously increasing, as shown in the series of figures 1/b-g. Consequently the integral value increases until:

$$P \approx 2.5 \tau,$$

/4/

than decreases again as in Fig.1/h.

The frequency-scan technique was used to characterize radiation damage centres in p-type silicon. The sample was implanted with H^+ at 300 keV and 10^{10} cm^{-2} flux. The results from one of the hole traps are shown in Fig.2

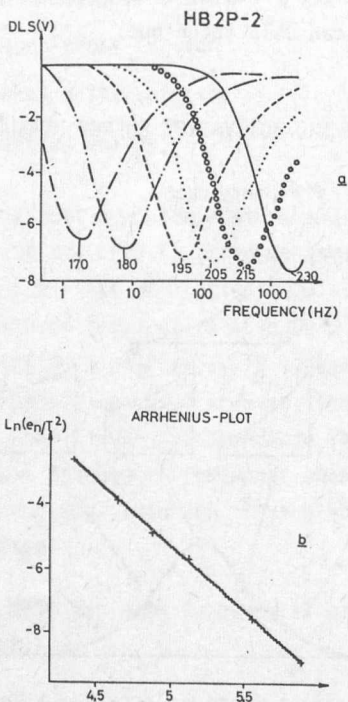


Fig.2

Frequency scan spectra taken at six fixed temperatures between 160 K - 230 K are shown in Fig.2/a. The corresponding Arrhenius plot is illustrated by Fig.2/b. The activation energy $E_T = 0.350 \text{ eV}$ and the regression coefficient

cient is 0.9997. The activation energy was independently determined by photocapacitance transient decay experiments which provided $E_T = 0.350$ eV as the optical ionisation energy. Since this trap is identified as $C_I - C_S$ pair, and the measured transition is $0/+$, no Franck-Condon shift is expected. We believe that this is the best reported agreement between thermal and optical ionisation data. The high degree of accuracy is due to the more accurate determination of the sample temperature provided by the thermal equilibrium conditions of the frequency scan measurements.

THE USE OF MERCURY-SEMICONDUCTOR CONTACTS FOR DEEP LEVEL STUDIES

Mercury probe is routinely used for shallow level profiling in semiconductor wafers³, but it has not been used until now for deep level characterisation. The advantages of the mercury probe for defect characterisation are obvious:

- No permanent junction need be prepared i.e. the modification of the defect structure due to diffusion, high temperature oxidation etc. can be avoided.
- No sample preparation is needed.
- Full size wafers can be analyzed (e.g. lateral mapping is possible).
- The technique is non-destructive.

For these studies a temperature controlled mercury probe was designed as illustrated in Fig.3

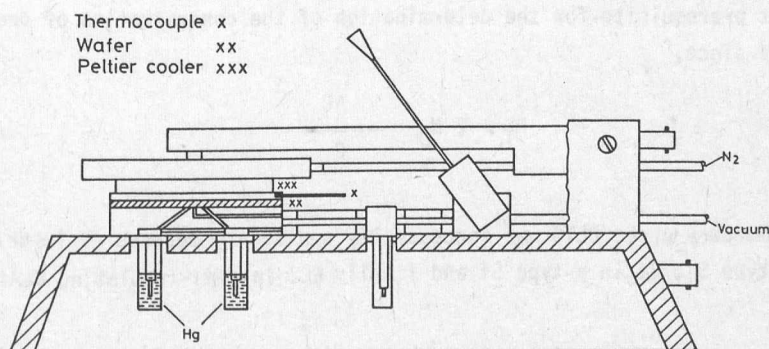


Fig.3

The rear contact of the probe is a Peltier element which can cool or heat the sample as desired. The temperature controlled mercury probe operates in the 240 K - 330 K temperature range. The lower temperature is limited by the freezing point of the liquid mercury. The upper limit is set by the vapour pressure of mercury which increases rapidly with temperature. Since mercury is poisonous it is not recommended to use the system at higher temperatures. Also, it is not necessary to do so. The activation energy and capture cross section of the most important deep levels are known from the literature. Using these input parameters and Eqns. 2-4 the position of a deep level peak in frequency at a given temperature can be calculated. The dynamic range of our DLS-82 is four orders of magnitude in frequency. Using typical parameters at 240 K the 0.1 eV - 0.3 eV activation energy range can be covered in a single frequency scan. At 330 K the corresponding activation energy range is 0.5 eV - 0.8 eV. These results illustrate that in the frequency scan mode the 0.1 eV - 0.8 eV activation energy range (i.e. half of the band gap) can be assessed by selecting three constant temperatures within the 240 K - 330 K range as contrasted with the temperature scan mode where the corresponding temperature interval is 80 K - 400 K. As it was demonstrated using frequency scan, the temperature range is significantly reduced. This made possible the use of a mercury probe for deep level characterisation which was not possible with the standard temperature scan DLTS. The mercury probe design shown in Fig. 3., enables the illumination of the contact area with monochromatic light. This way minority carrier injection is made possible and hence the full band gap can be analyzed by the mercury semiconductor contact technique. Finally it should be noted that exact knowledge of the area of the mercury contact is not prerequisite for the determination of the concentration of deep levels since,

$$N_T = 2 N_D \cdot \frac{\Delta C}{C} \quad /5/$$

Mercury probe DLTS was successfully applied to measure Au impurity in n-type Si, Fe in p-type Si and finally EL2 in semi-insulating GaAs.

REFERENCES

1. D.V.Lang
J.Appl. Phys. 45, 3023 (1974)
2. G.Ferenczi, P.Horvath, F.Toth and J.Boda .
U.S.Patent No: 4437060 (1984)
3. P.J.Severin and G.J.Poodt
J.Electrochem.Soc. 119, 1384, (1982)

OPTICAL PROPERTIES OF SELECTED SEMICONDUCTOR COMPOUNDS

M. Gál *

It is important to understand the roles of defects, impurities and interfaces in those semiconductor materials which hold significant promise for device applications. This knowledge is particularly significant in attempts to create devices based on new concepts such as ultra-high speed FETs based on GaInAs alloys lattice matched to InP substrates, or doping superlattices based on quantum-size effects in OMCVD grown InP. It is of similar importance to optimize and to improve existing devices and to be able to characterise materials grown for such device applications. These important questions were probed during the last 2-3 years, while the author was on leave of absence at the Department of Physics at the University of Utah. In the following, we shall give a brief description of our results in the following order:

- a) Quantum-size effects in InP doping superlattices
- b) Confined electron hole plasma in GaInAs-InP heterostructures
- c) Exciton dynamics in GaSe
- d) Electronic states in hydrogenated $a\text{:Si}_x\text{Ge}_{1-x}$

a) Quantum-Size Effects in InP Doping-Superlattices

More than a decade ago Dohler predicted that superlattice structures consisting of alternate n-doped and p-doped semiconductor layers would have interesting and potentially useful properties¹. Such doping superlattices, or "nipi" structures, were predicted to have a variable band gap depending on the concentration of free carriers in the conduction and valence bands and the layer thicknesses. The band gap was predicted to be indirect in the sense that the electrons and holes would be separated in

*On leave of absence at the Department of Physics,
University of Utah, Salt Lake City, UT 84112, USA

real space. These properties promised the possibility of a variable band-gap structure with very long minority-carrier lifetimes. Such structures would be potentially useful for a number of device applications including tunable light sources, extremely sensitive optical detectors, and novel field-effect transistors where the field would modulate both electron and hole conductivities.

We have reported the first doping superlattices grown by organometallic vapor phase epitaxy (OMVPE).² The superlattices were grown in InP with layer thicknesses as small as 200 Å. The 4 K PL peak energy was found to be considerably less than the band gap of homogeneous InP and to depend on excitation intensity (Fig.1).

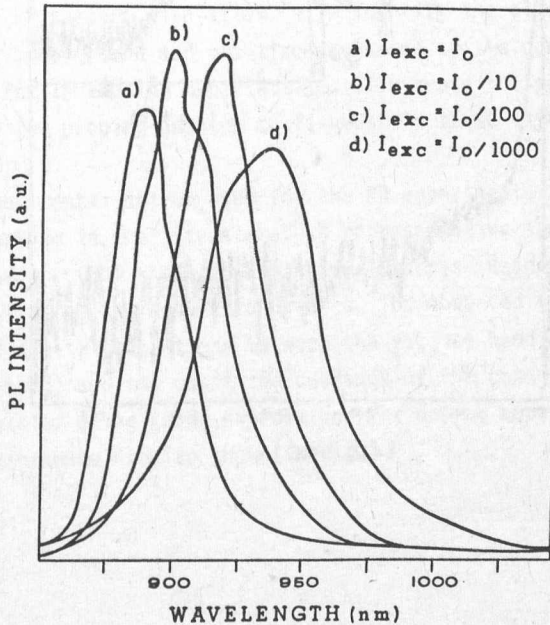


Fig.1
Photoluminescence spectra measured at 4 K with various excitation intensities for InP doping superlattice with layer thicknesses of 200 Å and n- and p-doping levels of 1×10^{18} and $2 \times 10^{10} \text{ cm}^{-3}$.

The luminescence was found to decay in distinct stages, each stage being approximately exponential, with a range of time constants from 6×10^{-8} to 7×10^{-4} s at 4 K, as expected for transitions which are indirect in real space between different quantum levels (Fig.2).

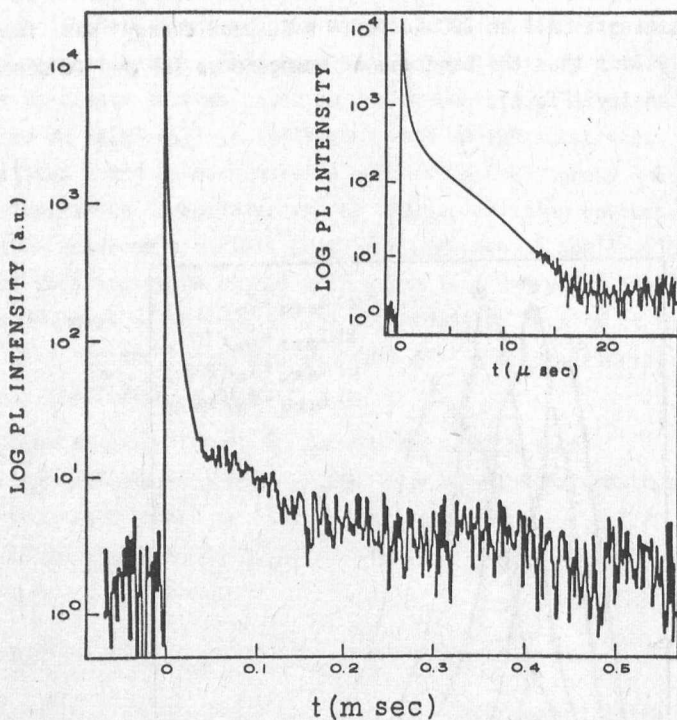


Fig.2

Photoluminescence intensity versus time after removal of excitation for InP superlattice

In addition to these unique features, the nipi superlattices also exhibit quantum size effects similar to those observed in quantum wells. The first observation of quantized subbands in GaAs/GaAlAs doping-superlattices was achieved by resonant spin-flip Raman scattering (RRS).¹ However, with the development of superlattices, which are not based on GaAs, RRS can become extremely difficult, due to the lack of resonant laser lines.

We have proposed and used an alternative technique to study quantum size effects in doping superlattices, using the photoreflectance (PR) method.³ This technique was often used in the past for understanding interband transitions in bulk semiconductors.⁴ Because optical modulation in the doping superlattices affects the real-space modulation of the band gap and the population of the subband levels in a very predictable fashion, a detailed and semi-quantitative understanding of the phenomena can be obtained.³ The PR spectra also allow us to identify the allowed transitions between the valence band and quantized subbands of the conduction band. Our results for InP doping superlattices illustrate the potential of the PR technique for probing quantum confinement in these layer structures.³

The experimental set-up used for the PR experiments was very similar to that described in the literature.⁴ A representative spectrum is shown in Fig.3. The spectrum shown in Fig.3. was observed using 1.2 mW cm^{-2} at 2.41 eV (5145 Å) as the modulation source. The observed features on the spectrum are due to transitions between the valence band (and the split-off valence band) and the quantized subbands of the conduction band, and can be calculated using known expressions for doping superlattices.³ The calculated lineshape is also shown in Fig.3.

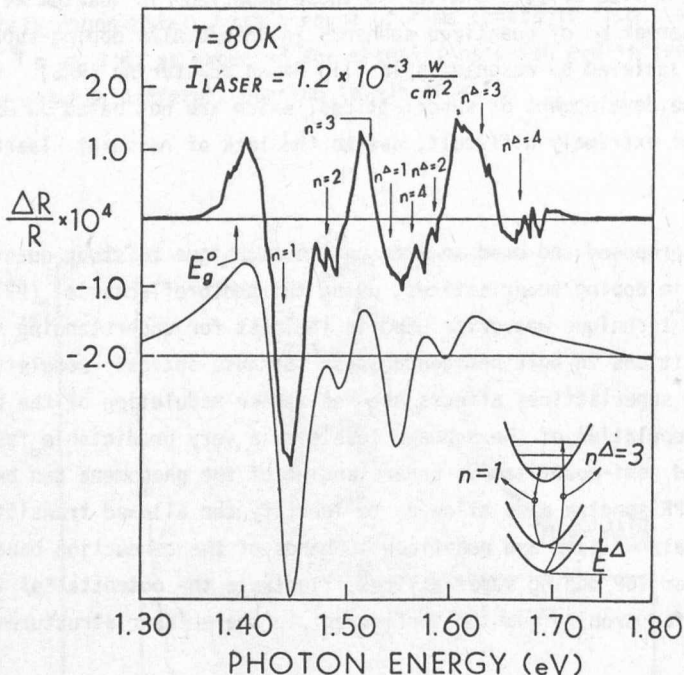


Fig.3

Low temperature (80 K) PR spectrum at low modulation intensity in an InP doping superlattice. E_0 denotes the band gap of bulk InP. The indices n and n^Δ refer to transitions from, respectively, the valence band and the split-off valence band to the subband levels in the conduction band. The lower trace is a calculated spectrum.

b) Confined Electron-Hole Plasma in GaInAs

$\text{Ga}_{0.47}\text{In}_{0.53}\text{As}$ lattice matched to InP is an important semiconducting compound due to its large potential for a number of optoelectronic and high-speed electronic applications. The main focus of recent spectroscopic work in these compounds has involved the study of excitonic and impurity related phenomena. We have observed a low-energy photoluminescence (PL) emission in $\text{Ga}_x\text{In}_{1-x}\text{As}$ heterostructures.⁵ The emission originates from an electron-hole plasma (EHP) confined in a 500 Å $\text{Ga}_y\text{In}_{1-y}\text{As}$ layer between the InP substrate and a wider band gap $\text{Ga}_x\text{In}_{1-x}\text{As}$ layer. A line-shape analysis

of the EHP emission yields electronic temperatures which essentially coincide with the bath temperature (Fig.4).

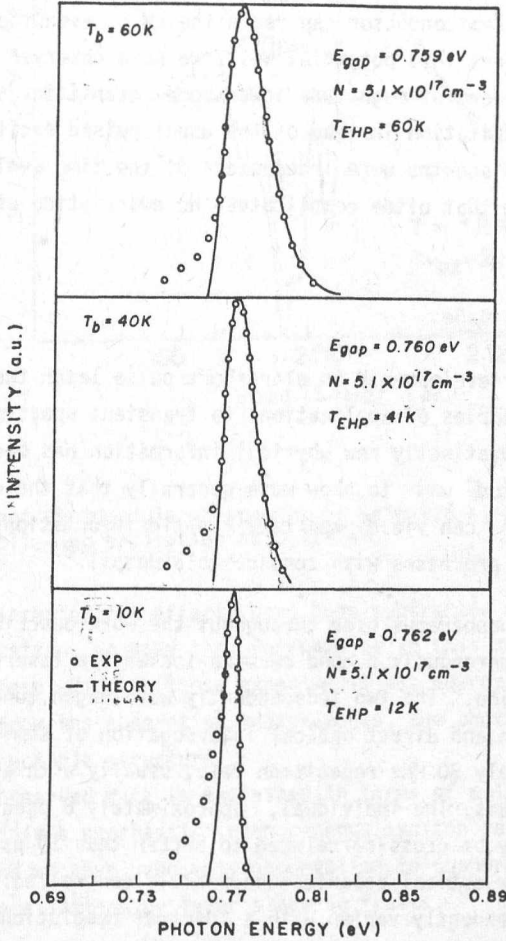


Fig.4

Luminescence spectra of GaInAs at constant excitation intensity for different bath temperatures (T_b). The circles represent the experimental points, while the solid curves are the calculated EHP lineshapes.

Linear polarization of the PL was observed which indicates a degree of strain in the confining layer. Studies in a magnetic field indicate that the carrier transport in the heterostructure studied is via free carriers and not via excitons.⁵

In a bulk semiconductor, substantial EHP density only occurs at very high excitation intensities due to the short lifetime and the rapid diffusion of the carriers out of the photoexcited volume.⁶ Typical excitation intensities in a bulk semiconductor can reach the kW or even the MW range.⁷ By confining the carriers in a potential well, we have observed EHP luminescence at several orders of magnitude lower pump intensities and thus we were able to use cw excitation instead of the usual pulsed excitation. As a result, our measured spectra were independent of the time evolution of the exciton-EHP system that often complicates the description of the phenomenon.⁵

c) Exciton Dynamics in GaSe

Following recent developments in ultrashort pulse laser technology, there are now many examples of applications to transient spectroscopy of semiconductors where distinctly new physical information has been obtained. The emphasis of our study was to show more generally that the experimental techniques in question can yield real time kinetic information of excitonic energy relaxation processes with considerable detail.⁸

The experimental apparatus used throughout the work described here employs a pair of synchronously pumped cw-mode-locked dye lasers in an excite-probe configuration.⁹ The two independently wavelength tunable lasers provide the excitation and direct optical interrogation of semiconductor samples at approximately 80 MHz repetition rate, usually with a small angle separating the two beams. The individual, approximately 6 psec pulses from each laser can usually be cross-correlated to better than 10 psec with good consistency, and their optical polarization readily controlled. The photon energies can be independently varied with a spectral resolution typically close to 0.3 meV. The arrival of a pulse of excitation at $t = 0$ injects, for example, an initially mono-energetic exciton gas into a sample. The presence of this excitation is measured as a weak optically induced modulation of the transmitted (or reflected) probe pulse intensities at a variable delay time. Figure 5 shows the time-resolved modulation spectra for three different delay times in the 5- μ m-thick GaSe sample at 1.8 K, following the excitation by a picosecond pulse within the $n = 1$ free-exciton region at $t = 0$.

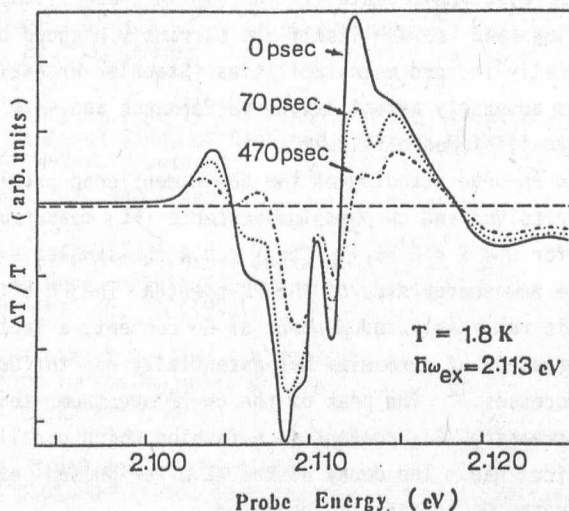


Fig.5

Transient photomodulated spectra of GaSe 1.8 K, recorded 70, and 470 psec following excitation at 2.113 eV.

(Optical interference effects have been subtracted automatically by our instrumentation, an easy task for samples in this range of thickness.) The time resolution in these experiments was approximately 15 psec. As expected from the absorption measurements, the photomodulated spectra shows appreciable structure.

The observed data is explained in terms of a lack of spectral diffusion within a stochastic inhomogeneous exciton resonance at low temperatures and we have used this observation to support arguments for partial exciton localization by layer stacking faults.¹⁰

d) Electronic States in Hydrogenated Amorphous SiGe Alloys

One important class of materials for photovoltaic conversion of solar energy is the group of thin film amorphous semiconductors based on hydrogenated amorphous silicon (a-Si:H). Important alloys include a-Si_xGe_{1-x}:H and a-Si_xC_{1-x}:H which are used to produce narrower gaps for tandem cells and lower band gaps for top-surface p-layers, respectively. Currently, little is known concerning the defects and impurities which create



enhanced densities of electronic states in the gap in these films. In addition, both the alloys and a-Si:H itself are currently plagued by electronically- and optically-induced metastabilities (Staebler-Wronski effect). These metastabilities adversely affect device performance and make projections of useful device lifetimes difficult.

In order to gain an understanding of the above mentioned problems, we have performed time resolved and cw photoluminescence (PL) measurements in $\text{a-Si}_{1-x}\text{Ge}_x\text{:H}$ alloys for $0 \leq x \leq 0.52$.¹¹ For $x \leq 0.4$ the samples exhibit a universal tail on the low-energy side of the PL spectra. The PL efficiency in this tail region is remarkably independent of Ge content, a fact which indicates that the presence of germanium has essentially no influence on the low-energy PL processes.¹² The peak of the cw PL spectrum shifts to lower energy with increasing Ge content in a fashion which parallels the narrowing of the optical gap. The decay of the PL after pulsed excitation becomes more rapid as the Ge content is increased.

The existence in hydrogenated silicon-germanium alloys of a universal PL low-energy tail, where the quantum efficiency is independent of x , suggest that the PL process is a property of the silicon in the network and essentially independent of germanium.¹³ This deduction in turn suggests that the low-energy PL process is a highly localized phenomenon.¹⁴

REFERENCES

1. For a review see, e.g., G.H. Dohler, Festkörperproblem, Vol.XXIII, p. 207, H.F. Queisser (ed.), Pergamon-Vieweg, Braunschweig (1983).
2. K.C. Yuan, M.Gal, P.C.Taylor and G. Stringfellow
Doping Superlattices in organometallic VPE InP
Appl. Phys.Lett. 47, 405 (1985)
3. M.Gal, J.S. Juan, J.M. Viner, P.C. Taylor and G.B.Stringfellow
Modulated-reflectance spectroscopy in InP doping-superlattices
Phys.Rev.Lett. (to be published)

4. F.L.Shay
Photoreflectance Lineshapes at the Fundamental Edge in Ultrapure GaAs
Phys.Rev. B2, 803 (1970)
5. M.Gal, J.Viner, P.C.Taylor, C.P.Kuo and G.B.Stringfellow
Photoluminescence Study of Confined Electron-Hole Plasma in $\text{Ga}_x\text{In}_{1-x}\text{As}$ Heterostructures
J.Appl.Phys. 58, 948 (1985)
6. C.Huber, A.V.Nurmikko, M.Gal and A.Wold
Magnetic polaron contribution to donor bound excitons in CdMnSe
Sol.State Comm. 46, 41 (1983)
7. M.Gal, Y.Hefetz, Y.Aya and A.V.Nurmikko
Luminescence in semimagnetic ZnMnSe
Phys.Rev. B28, 4500 (1983)
8. X.C.Zhang, M.Gal and A.V.Nurmikko
Transient photomodulation spectroscopy of bound excitons in doped GaSe
Bull. Am. Phys. Soc. 29, 477 (1984)
9. S.X.Zhang, M.Gal and A.V.Nurmikko
Exciton confinement by layers in GaSe: Direct evidence from sub-nanosecond time-resolved spectroscopy
Phys. Rev. B. Rapid Comm. 30, 6214 (1984)
10. X.C. Zhang, Y. Hefetz, M.Gal and A.V.Nurmikko
Kinetics of bound and free excitons at low densities in semiconductors.
Presented at Fourth International Conference of Ultrafast Phenomena, June 1984. Monterey, Ca.
11. M.Gal, J.Viner and P.C.Taylor
The existence of a universal low-energy tail in the photoluminescence of $\text{a-Si}_{1-x}\text{Ge}_x\text{:H}$ alloys
Phys.Rev.B. Rapid Comm. 31, 4060 (1985)
12. R.Ranganathan, M.Gal and P.C.Taylor
Temperature dependence of photoluminescence in $\text{a-Si}_{1-x}\text{Ge}_x\text{:H}$ alloys
Bull. Am.Phys.Soc. 30, 307 (1984)
13. M.Gal, J.Viner and P.C.Taylor
Alternative method for measuring optical absorption below the band edge in thin a-Si:H
Bull.Am.Phys.Soc. 30, 259 (1985)
14. M.Gal and P.C.Taylor
Temperature dependence of the absorption in a-Si and related alloys
11th Inter.Conf.on Amorphous and Liquid Semicond. Rome, Sep.2-6, 1985.

TERNARY AND QUATERNARY A^{III}B^V ANTIMONIDES

E. Lendvay

1. INTRODUCTION

The continuously growing field of microwave and optoelectronic applications is increasing rapidly the demand for new semiconductors with particular properties.

Optoelectronics requires laser, LED and detector materials in a wide optical range between 0.5 - 10.0 μm . The elementary semiconductors, being indirect materials, generally are not suited to these purposes. Similarly, the charge carrier mobility of Ge and Si is low for high frequency applications.

Among the different semiconductor compounds, quaternary systems have four degrees of freedom and therefore, a wide range of composition (as well as E_g) belonging to a definite a_0 lattice parameter value, and vice versa. This is the reason interest in quaternary A^{III}B^V alloys has been considerably aroused recently. Among the possible compounds only the GaInAsP has been thoroughly examined as a laser material. The similar GaAlAsSb alloy has also been studied but our knowledge about this phase is less than mentioned above. No detailed study of pseudo-ternary A^{III}B^{III}C^{III}D^V or A^{III}B^VC^VD^V compounds have been performed. In these systems one of the sublattices consists of three different ions. AlGaInSb¹⁻³, GaPAsSb^{4,5} and InPAsSb⁶ are the experimentally known quaternaries of this kind.

For laser and detector applications two antimonide heterosystems have been developed recently. The GaAlAsSb/GaAsSb/GaAs system was described earlier^{7,8}. Growing single and multilayer structures onto GaAs peritectic temperatures and miscibility gaps were found (750°C for GaAsSb and 715°C for GaAlAsSb). Above the peritectic temperature good quality epitaxial layers can be grown, while under the peritectic limit, owing to the miscibility gap microcrystalline, GaSb-rich layers were formed. This restricts the applications of the system. Numerous efforts were made, however, to

prepare DH laser structures. For the real application of these epitaxial structures further research is needed to determine the factors limiting device preparation. On GaSb substrates quaternary III-V compounds of the $A_x^{III}B_y^{III}C_{1-x-y}^{III}Sb$ and $GaA_x^VB_y^VSb_{1-x-y}$ types have also been investigated.

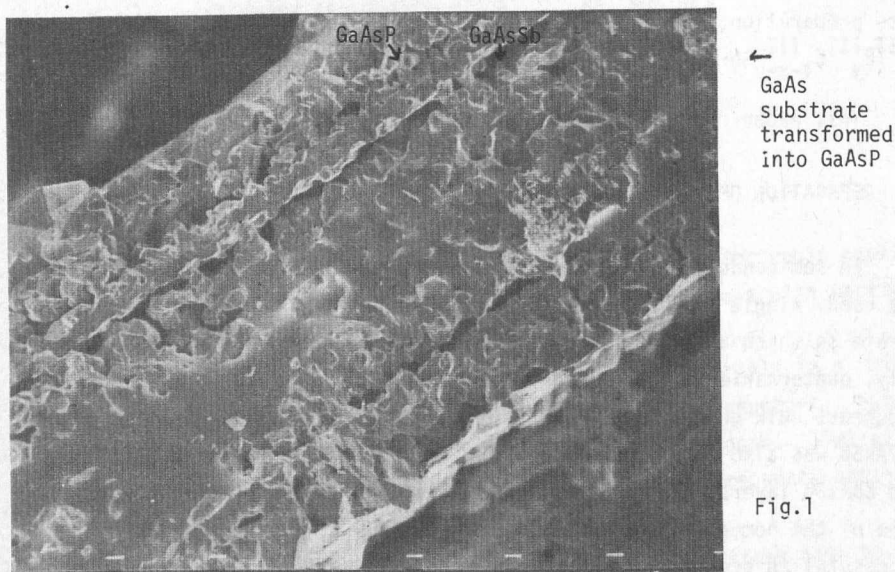
This paper reports the results achieved in these systems.

2. PREPARATION OF PSEUDO-TERNARY ANTIMONIDES

In semiconductor technology both single crystals and epitaxial layers are used. Single crystals are applied as a starting material or as a substrate on which a particular epitaxial layer structure can be built. Generally, quaternaries are known in the form of epitaxial layers because homogeneous bulk quaternary crystals can hardly be prepared. Earlier, the GaPAsSb was also known as an epitaxial intermediate layer between the GaAs and GaAsSb layers.⁴ No previous work has been published about the preparation of the homogeneous, bulk crystalline phase. Recently, we have been successful in preparing this phase using a transport process⁵. The GaPAsSb pseudo-ternary offers the possibility to develop light sources; in the composition diagram of the system the direct band gap region covers a remarkable part of the composition field. However, in order to get the suitable, homogeneous composition extended work has to be done. The design of an optimized p-n junction is an extremely complex subject because of the P segregation and the anomalous conversion of GaAs substrates to GaAsP. It was observed that after the LPE growth of the GaPAsSb onto GaAs the substrate transformed as a whole into a polycrystalline ternary material. In Fig.1. the cleaved [110] surface of a LPE grown wafer is shown. Instead of the planned double heterostructure (lattice matched GaPAsSb/GaAs/GaPAsSb/substrate system), a sandwich structure consisting of polycrystalline phases between the pseudo-ternary antimonides was formed. The mechanism of this fast reaction is not known, and detailed analysis is needed in the future to explain it.

Preparation of a single phase, bulk AlGaInSb alloy has also been shown to be difficult. The existence of an AlGaInSb phase was confirmed experimentally for the first time not so long ago¹. One problem which is clearly seen from the previous results is the strong segregation of Al in the quaternary system. Another problem to be considered in LPE experiments

is the so called lattice-pulling effect (substrate induced stabilization 15-16.



It was observed that lattice mismatch could play a role in determining the solidus composition. Owing to this phenomenon, the solid composition varies little from that of lattice matched to the substrate material in a wide range of melt compositions. This means that the measured solid composition can hardly be applied for the determination of the real solidus unless the substrate and the equilibrium quaternary solid phase have closely matched a_0^i values. ($i=s, e$ where s denotes the substrate and e corresponds to the epitaxial layer).

To study the role of the lattice matching, different binary III-V substrates were used for AlGaInSb growth. It was observed that the morphology of the epitaxial layer strongly depends both on the substrate and the supercooling. Near equilibrium LPE ($\Delta T < 2-5^\circ\text{C}$) results in a rough, polycrystalline overgrowth on GaAs where the lattice mismatch is large ($\Delta a_0^i/a_0 > 8\%$). A good quality epitaxial layer forms on GaSb if the supersaturation is high ($\Delta T > 10^\circ\text{C}$).

No satisfactory AlGaInSb layer growth was achieved in In-rich melts using InSb substrates because of the melt back phenomena. A similar effect

was observed using Ga-rich melts and GaSb substrates. The difference between the GaAs and InSb substrates using Ga-rich or In-rich melts probably involves the different chemical and thermodynamical activities as in the complex systems. Experiments in Ga and In-rich melts showed that this difference is most probably caused by the activity difference of Sb in the binaries, rather than by the activity difference of the cations in these compound. Practically no perfect layer growth was achieved in Ga-rich melts, whereas in In-based melts using GaSb substrates good quality AlGaInSb were grown. Similar effects have been observed for InP and GaP¹⁷ in the In-Ga-P system, and for GaAs and InAs in the In-Ga-As system^{18,19}. The activity difference results in the fact that InSb wafers do not allow complete saturation, while a GaSb substrate can provide saturation and layer growth.

3. STRUCTURE AND PHYSICAL PROPERTIES OF THE PSEUDO-TERNARY ANTIMONIDES

In a quaternary system such parameters as the lattice constant, a_0 and the alloy composition can be roughly approximated theoretically. The lattice parameter values in the AlGaInSb system satisfy Vegard's law fairly well. The experimental values, however, strongly differ from those previously predicted in ref.20. Owing to this difficulty, the properties mentioned (a_0 and the composition parameters) have to be determined experimentally.

The alloy compositions were determined directly from EPMA measurements. For the a_0 measurements the usual X-ray methods (rocking curve technique) were applied. In Fig.2, two characteristic rocking curves are shown. Diffraction from the GaSb substrate rear side (curve 3 in Fig.2) was used to determine the resolution of the system and to compare sample traces. The rocking curve of the thick epitaxial layer was measured on the front side of the sample (layer thickness 2-5 μm), while the traces of both the substrate and the epilayer were recorded at the epitaxial layer edge, where the layer thickness was sufficiently thin to give diffraction from both materials. Curve 1 exhibits a well defined and laterally uniform lattice constant of 0.61355 nm. The layer was grown at optimal supercooling ($\Delta T = 12^\circ\text{C}$), with a cooling rate of $0.4^\circ\text{Cmin}^{-1}$, starting the growth from 650°C . Using an $a_0(\text{GaSb}) = 0.60970$ nm value, the mismatch ($\Delta a_0/a_0$) found in the AlGaInSb/GaSb system was about $6.3 \cdot 10^{-3} \%$. EPMA measurements showed that the composition parameters of the $\text{Al}_x\text{Ga}_y\text{In}_z\text{Sb}$ layer investigated were $x = 0.979$, $y = 0.14$ and $z = 0.012$ ($z=1-x-y$).

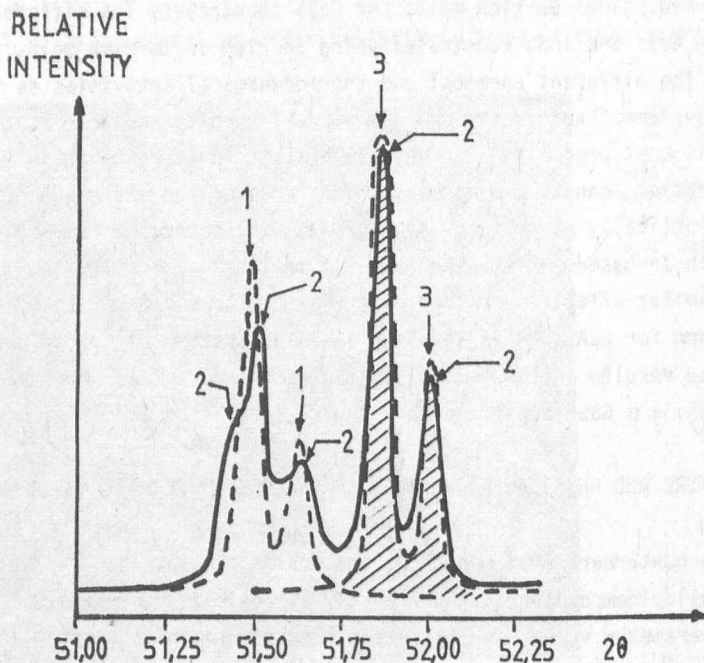


Fig.2

The sharpness of the diffraction peaks indicates that the lattice constant variation, in the direction normal to the layer surface, is small in comparison, with that of graded structures.

The half width of the rocking curve is the most important parameter in characterizing the layer perfection, while the separation of the substrate and layer diffraction peaks show the degree of lattice matching. Both the half-width ($\Delta\theta$) and the diffracted intensity depend on the layer thickness. While $\Delta\theta$ increases abruptly when the layer thickness (d) decreases, the diffracted intensity increases with increasing d ²¹. The half-width of a high quality III-V binary substrate (GaAs, InP) is usually in the order of 15-50 seconds; for GaSb a value of 40-45" was published²². According to our measurements the perfection of the GaSb substrate used was slightly inferior to the one mentioned above but the layer perfection with a value of $\Delta\theta \sim 150''$ is sufficiently good.

For ternary InAsSb and InGaSb, eg. values of 300" and 600", were also published²²; while for pseudo-ternary AlGaInAs a value of 100" ²³, and for

InPAsSb values of 150-300" ²⁵ were found. In the case of GaInAsP prepared by the most advanced LPE technologies, values from 15" (d ~ 1,5 μm) up to 190" (d ~ 0.1 μm) were measured ²⁴.

Using high supercooling values ($\Delta T \sim 18^\circ\text{C}$) complex rocking curves can also be observed, indicating a double layer. The compositions of the first and second layers are different, but close to each other. It can be concluded that the lattice pulling effect does not appear for the first layer, and the second (outer) layer is assumed to have a near-equilibrium composition. These suppositions are supported by the fact that the a_0 value for the first layer joining the GaSb ($a_0 = 0.61409 \text{ nm}$) is rather far from the lattice constant of GaSb and farther than the lattice constant of the second layer ($a_0 = 0.61355 \text{ nm}$). Between the two AlGaInSb layers there is only a $8.8 \cdot 10^{-2}\%$ mismatch. The $\Delta a_0/a_0$ value between the substrate and the first layer, however, is 0.72 %.

Similar to the undoped GaSb and ternary antimonides the undoped pseudo-ternary AlGaInSb showed p-type conductivity that was probably also caused by Sb vacancies. Using a p-GaSb ($p = 2 \cdot 10^{17} \text{ cm}^{-3}$, $\mu = 500 \text{ cm}^2 \text{V}^{-1} \text{s}^{-1}$) substrate and doping the melt with Te p-GaSb/p-AlGaInSb/n-AlGaInSb, structures were also grown. Although, the p-n junctions show diode-characteristics, their semiconductor parameters (doping levels, transport, etc.) and diode properties (I-V characteristics, photoresponse etc.) have still to be studied in order to achieve optimum performance photodiodes.

In the $\text{GaP}_x\text{As}_y\text{Sb}_{1-x-y}$ ($x = 0.366$ and $y = 0.619$) system the most characteristic feature was that, upon exciting the semiconductor at 4 K by Ar-ion laser and also during SEM investigations, bright, red luminescence was observed.

The recombination properties indicates that this pseudo-ternary, the GaPAsSb, offers a possibility to develop light sources. The lattice matching - in principle - can be achieved for both GaAs and InP. InP suits to GaPAsSb compositions falling into the direct band gap region, while to GaAs both direct and indirect band gap GaPAsSb quaternaries could be lattice matched. This means that good quality substrate materials for a prospective development are available. But phase relations, solid state reaction with GaAs and segregation effects as mentioned have to be investigated for the further technological progress.

REFERENCES

1. Zbitnew, Z. and Wolley, J.C.
J.Appl.Phys. 52 6611 (1981)
2. Lendvay, E.
Electronics Lett. 18, 407 (1982)
3. Lendvay, E.
in "Defect Complexes in Semiconductor Structures"
Lecture Notes in Phys. Vol.175
Springer-Verlag, Berlin, p.163
4. Nishitani, Y., Akaita, K., Yamaguchi, A. and Kotani, T.
J.Electrochem.Soc. 127, 949 (1980)
5. Lendvay, E.
J.Cryst.Growth 60 447 (1982)
6. Kobayashi, N. and Horikoshi, Y.
Japan J.Appl.Phys. 20 2301 (1981)
7. Lendvay, E.
J.Cryst.Growth 53 591 (1981)
8. Lendvay, E., Görög, T., and Toth, L.A.
"Intl.Symposium on GaAs and Related Compounds" 1980, Vienna Inst. of
Physics Conf. Ser. 56 p.139 (1981)
9. Hsieh, J.J.
IEEE J.Quant.Electron. QE-17 118 (1981)
10. Pearsall, T.P. Quillex, M. and Pollack, M.A.
Appl.Phys.Lett. 35, 342 (1979)
11. Houston, P.A.
J.Mater.Sci. 16 2935 (1981)
12. Ishida, K., Matsumoto, Y., and Taguchi, K.
phys.stat.sol. (a) 70 277 (1982)
13. Lendvay, E.
to be published
14. Stringfellow, G.B.
J.Apply.Phys. 43 3455 (1973)
15. Quillex, M., Launois, H., and Joncour, M.
J.Vac.Sci.Technol. 31 238 (1983)
16. Morrison, C.B. and Bedair, S.M.
J.Apply.Phys. 53 9058 (1982)

17. Panish, M.B.
J.Chem.Thermodyn. 2 319 (1970)
18. Blom, G.M.
J.Electrochem.Soc. 118 1834 (1971)
19. Ettenberg, M. and Lockwood, H.
"GaAs and Related Compounds" Inst.Phys.Conf.Ser. 24 102 (1975)
20. Williams, C.K., Glisson, T.H., Hauser, J.R., and Littlejohn, M.A.
J.Electron.Mater. 7 639 (1978)
21. Komiya, S., Nakajima, K., Umebu, I., and Akita, K.
Japan.J.Appl.Phys. 21 1313 (1982)
22. Abrokwhah, J.K. and Gershenzon, M.
J.Electronic Mater, 10 379 (1981)
23. Nakajima, K., Tanashi, T., Komiya, S. and Akita, K.
J.Electrochem. Soc. 130 1927 (1983)

INVESTIGATION OF CLUSTER MODELS

J. Kertész

Many physical processes lead to the formation of clusters; examples are parts sticking together during sintering, aggregation of small particles, gelation and nucleation. But in some senses the patterns formed in surface instabilities can also be mentioned here. The circumstances of cluster formation, the geometry and statistics of clusters and the physical processes taking place on them are of fundamental relevance. In this short report I give an account of the recent research in this field in which I participated.

The simplest non-regular cluster model is the percolation model: the realization of which can be a lattice with randomly occupied sites. In the last decade much information accumulated about this model. The statistics of clusters turned out to be closely related to thermal phase transitions and therefore concepts like universality and scaling taken from the critical phenomena, can be applied. In this analogue the percolation threshold, the concentration where an infinite cluster first appears, plays the role of the critical point. A coherent picture of the statistics of clusters in random percolation has now emerged and the research in this field is focused either on applications of percolation models or on phenomena taking place on the clusters. Percolation is a par excellence droplet model, therefore it is of interest to check the predictions of the simple nucleation theory for percolation clusters¹. Alternatively percolation theory helps to find the physical droplets in describing collective phenomena in thermal systems².

There is of course much effort made in refining the earlier results. Using Beleznyay's method we achieved very precise numbers for two dimensional percolation³. New types of percolation problems have also been introduced such as percolation of surfaces⁴.

If physical processes are considered on clusters, the time dependence comes in a natural way. The most investigated phenomenon is diffusion - its importance can be understood from the Einstein relation which connects

electrical conductivity with diffusivity:

$$\sigma(\omega) = \text{const } D(\omega) \quad /1/$$

where $\sigma(\omega)$ is the frequency dependent conductivity and $D(\omega)$ is the frequency dependent diffusion coefficient which can be determined from the mean square displacement (averaged over configurations and initial positions) of a particle.

One of the interesting questions concerning this aspect is whether the dynamic behaviour at the threshold can be related to the static critical behaviour of the cluster statistics. Recently, several attempts have been made here and our contribution to this topics can be found in Ref.5,6.

The theory of critical phenomena gives a proper description of percolation phenomena near to the threshold. However, it is of general interest to construct approximation theories for the whole parameter range, although it is clear from the beginning that they must fail near to the critical point. An important question which arises is what, far from criticality means, i.e. what is the region of validity of an approximate theory. In the case of mean field theory the Ginzburg criterion solves this problem and our aim therefore was to find the main physical reasons for the break down of the theories of diffusion in percolation systems in order to find a similar criterion⁷. The best theory of this kind is the so called effective medium theory (EMT), originally due to Bruggemann. In a percolation system the correlation length ξ diverging as $\propto |\epsilon|^{-\nu}$ is characteristic for both finite and infinite clusters, where $\epsilon = c_p - c$ represents the distance from critical concentration of blocking elements c_p , and ν is a critical exponent. (Here and henceforth we restrict ourselves to the conducting region $c < c_p$.) The characteristic finite clusters with radius ξ give the main contribution to the diverging moments of the cluster distribution. The infinite cluster is homogeneous on larger length scales but it is self similar ('fractal') on much shorter length scales. This structure is reflected in the diffusion of a particle on percolation clusters. According to the scaling form of the mean square displacement:

$$\langle r^2(t) \rangle \propto \epsilon^{-2\nu+\beta} f(t/\tau) \quad /2/$$

at time t for $\epsilon \rightarrow 0$, where $\tau \propto |\epsilon|^{-2\nu+\beta-\mu}$ is the characteristic time, μ and β

are respectively the critical exponents of the diffusion coefficient ($D \propto \epsilon^u$) and of the percolation probability. For times $t \ll \tau$ the critical behaviour can be observed; which is an anomalous diffusion similar to that at the threshold. For $t \gg \tau$ the long time asymptotics set in

$$\langle r^2(t) \rangle / 2d = Dt + r_0^2 + \ell(t) \quad /3/$$

$\ell(t)$ being determined by the long time behaviour of $K(t)$, the time dependent diffusion coefficient and for $\epsilon \rightarrow 0$ $r_0^2 \propto \epsilon^{-2\nu+\beta}$, τ of eq./2/ can be calculated as r_0^2/D . This is the time needed for the particle either to notice the boundaries of a typical finite cluster or to cross a self similar blob in the infinite cluster. In eq./3/ the term r_0^2 expresses that the particle remembers, even for t going to infinity, the typical finite clusters and the structure of the infinite one, i.e. features carrying criticality at c_p . Taking now r_0^2 and D from an approximation theory, we can define

$$\tau_s = r_0^2/D \quad /4/$$

as the characteristic time for the short time behaviour. $\ell(t)$ is a typical hydrodynamic term. Accepting universality arguments, as they are established in the case of classical liquids, we assume:

$$\ell(t) = -at^{-(d/2-1)} \quad /5/$$

where the exponent is taken from the exactly known $c \rightarrow 0$ limit. A quantity with the dimension of time is therefore $(a/D)^{2/d}$. Because of eqs. /2,3/ this should yield τ again, as far as order of magnitude and divergence properties are concerned. For $t \gg \tau$ one should observe the long time asymptotics. The long time tail of $K(t)$ is due to memory effects and the time scale where it becomes observable, corresponds to the returning time. If a and D are now taken from EMT, one can define:

$$\tau_h = (a/D)^{2/d} \quad /6/$$

as a characteristic time for the hydrodynamic limit. We argued that in the

approximation theories the short and long time scale should not be mixed up:

$$\tau_s \leq \tau_h \quad /7/$$

and we proposed this relation as a criterion for the region of validity of approximation theories.

Applying the criterion /7/ to EMT we get for the region of validity in d dimensions:

$$c \leq c_p (1 + x(d))^{-1} \quad /8/$$

where $x(d)$ is a dimension dependent factor. One important consequence is that, contrary to the mean field theory of thermal phase transitions, there is no upper critical dimension above which the theory becomes correct. Furthermore, it turns out that $d=2$ is a special case, where criterion /7/ is never violated. In fact, EMT is excellent in two dimensions. If we take into account, that such a criterion is to be considered as an order of magnitude estimate, the agreement with the comparison of EMT with computer simulations is good. Similar results were obtained also for Götze's self consistent current relaxation theory, which considers diffusion in a continuum percolation system. In a work on hopping to further neighbours on percolation clusters the power of EMT has again been shown⁸.

Another important class of clustering is the aggregation of particles (see T. Vicsek's article in this volume). A very simple case is the Witten-Sander model of diffusion limited aggregation (DLA), where particles diffuse from infinity and stick at a seed where they hit it. This model is closely related to the phenomenon of dendritic crystal growth and other diffusion controlled pattern forming processes. In the work described below we investigated this relationship^{9,10}. We want to describe two-dimensional dendritic solidification in an (x,y) frame as grown from the $y = 0$ line in the positive y direction. Let us consider the following set of equations⁴:

$$\Delta u = 0 \quad /9a/$$

$$u(\underline{r}_\xi) = -d_0 k(\underline{r}_\xi) \quad /9b/$$

$$v_n(\underline{r}_\xi) = -D(\nabla u) \cdot \underline{n}(\underline{r}_\xi) \quad /9c/$$

$$u(y_0) = \varepsilon y_0 \quad /9d/$$

where u is the dimensionless temperature in the liquid, D the diffusion constant, a_0 is the capillary length, the vector \underline{r}_ξ is a point on the boundary represented by ξ (we restrict ourselves to two-dimensional problems), k is the curvature at such a point, \underline{n} is the normal vector and v_n the normal velocity of the interface, y_0 some large distance and g the value of u at y_0 . We neglected the time derivative in the eq./9/ which means that the diffusive relaxation is much faster than the growth of the crystal. In order to get instabilities, perturbations to eq./9/ should be added, but due to the MC noise they are always present in our simulation.

The standard MC method of solving the Laplace equation on the region S when the function is prescribed on the boundary ∂S is the following. N random walkers are started at a point $r \in S$ and at some time they hit the boundary which is a sink for them. The average of the values of u at the terminating points will converge to the solution at r if $N \rightarrow \infty$. We apply this method to eq./9a/ considering also eqs./9b,c/ in a numerical way.

We discretise the problem by putting a square lattice mesh on the plane and occupied (empty) sites on it will belong to the solid (liquid) phase. Since we are interested in the shape of the interface which is governed by eq./9c/ it is enough to determine u on the boundary, eq./9b/, and next to it, in order to calculate the gradient in the rhs of eq./9c/. In the discretised version of eq./9b/ the curvature is determined by Vicsek's method from the occupation ratio of a 7×7 square. Random walkers are started from the sites neighbouring the boundary. One sweep along these sites means one MC step/site (MCS/s) which is the time unit. The information about the gradient is stored in an array F : if the walker hits the boundary the quantity D times

$$u(\text{on boundary next to the start}) - u(\text{at terminal}) \quad /10a/$$

is added to it. After N MCS/s we have an approximation of

$$F = DN \nabla u \quad /10b/$$

If at some site F becomes unity, this point is occupied i.e. it freezes out. The velocity v of the boundary at this point is then

$$v = 1/N$$

/11/

(distances measured in lattice units). For more details on the algorithm see Ref.8.

Let us first see the connection of this model to DLA. The latter is often referred to as the solution of eq./1/ in the limit of vanishing surface tension ($d_0=0$). But in the case of the finite heat diffusion coefficient, we have an averaging effect due to the fact that the time N between two motions at the interface will be finite and this can lead to a relevant smoothening of the pattern. For $D \rightarrow \infty$, $N \rightarrow 0$ i.e. the crystal grows infinitely fast eq./11/. (Of course in the computer simulation $D \rightarrow \infty$ means that it is large enough to reach $F=1$ whenever the difference in eq./2a/ is positive). Only in this limit will our model coincide with the DLA. All the patterns on Fig.1 were generated under the condition of vanishing surface tension. Fig.1a (large D limit) has the same properties as DLA grown on a line substrate and this is reflected also in the measured fractal dimension ~ 1.7 . If smaller values of D are taken the pattern and probably also the fractal dimension changes (Fig.1b,c). The reason why the 'clusters' are much less ramified and more elongated is that the finiteness of the diffusion constant slows the procedure and the attractive power of the gradient can better act. At the moment we do not know if the change in the effective exponent is due to the appearance of a crossover to a different universality class or that one should go to much larger sample sizes to see the DLA exponent again.

Fig.2. shows the time evolution of a dendritic pattern grown in our model, where the time between two snapshots was always 2000 MCS/s. Due to the MC, noise fluctuations occur and then after some time, a characteristic length is observable in Fig.2c,d, corresponding to $d_0/2$. During further growth some branches become eventually larger and they screen the smaller ones in a 'struggle for life', which leads to the appearance of a longer characteristic wavelength as shown in Fig.2d,e. Fig.3 shows how the sequence of wavelengths appears as a function of time.

In this brief summary we could give only insights into the investigation on cluster models which emerged in our institute from problems

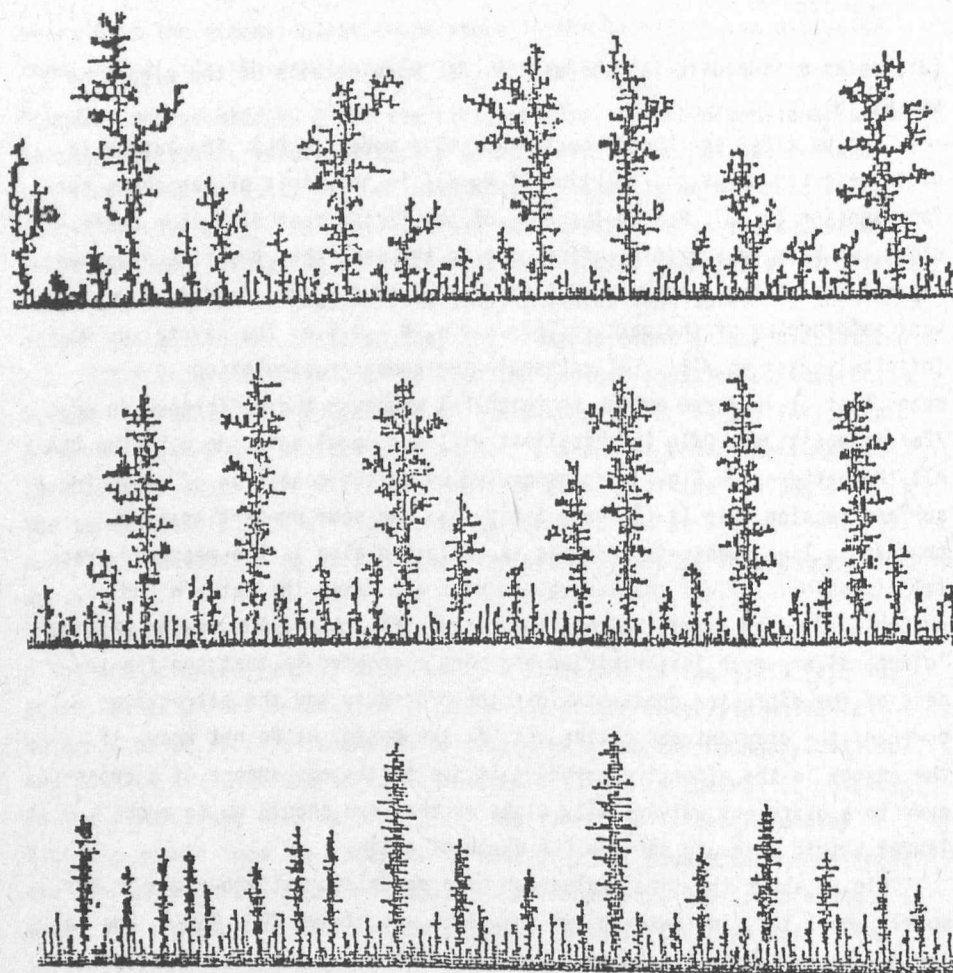


Fig.1 Patterns generated with $d=0$. The averaging is increasing from top to bottom.

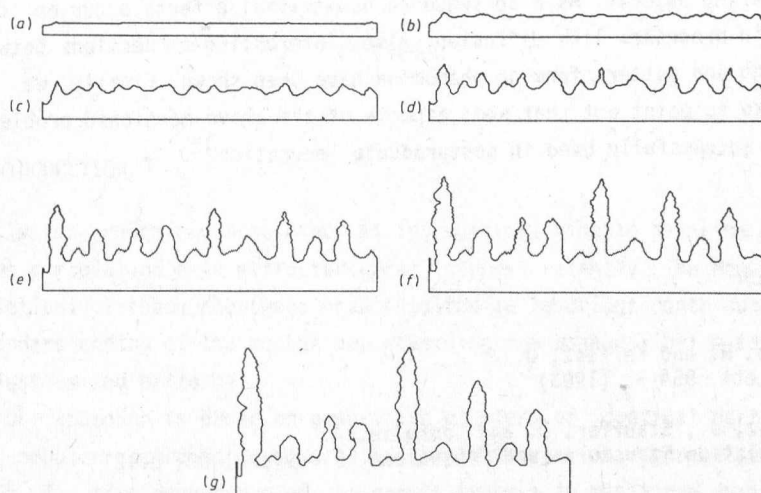


Fig.2 Evolution of a pattern in time

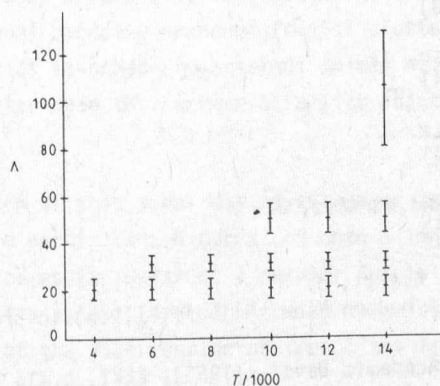


Fig.3 The characteristic wavelenths Λ as a function of time

suggested by practical field of research¹¹. The common features of the investigated cluster models are the randomness and the fractal dimension of the appearing objects. As a consequence non-trivial effects occur on the cluster in processes like diffusion. Also, interesting connections between clustering and pattern forming phenomena have been shown. Finally, we would like to point out that some aspects of the above-mentioned problems has been successfully used in postgraduate education¹².

REFERENCES

1. Franke, H. and Kertész, J.
Phys.Lett. 95A 52 (1983)
2. Kertész, J., Stauffer, D. and Coniglio, A.
'Percolation Structures and Processes', Elsevier 1983, p.121
3. Kertész, J.
J.Phys.A, in press
4. Kertész, J. and Herrmann, H.J.
J.Phys. A, in press
5. Kertész, J.
J.Phys.A 16 L471 (1983)
6. Kertész, J. and Metzger, J.
J.Phys.A 16 L735 (1983)
7. Kertész, J. and Metzger, J.
J.Phys.A 17 L501 (1984)
8. Metzger, J. and Kertész, J.
J.Phys.C 17 5153 (1984)
9. Szép, J., Cserti, J. and Kertész, J.
J.Phys.A 18 L413 (1985)
10. Kertész, J., Szép, J., Cserti, J.
in 'Growth and Form - A Modern View' Nijhoff, (1985) in press
11. Nagy, E., Kertész, J.
in 'Swedish-Hungarian Academic Days', (1985), KFKI, p.115
12. Kertész, J., Cserti, J., Szép, J.
Eur. J. Phys., in press.

FRactal Structure and Dynamics in Aggregation Phenomena

T. Vicsek

1. INTRODUCTION

Cluster growth processes such as aggregation, kinetic gelation or invasion percolation have attracted great interest recently. The Monte Carlo simulations of these phenomena have resulted in important contributions to the understanding of the mechanisms governing the nonequilibrium formation of clusters and patterns.

Our approach is based on generating clusters of identical particles in a computer according to some rules simulating various aggregation phenomena. The time dependence of the growth process is monitored during the numerical experiment, while the structure is usually determined when the growth is completed.

2. STRUCTURE

The first process we studied is called diffusion-limited aggregation (DLA) which had been proposed by Witten and Sander in 1981. In the simulations of this model randomly branched, fractal clusters are generated as diffusing particles launched from distant points stick to the surface of the growing cluster when they arrive at a site adjacent to the aggregate. (Fig.1.)

2.1. A version of this model was investigated in which instead of a seed particle the particles are deposited onto a line of seed particles. This model enabled us to construct a regular fractal model^{1,2} for DLA and to study the statistics of "trees"³ growing on this one dimensional surface. The study of the distribution of tree sizes led us to a scaling assumption and a new scaling law.

Calculations of the radial and tangential correlations in the DLA clusters resulted in an unexpected conclusion, namely, that the diffusion-limited aggregates are internally anisotropic and the power law decay of correlations within the clusters are orientation dependent^{4,5}.

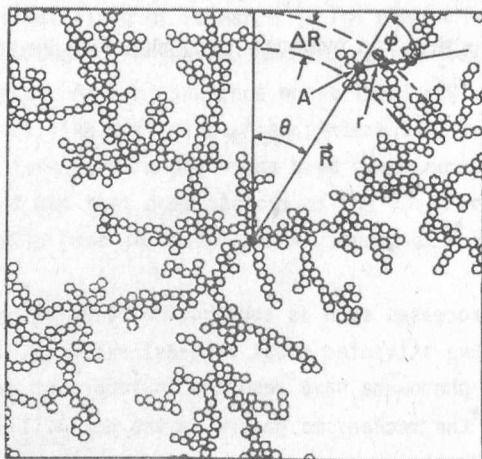


Fig.1

Central part of an off lattice diffusion-limited aggregate. The tangential correlations were determined in a layer of width ΔR at a distance R from the origin as a function of the angle. The arguments of the orientation dependent correlation function $c(r, \phi)$ at the point A are the distance from this point r and the local angle ϕ .

Figure 2 shows that the tangential correlations decay with an exponent -0.41 , while the corresponding value in the radial direction is -0.29 .

2.2. The above model is called ballistic aggregation if the particles move along straight trajectories. We have studied the width of the surface of ballistic deposits and found nontrivial scaling as a function of the height and the length of the aggregates⁶.

2.3. The shape of the so called lattice animals and percolation clusters has also been investigated⁷. According to our results, although these systems are completely isotropic, the overall shape of the random fractal clusters generated in the above models is anisotropic.

2.4. We modified the standard real space renormalization group in order to calculate the fractal dimension of the DLA clusters. The resulting method is very efficient and can be applied to a large variety of related models⁸.

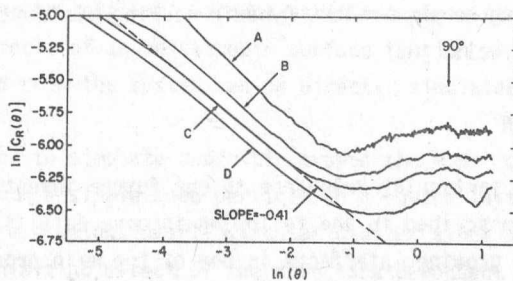


Fig.2.:

Tangential correlations in off lattice diffusion-limited aggregates. Curves a-d were obtained for 44 clusters of 50.000 particles by making an average over the intervals $\delta R = R \pm 0.05 R$ with a) $R = 75$; b) $R = 150$; c) $R = 225$ and d) $R = 300$. The position of the minimum of these correlation functions does not seem to change with the increasing distance R from the origin, showing that the aggregates are built up from a few large treelike branches. The slope of the straight line drawn through the curve d is $\alpha_{\perp} = 0.42$.

3. DYNAMICS

3.1. In the cluster-cluster aggregation model the system initially consists of randomly distributed particles at the sites of the lattice. These particles undergo random walks and stick rigidly together on contact. The resulting clusters continue to diffuse and build larger ones by joining when touch each other. The diffusivity of the clusters may depend on their sizes. Our results showed that the temporal evolution of the cluster size distribution can be described in terms of dynamical scaling. A new scaling relation was established^{9,10} among the critical exponents describing the power law behaviour of the various quantities. The cluster size distribution was shown to be nonuniversal as a function of the diffusivity¹¹ and the sticking probability^{12,13} of the clusters.

3.2. The cluster size distribution function has also been determined in the steady-state version of the above cluster-cluster aggregation model¹⁴, where single particles are added to the system and larger particles are removed according to some rules. Dynamic scaling was shown to exist for this problem as well.

4. PATTERN FORMATION

Because of its particular relevance to our future investigations this study¹⁵⁻¹⁷ will be described in the following in more details. The formation of patterns by growing interfaces is one of the main processes in a wide range of phenomena in science and technology. Such behavior is exhibited during solidification, when the crystalline phase is growing in super-saturated vapor or undercooled melt. Examples for formation of solidification patterns include the evolution of a snowflake in the atmosphere or directional solidification in a number of metallurgically important situations.

4.1. The following rules¹⁵ will be used to simulate the process of solidification:

- i) Random walks by the particles (as in DLA),
- ii) Sticking to the surface of the growing cluster with a probability depending on the local interface curvature,
- iii) Relaxation to a position with the highest number of occupied nearest neighbours.

The first rule simulates the effects of a non-local diffusion field as it was discussed by Witten and Sander and by Kadanoff. This destabilizing force is compensated by the surface tension which is taken into account by rule ii). (The growth is slowed down at places with large curvature.). The third rule is needed in order to get compact clusters with a low density of local defects (holes). A detailed description of the model can be found in Ref.15.

Application of the above model to the solidification problem has a number of advantages. The numerical method is simple and effective. Relatively complex geometries can be generated easily. Second, the fluctua-

tions which are always present in a thermodynamical system (and play an important role during the growth process) are included in a natural way through the random walks of the particles. Finally, the model can easily be modified in order to take into account various experimental conditions. For example, the effects of an anisotropic surface tension or a temperature gradient imposed upon the system can be directly simulated.

4.2. In order to simulate dendritic growth the model described in Sec. 4.1. was used with a single seed particle on a square lattice¹⁵. The process starts with a growing, nearly circular cluster since at this stage the surface area minimizing effect of the curvature dependent sticking probability dominates the growth.

As the process goes on, the initially structureless behaviour crosses over into dendritic growth as it is demonstrated in Fig.3, where we show the number of surface sites, N_s versus the number of sites in the cluster, N , in a log-log plot.

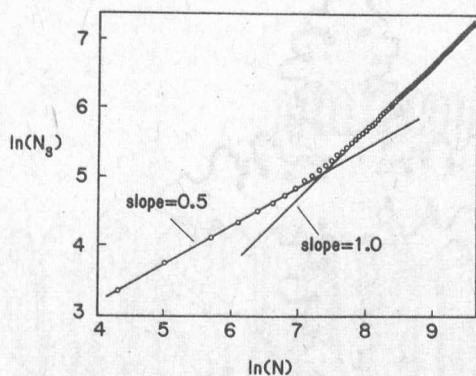


Fig.3

Dependence of the number of surface sites, N_s , on the number of particles in the cluster, N . The change in the slope of the curve indicates the crossover from compact to dendritic growth.

For relatively small sizes the slope of the straight line connecting the data is approximately equal to $1/2$ in accordance with the growth of a circular cluster. At later stages, however, the number of surface sites becomes linearly proportional to N (resulting in a slope nearly equal to 1) which corresponds to the development of dendrites.

The effects of an anisotropic surface tension can be investigated in the present model by introducing a sticking probability, p_{an} , depending on the local slope of the surface.

In Fig.4. a cluster of 25.000 particles is shown which was generated using an anisotropic surface tension enhancing the growth along the main axes of the square lattice. This pattern exhibits a number of properties typical of dendritic solidification and it appears to be stable in the sense of the absence of any tip splitting. However, this cluster is still not as regular as most of the solidification patterns observed in the experiments. This is due to the fluctuations which are relatively large for small surface tension.

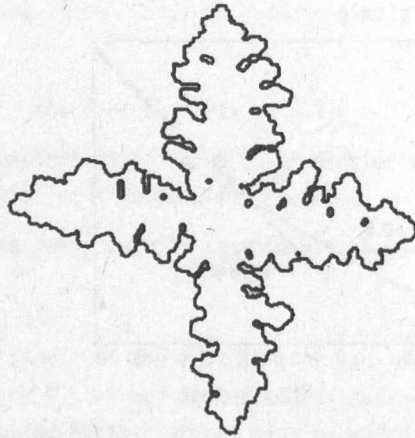


Fig.4

The effect of a sticking probability depending on the local orientation of the surface. This figure shows a cluster of 25.000 particles generated using a condition for the sticking probability which enhances growth along the axes of the square lattice. Only the surface sites (those which have less than four occupied nearest neighbours) are plotted.

For larger values of A more regular patterns are expected to grow in this model. On the other hand, we had to keep A relatively low in order to have larger curvatures and more complex patterns in our medium scale simulations.

4.3. In this section we consider a version of the model^{16,17} in which the particles are deposited onto a line instead of a single particle in order to simulate the conditions of directional solidification experiments. During these experiments the working material (usually a long rod or a thin strip) is drawn with a given velocity through a fixed temperature gradient.

To account for the fact that the working material is moving we introduce a biased random walk by increasing the probability of jumping into the direction of the interface or "downward", p_{down} , with regard to the probability of jumping "upward", p_{up} . The simulations for several values of the ratio $R = p_{\text{down}}/p_{\text{up}}$ result in patterns which are more regular for $R > 1$ than in the unbiased case. In fact, these patterns look very similar to those observed in the experiments of Heslot and Libchaber on directional solidification of thin samples of succinonitrole. This is demonstrated in Fig.5, where both the simulation and the experimental results are shown.

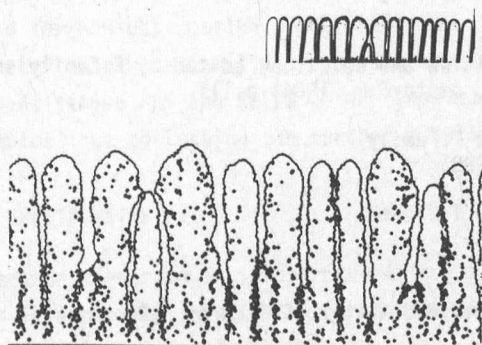


Fig.5

This pattern was generated using biased random walks with a ratio of down- to upward jumps of $R=1.1$. The insert shows the experimental results of Heslot and Libchaber on the directional solidification of succinonitrole

REFERENCES

1. T.Vicsek
J.Phys.A.: Math.Gen.16, L647 (1983)
2. Z.Rácz and T.Vicsek:
in Kinetics of Aggregation and Gelation, edited by F.Family and D.P.
Landau (North-Holland, Amsterdam, 1984) p.255
3. Z.Rácz and T.Vicsek
Phys.Rev.Lett. 51, 2382 (1983)
4. P.Meakin and T.Vicsek
Phys.Rev. A32, 685 (1985)
5. P.Meakin and T.Vicsek:
in Fractals in Physics, edited by L.Pietronero and E.Tosatti:
(North-Holland, Amsterdam, 1985)
6. F.Family and T.Vicsek
J.Phys. A18, L75 (1985)
7. F.Family, T.Vicsek and P.Meakin
Phys.Rev.Lett. 55 641 (1985)
8. L.M.Montag, F.Family, T.Vicsek and H.Nakanishi
Phys.Rev. A32, Oct. (1985)
9. T.Vicsek and F.Family,
Phys.Rev.Lett. 52, 1669 (1984)
10. T.Vicsek and F.Family:
in Kinetics of Aggregation and Gelation, edited by F.Family and D.P.
Landau (North-Holland, Amsterdam, 1984) p.111
11. P.Meakin, T.Vicsek and F.Family
Phys.Rev. B31, 564 (1985)
12. F.Family, P.Meakin and T.Vicsek
J.Chem.Phys. Nov. (1985)
13. F.Family and T.Vicsek:
in Physics of Finely Divided Matter, Edited by M.Daoud,
Springer Verlag (1985)
14. T.Vicsek, P.Meakin and F.Family
Phys.Rev. A32, 1122 (1985)
15. T.Vicsek
Phys.Rev.Lett. 53, 2281 (1984)
16. T.Vicsek
Phys.Rev. A.Sept. (1985)
17. T.Vicsek, in Fractals in Physics, edited by L. Pietronero and
E. Tosatti: (North-Holland, Amsterdam, 1985)

NEW DEVELOPMENTS AND RESULTS IN SURFACE ANALYSIS

G. Gergely

In this report a brief review is given on research and developments in the field of surface analysis and additionally as applied to thin films. Besides materials research associated with electronics and metallurgy some new methods have been developed which are useful for non-destructive depth profiling and for determining the inelastic mean free path (IMFP) of electrons. Surface and thin film analysis is made by electron and ion spectroscopy, mainly with Auger electron spectroscopy (AES), combined with ion sputtering. In our laboratory considerable efforts have been devoted to two auxiliary methods:

- Electron energy loss spectroscopy in reflection mode (REELS)
- elastic peak electron spectroscopy (EPES)

The aim of these developments was to extend the application of our simple CMA electron spectrometer beside the AES and to identify chemical compounds and for non-destructive depth profiling. In this development of the spectrometer mainly nationally produced components and units have been used. For quantitative AES and REELS better knowledge of IMFP was needed for many samples thus motivating the further developments of EPES.

1. ELECTRON SPECTROMETER

The electron spectrometer is operated with a Riber OPC 103 CMA analyser and lock in amplifier (KFKI NV255) or in the DC mode (Analog Devices 272J). Surface analysis is made in UHV (10^{-8} Pa), using Ar^+ ion milling for cleaning or depth profiling and fracture in UHV resp. (Gergely, Menyh rd, 1984). An on line computer system has been constructed (Menyh rd, Sulyok 1984), using a MMG SAM 85 type microcomputer with peripheries. The main features of the system are:

- Digital scan of ramp in arbitrary steps from 0.1 V.
- Matching and recording the scanned, selected energy range (ramp and CMA) with suitable energy resolution.

- Data acquisition by a selected number of runs, required by the signal/noise ratio.
- Averaging and smoothing of the spectra.
- Processing operations depending on the type of analysis (e.g. quantitative AES, low signal level REELS etc.)
- Computer corrections with the backscattering factor, IMFP etc.
- Background subtraction and deconvolution (inelastic tail of peaks).
- Integration of selected peaks (AES, REELS).
- Computer evaluation of surface and thin film analysis.

2. MATERIALS RESEARCH

Materials research used mainly AES with depth profiling, in some cases REELS. This section is confined to five topics:

2.1. Oxidation of tantalum thin films

Tantalum based thin films have been studied in cooperation with Microelectronics Co. (Kolonits et al. 1985). The distribution of oxygen within the films has been determined by AES depth profiling thus revealing the effects of annealing.

2.2. AIS M2 high speed steel

AIS M2 high speed steel has been investigated in cooperation with the Res.Inst.Ferrous Metallurgy (Budapest). The hot deformability of this steel alloy is strongly affected by some impurities like S and Sn. AES fractography revealed enrichment of S and P on carbide phases (Szilvásy et al. 1984). The isolated carbide phase has been studied by XPS in the Res.Lab. Inorganic Chemistry. Hung.Acad.Sci. (Budapest), identifying the carbide compounds (Menyhárd et al, Bertóti 1984).

2.3. Iron in tungsten

AES analysis participated in the tungsten research program. The segregation of iron on grain boundaries of tungsten was studied by AES fractography, showing its occurrence at temperatures where bulk diffusion is

still negligible. (Uray, Menyh rd 1984).

2.4. Ordered Al50-Co50 alloy

Al_xCo_{1-x} alloys have been investigated in cooperation with the Inst. Physical Chemistry of the Polish Acad.Sci (Warsaw). Enrichment of Co on the surface of Al50-Co50 ordered alloy was shown using AES (Mrozek et al. 1984) in our laboratory.

2.5. Natural oxide layers on Al thin films

Electron spectroscopy contributed to the research of aluminium thin films (Barna et al 1985). The IMFP of electrons in Al_2O_3 has been determined by elastic peak electron spectroscopy in the 1 - 3 keV kinetic energy range (Gergely et al. Acta Phys.Hung. 1985). The plasmon loss spectra exhibited the attenuation of electrons, backscattered elastically from the substrate by the oxide film. (Gergely 1985).

3. REFLECTION ELECTRON ENERGY LOSS SPECTROSCOPY (REELS)

The development of our highly sensitive electron spectrometer using signal storage and processing achieved progress in REELS. It was verified by the experimental evidence; that the loss peaks are formed mainly by electrons reflected elastically before or after the inelastic scattering (Sulyok 1985). Mainly core level ionization loss spectra (ILS) was studied, REELS supplying much additional information with respect to AES. (Menyh rd 1984, Meny rd, Sulyok and Gergely 1984-85.).

The main features are:

- REELS can be made quantitative by means of the elastic peak as reference (Gergely 1984)
- Chemical identification of compounds and alloys (Menyh rd, Sulyok 1984), possible band structure studies.
- In some cases REELS might be more sensitive than AES.
- Larger information depth of analysis with respect to AES.
- Depth profiling possibilities (Gergely, Meny rd and Sulyok 1985).

To illustrate the magnitude of signals, the Auger peak of Ti, its L_2 ILS

peak and the elastic peak are shown in Fig.1 for a very thin Ti film deposited on a Si substrate.

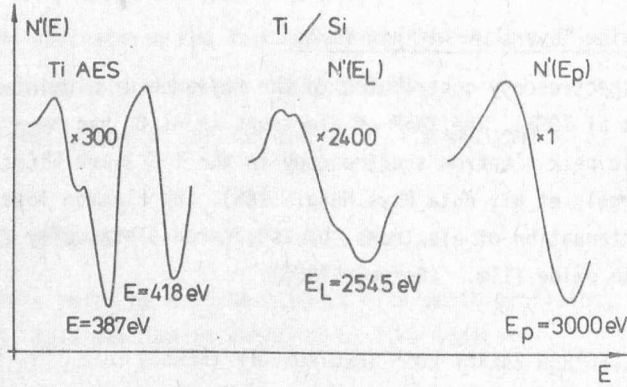


Fig.1

The shape of the ILS peak is determined by the distribution and density of local states in the solid. This is illustrated in Fig.2., showing four different alloys and compounds of Cu. (Menyhárd, Sulyok 1985).

Non destructive depth profiling has been elaborated by using REELS combined with EPES. In thin film analysis depth profiling with ion milling is widely used. In many cases, however, it is disadvantageous (limited depth resolution, ion beam artifacts etc.). According to (Gergely, Menyhárd 1985), the ratio of the ILS peak $N(E_L)$ to the elastic peak $N(E_p)$ is given by Eqn /1/:

$$\frac{N(E_L)}{N(E_p)} = N_A f \sigma_i(E) \frac{\lambda_L \cos \alpha}{\lambda_p + \lambda_L \cos \alpha} \left[\lambda_p + \frac{\sigma_e(E_L)}{\sigma_e(E_p)} \lambda_L \right] \quad /1/$$

denoting N_A as the density of atoms, λ_p and λ_L resp. the IMFP for E_p and E_L energies, $\sigma_i(E)$ the ionization, $\sigma_e(E)$ the elastic reflection cross sections resp. $\alpha = 42^\circ$ (CMA angle). Scanning the primary energy E_p λ_p can be

varied, achieving depth profiling. In the $E_p = 1 - 3$ keV range λ_p covers a 1.5 - 5 nm information depth, with excellent resolution (0.2 nm at 3 keV). The oxide overlayer on Al has been studied in this way. (Barna et. al 1985, Gergely, Menyh rd, Sulyok 1985).

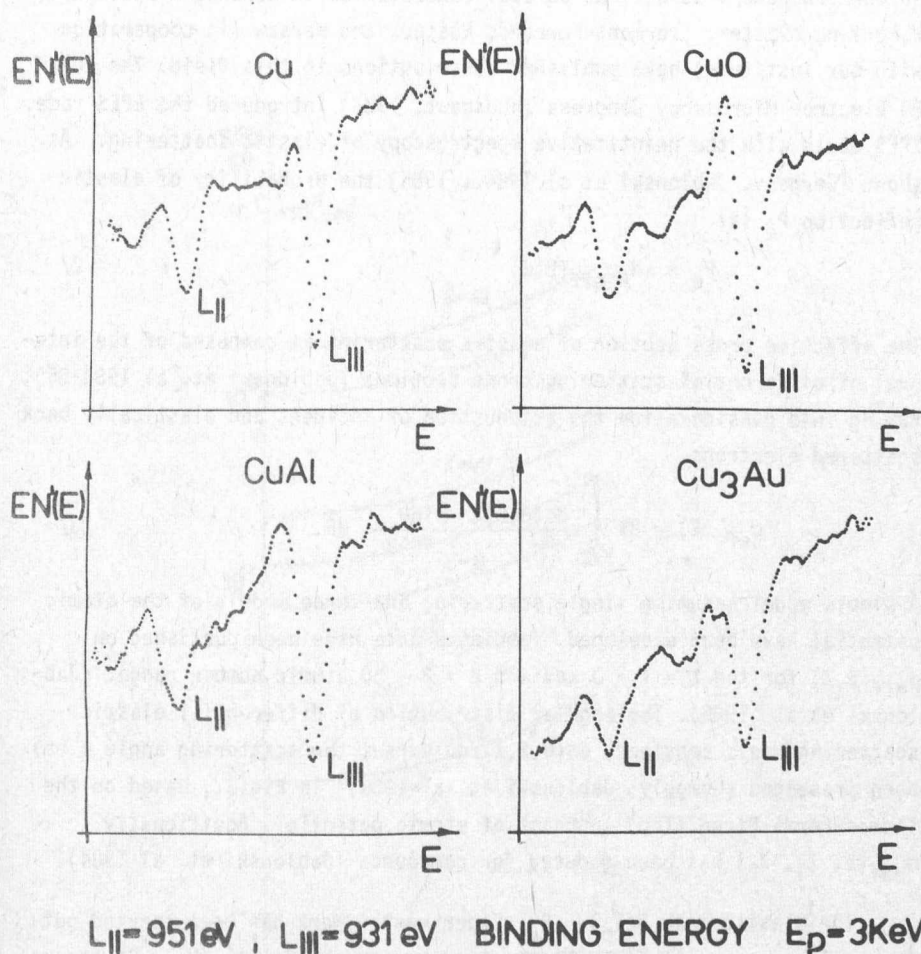


Fig.2

4. ELASTIC PEAK ELECTRON SPECTROSCOPY (EPES)

Elastic peak electron spectroscopy was developed in our laboratory in 1981 and reported in MFKI'82/83 Yearbook. Nowadays electron spectroscopy is using 25-30 methods, little attention however having been paid to the elastic scattering of electrons which are useful for surface and thin film analysis. During 1984-85 though considerable development has been achieved in our laboratory as well as abroad: laboratories in Hohenheim-Stuttgart, W.Berlin, Münster, Clermont-Ferrand, Rostock and Warsaw (in cooperation with our Institute) have published contributions in this field. The EUREM 84 Electron Microscopy Congress (Budapest, 1984) introduced the EPES code. EPES deals with the quantitative spectroscopy of elastic scattering. As shown (Gergely, Jablonski et al 1984., 1985) the probability of elastic reflection P_e is:

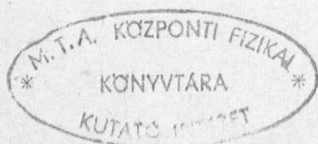
$$P_e = \lambda N_A \sigma_{\text{eff}}(E, Z) \quad /2/$$

The effective cross section of elastic scattering is composed of the integral of differential scattering cross sections (Jablonski et. al 1984-85), taking into consideration the attenuation of incident and elastically back scattered electrons.

$$\sigma_{\text{eff}}(E) = 2\pi \int_{\pi/2}^{\pi} \frac{d\sigma(\theta, E)}{d\Omega} \frac{\sin\theta}{1 - \sec\theta} d\theta \quad /3/$$

A simple model assuming single scattering and three models of the atomic potential have been developed. Tabulated data have been published on $\sigma_{\text{eff}}(E, Z)$ for the $E = 1 - 3$ keV and $Z = 3 - 50$ atomic number range. (Jablonski et.al 1985). The angular distribution of differential elastic scattering cross sections, $d\sigma(\theta, E, Z)/d\Omega$ versus the scattering angle θ has been presented (Gergely, Jablonski et. al 1985) in Fig.3, based on the Thomas-Fermi-Dirac (TFD) approach of atomic potential. Additionally $\sigma_{\text{eff}}(E, Z_1, Z_2)$ has been deduced for compounds (Jablonski et. al 1984).

The elastic peak $N(E_p) \sim P_e$. Experimental work has been carried out in our laboratory with our CMA spectrometer and by Seiler (Univ.Stuttgart-Hohenheim), working with a retarding field analyser (RFA). For a CMA or RFA, the angular window of the spectrometers should be taken into consideration. Comparing the elastic peaks of two samples measured with the



CMA or RFA spectrometer, using Eqn/2/ and tabulated $\sigma_{\text{eff}}(E, Z)$ data, the IMFP λ can be determined with simple electron reflection measurements without needing a perfect, uniform thin film, transparent for electrons. λ has been determined for a number of elements and compounds, like SiO_2 , Si_3N_4 , GaAs, GaP, GaSb etc. Results are presented in papers (Jablonski et al. 1984, Gergely, Jablonski et al. 1984-1985). Some λ data determined by our CMA measurements are recollected in Table I.

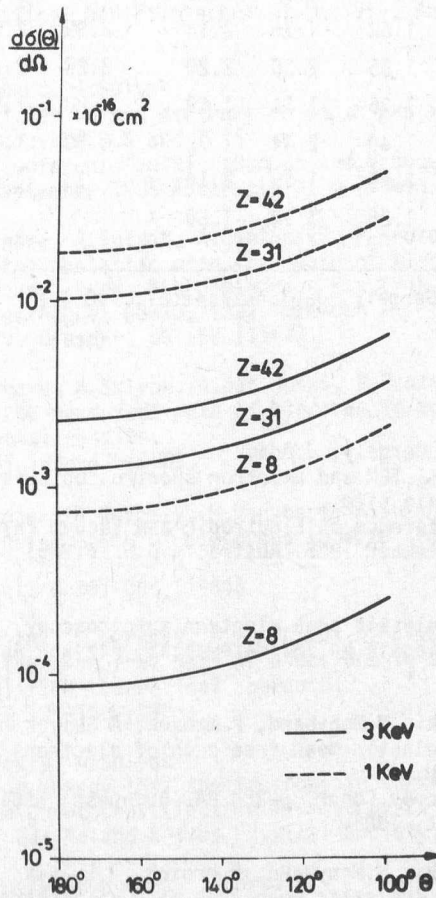


Fig.3

TABLE I. λ [nm]

E keV	1		1.5		2	
Sample	TFD	Lit	TFD	Lit	TFD	Lit
Al	1.92	2.12	2.86	2.91	3.64	3.63
V	1.78	1.55	2.62	1.90	3.39	2.31
Fe	1.64	1.41	2.54	1.72	3.21	1.99
Cu	1.53	1.62	1.75	2.14	2.99	2.62
Ag	1.28	1.65	2.30	2.20	3.20	2.70
Co	1.22	1.36	1.51	1.69	2.83	1.93
CoAl	1.51	1.40	2.44	1.72	3.29	1.98
Ta	0.73	1.75	1.16	2.14		
W	0.78	1.25	1.24	1.59		

Lit. data cited in (Gergely, Jablonski et al. 1985).

REFERENCES

- P.B.Barna, Z.Bodo, G.Gergely, J.Adam
Spectral ellipsometric, TEM and electron spectroscopic investigations on oxidized aluminium thin films.
7th Czechoslovak Conference on Electronic and Vacuum Physics
Bratislava, 3-6, September 1985. Abstracts p.5. (1985)
- G.Gergely
New developments in elastic peak electron spectroscopy.
Acta Univ. Wratislaviensis No.782 Matematyka, Fizyka, Astronomia, 45
27-35 (1984)
- G.Gergely, A.Jablonski, M.Menyhard, P.Mrozek, A.Sulyok
Estimation of the inelastic mean free path of electrons by elastic peak electron spectroscopy.
Proc.Electron Microscopy Congr. EUREM 84. Budapest, 1984. 457-458
Ed.: MOTESz, Budapest, 1984.
- G.Gergely, A.Jablonski, M.Menyhard, P.Mrozek, A.Sulyok
Determination of the inelastic mean free path of electrons by elastic peak electron spectroscopy.
Acta Univ. Wratislaviensis, No.847 Proc.8th Sem.Surface Physics. 46 17-23
(1985)

G.Gergely

Ellipsometric and electron spectroscopic studies on oxide overlayers on Al
Proc.5.Symp.Oberflächen- und Elektronenphysik, 4-8 März. 1985, Gaussig
Ed: Technische Universität, Dresden. (1985)

G.Gergely, M.Menyhard

Auger electron spectroscopy in fractography. Electron-microscopic investigations of fracture and crack formation processes in solids.
Halle/S April 2-8 1984. Abstracts 18-19 (1984)

G.Gergely, M.Menyhard

Some problems of in-depth profiling of layer structures. New ways, possibilities.

Proc.Symp.Electronics Technology, 16-19 April 1985.

Ed. Optical, Acoustical and Filmtechnical Society, Budapest 1 111-116
(1985)

G.Gergely, M.Menyhard, A.Sulyok

Some new possibilities in non destructive depth profiling using secondary emission spectroscopy: REELS and EPES

7th Czechoslovak Conference on Electronics and Vacuum Physics

Bratislava, 3-5 September 1985 Abstracts p.10 (1985)

G.Gergely, M.Menyhard, A.Sulyok, A.Jablonski, P.Mrozek

Determination of the inelastic mean free path of electrons by elastic peak electron spectroscopy. Proc. 5th Seminar on Electron Spectroscopy of

Socialist Countries August 26-29, 1984. Dresden

Ed: Technical Univ. Dresden, p51-52 (1984)

G.Gergely, M.Menyhard, A.Sulyok, A.Jablonski, P.Mrozek

Determination of the mean free path of electron in solids from the elastic peak.II. Experimental results.

Acta Phys.Hung. 57 139-147 (1985)

A.Jablonski, P.Mrozek, G.Gergely, M.Menyhard, A.Sulyok

The inelastic mean free path of electrons in some semiconductor compounds and metals.

Surf.Interface Anal. 6 291-294 (1984)

A.Jablonski, P.Mrozek, G.Gergely, M.Menyhard, A.Sulyok

Determination of the mean free path of electrons in solids from the elastic peak. I. Simplified theoretical approach.

Acta Phys.Hung. 57 131-138 (1985)

M.Menyhard, G.Gergely, A.Sulyok

Reflection electron energy loss spectroscopy in surface studies.

Hungarian-Austrian Joint Conf.Electron Microscopy 25-27 April, 1985.

Balatonaliga, p36 Ed: Roland Eötvös Physical Society, Budapest (1985)

M.Menyhard, G.Gergely, A.Sulyok, I.Bertoti

Electron spectroscopy study of carbides in AISI M2 high speed steel.

Proc. 5th. Seminar on Electron Spectroscopy of Socialist Countries.

August 26-29, 1984. Dresden. Ed: Technical University, Dresden p.83-84
(1984)

V.P.Kolonits, M.Czermann, O.Gesztzi, M.Menyhard
The oxidation of tantalum-based thin films
Thin Solid Films 123 45-55 (1985)

M.Menyhard
Ionization loss spectroscopy in reflection mode
EPS Europhysics Conf.ABSTRACTS 8B ECOSS-6. 1-5 April, 1984, York p.247
(1984)

M.Menyhard, A.Sulyok
Electron spectrometer-computer system
Proc.5th Seminar on Electron Spectroscopy of Socialist Countries
August 26-29, 1984. Dresden, Ed: Technical University, Dresden p.85-86
(1984)

M.Menyhard, A.Sulyok
Ionization loss spectroscopy
Acta Univ. Wratislaviensis, No.847 Proc.8th Sem.Surface Physics, 46 57-64
(1985)

M.Menyhard, A.Sulyok, G.Gergely
Core level electron energy loss spectra determined by REELS
Internat.Conf.X-ray and Inner-Shell Processes in Atoms, Molecules and
Solids X84, August 20-24, 1984. Leipzig, Abstracts 2 307-308 (1984)

M.Menyhard, A.Sulyok, G.Gergely
Ionization loss spectroscopy in reflection mode
Proc.Electron Microscopy Congr. EUREM 84, Budapest, 1984
Ed: MOTESz Budapest, 459-460 (1984)

P.Mrozek, M.Menyhard, J.Wernisch, A.Jablonski
Surface composition of the ordered Al50-Co50 alloy.
phys.stat.sol(a) 84 39-48 (1984)

A.Sulyok
Intensity of core level electron energy loss peaks of Ti
ECOSS 7. 1-4 April 1985, Aix-en-Provence, EPS Europhysics Conf.
Abstracts 9C 211 Ed: University Aix-Marseille (1985)

Cs.Szilvasy, M.Menyhard, G.Gergely
Auger electron spectroscopy studies of impurity effects on the hot de-
formability of AISI M2 high speed steel.
Crystal Res.Technol. 19 187-194 (1984)

L.Uray, M.Menyhard
The segregation of iron in tungsten
phys.stat.sol. (a) 84 65-72 (1984)

ACKNOWLEDGEMENTS

This report contains works achieved with coworkers Dr.M.Menyhard and A.Sulyok, partly in cooperation with Dr.A.Jablonski and P.Mrozek (Institute of Physical Chemistry of the Polish Academy of Sciences, Warsaw). Author appreciates their cooperation.

ENERGY DISPERSIVE X-RAY MICROANALYSIS AND FLUORESCENCE ANALYSIS

J.L. Lábár and I. Pozsgai

To be able to meet the demands of practical applications we have made efforts in the past years to further develop the analytical techniques, available in the Laboratory for Scanning Electron Microscopy. An improved standardless microanalytical program and improved detection limits of X-ray fluorescence analysis in the electron microscope were therefore both attractive tasks for us. Correspondingly we are reporting about developments in these two fields.

1. THE EFFECT OF RELATIVE L-LINE INTENSITY RATIOS ON THE ACCURACY OF STANDARDLESS X-RAY MICROANALYSIS

a) Introduction

During the last decade a large number of papers demonstrated that the long term stability of detection efficiency of ED X-ray spectrometers can be used to spare the repetitive measurements of standards which are usual in conventional microanalysis. This fact considerably reduces the time required for analysis and makes the examination possible even in those cases when standards for certain elements are not available. The X-ray intensity of standards can be derived either, from empirical calibration curves or from calculations based on physical principles.

A modern standardless method should incorporate both spectrum processing and concentration calculations, and should be capable of handling complicated K and L spectra. As both overlap correction and calculation of X-ray intensities for standards (or alternatively the first concentration guess), require exact relative line weights this paper examines the effect of relative L-line intensities on the accuracy of the standardless X-ray micro-analysis. We regarded the K-alpha/K-beta ratio as known¹ and did not vary it during the test.

b) Theory

Our standardless program was developed from the FRAME-C quantitative EDS microanalytical program.² The calibration routine evaluates not only the detector window parameters but can also take into consideration the actual parameters of the multichannel analyzer i.e. gain, offset, the value of the resolution and its energy dependence. In contrast to the original FRAME-C in our program the standard intensities are not measured but calculated and stored on floppy disk. The data reduction of measured unknown spectra includes background subtraction, overlap and ZAF corrections in a common loop as in Ref.2. A further difference is that the total concentration is normalized to unity in each step of iteration and a convergence test was built in, both in overlap correction and ZAF correction loops. The maximum number of iterations was fixed to 10 in each case.

Two versions of our standardless program were tested. In version A/ we used the original relative line intensities of FRAME-C. Into version B/ we built in the atomic number (Z) dependent L relative line intensities proposed by Schreiber and Wims.³ An example of the modifications is shown in Fig.1. The other details of the two programs were totally identical. For more details of the calculation see Ref.4.

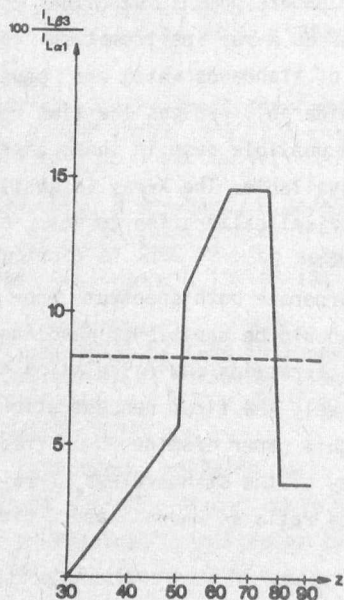


Fig.1

Plot of intensity ratio of L-beta3 to L-alpha1 line vs. atomic number (Z).

Full line:
values of Schreiber and Wims³

Dashed line:
values taken from FRAME-C.²

c) Experimental

The new standardless microanalysis program was implemented on an LSI-11 microcomputer built into a type EEDS-II ORTEC X-ray spectrometer, using a Si(Li) crystal manufactured by ATOMKI and having an energy resolution 175 eV at Mn K-alpha. The EDS system was connected to a type JSM-35 scanning electron microscope. The incidence and the take-off angles were respectively 90 and 35 degrees. The nominal Be window thickness was 7.5 micrometers but because of a contamination build-up an effective value of 17 micrometers was measured at the time of analysis.

L-alpha1 line intensities were measured at 15 kV on polished high-purity metal samples for comparison with calculated values (Fig.2).

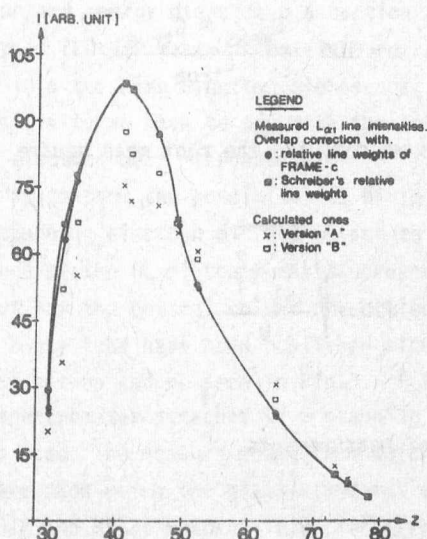


Fig.2

Comparison of measured and calculated L-alpha1 line intensities for pure elements as a function of atomic number (Z).

The two sets of intensities in Fig.2. originate from the same measured spectra. In one case they were processed by the original FRAME-C program, in the other case by a modified FRAME-C as standard spectra. The modified

version contained Schreiber and Wims' relative L-line intensities. The two kinds of data processing resulted in slightly different intensity values due to the overlap correction for other lines of the parent element.

Compound standards considered as "unknown" were also measured to test the overall analytical capabilities of each program. The samples examined were microanalytical standards from SY-LAB (anhydrite and orthoclase), from NBS (483:Si-Fe), garnet (YIG, YAG, GGG, $\text{Sm}_3\text{Fe}_5\text{O}_{12}$, $\text{Er}_3\text{Fe}_5\text{O}_{12}$, $\text{Ho}_3\text{Fe}_5\text{O}_{12}$, $\text{Yb}_3\text{Fe}_5\text{O}_{12}$, $\text{Ca}_3\text{Ga}_2\text{Ge}_3\text{O}_{12}$) and binary semiconductor (CdTe, ZnTe, ZnSe, GaAs, InAs, GaP) where the stoichiometry was accepted as a true value. Measurements were made at 10 and 15 kV accelerating voltages. For analysis we used only K and L lines in order not to mask error distribution with errors from the less well controlled M line analysis.

The relative error of the measurement is given as:

$$\epsilon = 100 \frac{C_{\text{meas}} - C_{\text{true}}}{C_{\text{true}}} \quad /1/$$

For 69 analysis results we computed the root mean square (RMS) of error as:

$$\text{RMS} = \sqrt{\frac{\sum_{i=1}^N \epsilon_i^2}{N}} \quad /2/$$

where N is the number of measurements.

d) Results

Measuring and computing the intensities of 12 elements in the $30 \leq Z \leq 78$ range, Fig.2. demonstrates a significant improvement in pure element intensity calculations in the whole region. The RMS was reduced from 23.5 to 13.1 % computed on the basis of these 12 analyses using the results of version "A" and "B" respectively.

During compound sample analyses, version "A" resulted in $\text{RMS}=15.2\%$ while version "B" improved this result to $\text{RMS}=8.5\%$. This improvement

indirectly supports the conclusions drawn from Fig.2; that the application of the new relative L-line weights by Schreiber and Wims improves the agreement between the measured and the calculated intensities.

We can conclude that the exchange of relative line intensities for new values improved the overall analytical capabilities of the method.

2. THE ATOMIC NUMBER DEPENDENCE OF THE X-RAY FLUORESCENCE ANALYSIS IN THE ELECTRON MICROSCOPE

Appart from some special cases when X-rays are utilized,^{5,6} in the electron microscope electron excitation is applied to chemical analysis. The use of X-ray excitation is justified by a lower background radiation and, as a consequence, by lower detection limits compared to electron excitation. Approximately 1000 ppm detection limits can be achieved by electron excitation and energy dispersive detection of X-rays. The X-ray fluorescence analysis (EDXRF) makes it possible for trace element analysis to be carried out in a scanning electron microscope; but for the gain in concentration sensitivity we have to pay with the loss of the good lateral resolution of the electron beam microanalysis.

Now, our aim is to show the possibilities of improving the detection limits (DL) in a scanning electron microscope and to demonstrate the atomic number dependence of the DL of the X-ray fluorescence analysis.

The details of how the optical column of an electron microscope can be converted to a X-ray tube have been published elsewhere^{7,8}. The scheme of the experimental set-up can be seen in Fig.3. A type EEDS-II energy dispersive X-ray spectrometer attached to a scanning electron microscope of type JSM 35 was used. The measurements, from which the detection limits were calculated were made using the glass standards of the National Bureau of Standards, No.612 and K1727 respectively. For X-ray sources Mo, GaAs, Ti and Al thin targets were applied and for each target we tried to find the optimum thickness and the optimum acceleration voltage for the microscope. The diameter of the exciting X-rays on the specimen surface was 6 mm. The count rates were about 5000 counts/s. The DL referring to 1000 livetime measurements (total time about 1300 s) were calculated⁹ according to equ. (3).

$$c_{\min} = \frac{2.33\sqrt{B} c_0}{|P-B|} \quad /3/$$

where P stands for peak height, B - background, and c - concentration of element in the standard.

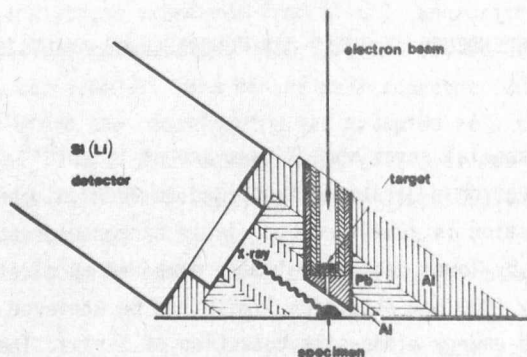


Fig.3

The scheme of attachment for X-ray fluorescence analysis in the scanning electron microscope

In order to achieve the optimum excitation condition for elements in different ranges of the atomic number, different target foils were applied. Mo target $100\ \mu\text{m}$ in thickness provided a DL between 1 and 7 weight ppm in the range $Z=26-38$ at an accelerating voltage of 35 kV for the microscope. (Fig.4). GaAs target $70\ \mu\text{m}$ in thickness irradiated at 25 kV ensured a DL from 1 to 12 ppm in the range $Z=22-29$. (Fig.5.) Ti foil $4\ \mu\text{m}$ in thickness proved to be effective at 15 kV for Ca and K analysis (DL=11.4 and 17.7 ppm respectively). (Fig.6.) Finally $7\ \mu\text{m}$ Al foil was the X-ray source for Na and Mg analysis at 12 kV. (Fig.7.). The DL's obtained were 29 and 14 ppm respectively.

Summarizing the results, (Fig.8.) it can be concluded that by means of X-ray fluorescence analysis the detection limits in the scanning electron microscope can be improved by 1 to 3 orders of magnitude, depending on the atomic numbers of the elements.

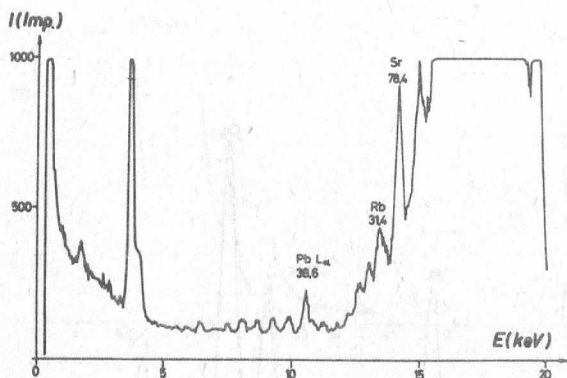


Fig.4

EDXRF spectrum of NBS 612 glass standard (MoK_α excitation, livetime 400 s)

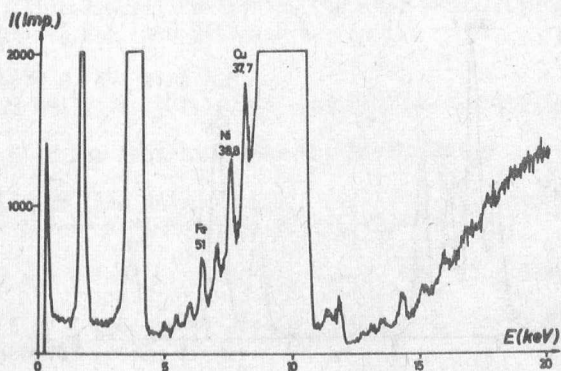


Fig.5

EDXRF spectrum of NBS 612 glass standard (GaAs excitation, livetime 400 s)

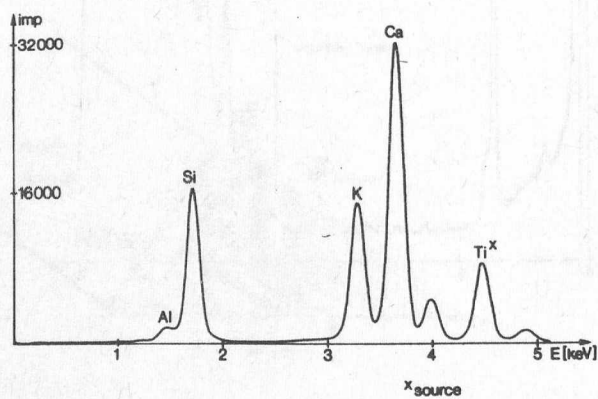


Fig.6
EDXRF spectrum of K1727 standard (TiK α excitation)

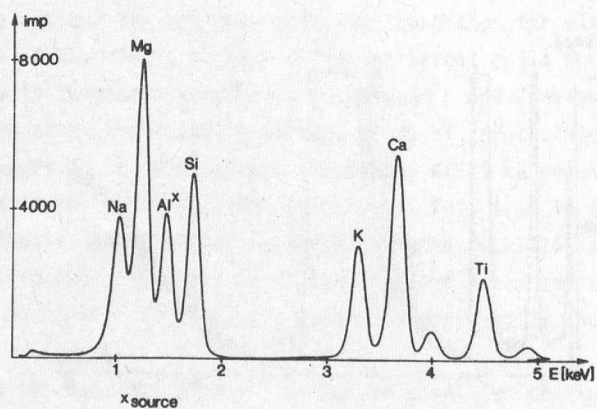


Fig.7
EDXRF spectrum of K1727 standard (AlK α excitation)

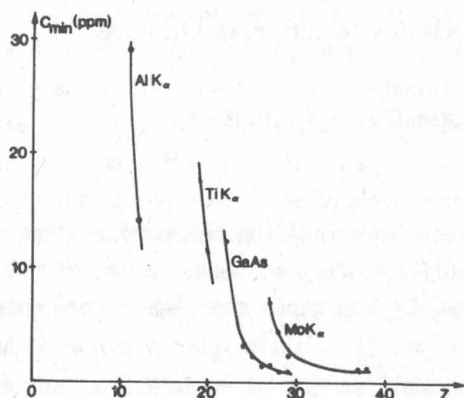


Fig.8

Atomic number dependence of the detection limits of EDXRF in the Z=11-40 range

REFERENCES

1. Heinrich K.F.J., Fiori C.E. and Myklebust R.L., J.Appl.Phys.50 (1979) p.5589
2. Myklebust R.L., Fiori C.E. and Heinrich K.F.J., NBS Technical Note 1106 (1979); also in NBS Special Publication 604 (1981) p.365; 8th Int.Conf.on X-ray Optics and Microanalysis, Boston (1977) p.116. Pendell Publishing Company, Midland (1980) (eds. Beaman D.R., Ogilvie R.E. and Wittry D.B.)
3. Schreiber T.P. and Wims A.M., Microbeam Analysis 1982. p.161. San Francisco Press (ed.Heinrich K.F.J)
4. Lábár J.L. to be published in X-Ray Spectrometry
5. Middleman L.M. and Geller J.D. Scanning Electron Microscopy, Vol.1. 171-177 (1976)
6. Linneman and Reimer L.: Scanning Vol.1. 109-117 (1978)
7. Pozsgai I.: 10th International Congress on Electron Microscopy, Hamburg Vol.1. 681-682 (1982)
8. Pozsgai I.: 8th European Congress on Electron Microscopy Budapest, Vol.1. 453-454. (1984)
9. Jenkins R., Gould R.W., Gedcke D.: Quantitative X-ray Spectrometry, Marcell Decker Inc. N.Y. 516. (1981)

GRAIN BOUNDARIES IN THIN METALLIC FILMS

G. Radnóczy and P.B. Barna

Grain boundaries (GB) develop during the coalescence stage of the film growth. As they form they influence further the processes of film growth and the final film structure. In this paper some aspects of these processes will be discussed.

THE EXPERIMENTS

Experiments were carried out on aluminium and gold films deposited in 10^{-4-5} Pa and 10^{-8} Pa respectively and onto NaCl, mica, Si single crystals, glass and amorphous carbon (a-C) substrates. The thickness of the Al films ranged between 10 -1000 nm and that of the Au films between 2-200 nm. The temperature of deposition for the Al was 200-400 °C, for Au 250-300 °C. The films were investigated using JEM 100U and JEM 100CX electron microscopes. Thick films of Al were thinned by ion beam milling from their substrate side in order to preserve their surface morphology².

The surface morphology of the films was investigated using both the Pt shadowing method and the dark field image thickness contour method³.

THE FORMATION OF GRAIN BOUNDARIES

The processes taking place during the film formation and controlling the formation of GB's were discussed in detail in Ref.4. It can be concluded that GB's form during solid state coalescence and that their orientation distribution is determined by selection processes such as nucleation, coalescence and either grain growth or recrystallization in the films⁴.

Examples of the selection processes and their importance are shown in Figs. 1. and 2. Fig.1. shows Au films deposited onto NaCl and a-C substrates. The deposition was carried out on a single crystal of NaCl, half of which had been covered by a-C. The temperature of deposition was 300 °C. The number of grains on air-cleaved NaCl is almost one order of magnitude lower

than that on a-C (10^9 and 10^{10} mm^{-2} resp.) The reason for this difference may possibly be the different density of nucleation sites on the two substrates, the different mobility of the islands on the substrates, and/or the differences in adsorption energies. The orientation distribution of crystallites is also different on the two substrates. On NaCl a well pronounced $\langle 111 \rangle$ texture with many twin positioned and $30^\circ/[111]$ misoriented particles were detected. The presence of these orientations is indicated by the appearance of a $1/3 \{422\}$ ring⁵ in the diffraction pattern and its 12-fold symmetry (Fig.1.a). This ring is missing from the diffraction pattern of the Au film, deposited onto a-C (Fig.1.b.), where the crystals are randomly oriented and no selection took place until the growth stage. The selection resulting in the texture shown in Fig.1.a took place at the nucleation stage and was preserved during coalescence on NaCl. In Fig.2 the decrease of the number of individual grains with film thickness is shown for Al films. In the thickness range 10- 80 nm the number of grains decreases nearly five times, so a large selection of orientations should take place during coalescence and grain growth.

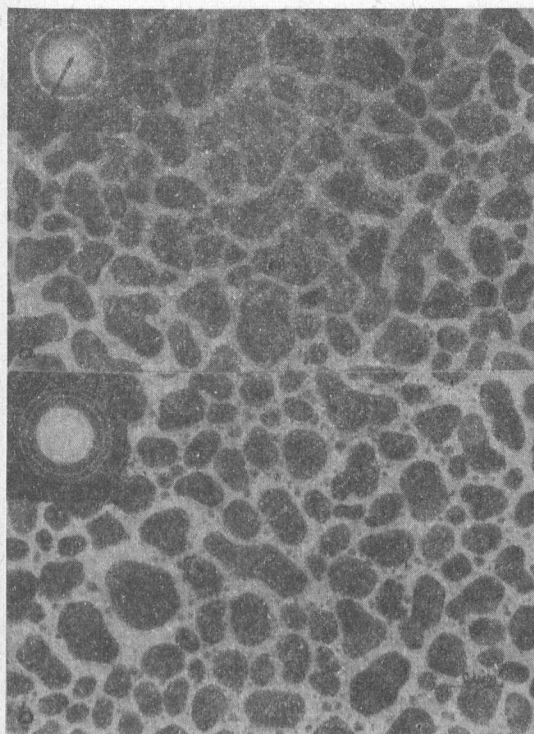


Fig.1

10 nm Au films deposited simultaneously in UHV (10^{-7} Pa) onto air cleaved NaCl (a) and amorphous carbon (b) substrates.

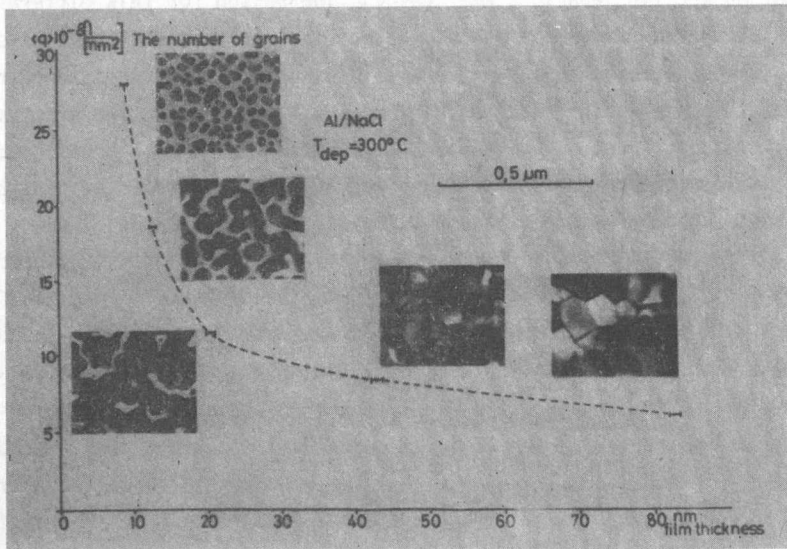


Fig.2

The dependence of the number of grains on the film thickness in Al films deposited in 10^{-5} Pa. Inserts show the type of structure at the thicknesses where measurements have been made.

THE INFLUENCE OF GB-PROCESSES ON THE STRUCTURE OF THE FILMS

Columnar structure, grain size, GB-morphology

The coalescence stage is one of the most important stages during the film formation. It is strongly influenced by the lateral face of coalescing particles. When this surface is covered by impurities the coalescence is hindered⁶ and the lateral growth of grains by GB movement is stopped at a certain stage. Grains can grow further only on their top surface. This kind of growth mechanism leads to a columnar structure. This can be realised under various deposition conditions. Inhibition of GB movements, leading to columnar structure, can be achieved also by varying the deposition parameters like deposition temperature, deposition rate and the nature of the substrate in pure as well as alloyed films⁷.

When the growth is also restricted on the top surface of grains, secondary nucleation takes place and new grains form on the surface^{6,8}.

Globular, fine grained structures can be formed in this way. The GB's of such systems are usually saturated by impurity atoms and even foreign phases can be present on them. In the case of Al, oxygen is very effective in blocking GB movement and crystal growth by forming oxide particles or a continuous oxide layer⁹.

GB's developed in the coalescence stage can play a different role in further growth processes depending on their purity. Pure GB's serve as sources for growth steps. In this case growth steps move from the GB into the grain area¹⁰. Oxide particles formed on the growing surface in the case of Al films pin these growth steps. This process leads to the formation of growth hills above the GB¹⁰. However GB's covered by impurities can also act as sinks for further impurity atoms. Growth steps cannot be generated at these GB's, they are nucleated in the grain surface area and sweep the impurities to the GB. Accumulation of impurities can develop and cover the GB, extending also to the surfaces of adjacent crystals. The movement of growth steps is stopped near to the GB if the surface coverage of impurities becomes continuous^{8,10}. Deep grooves form at the GB in this case.

The impurity content of a film surface depends not only on the vacuum conditions, but also on the adsorption properties of the substrate surface. Al films were deposited simultaneously onto NaCl, mica and glass substrates. The surface topography of the films is shown in Fig.3. On glass we find deep grooves, while on NaCl there are hills at the GB's. The smoothest surface is on mica although both hills and grooves are present.

In thin films GB's form an anisotropic network. The majority of GB's in pure films are parallel to the film normal. Faceting of GB's is characteristic for FCC metal films^{4,5,11}. Faceting takes place in planes both parallel and perpendicular to the film plane^{4,5}. Kinks and ledges are often observed as well. Many special misorientations are present^{4,11}, twin and $30^\circ/[111]$ misorientations being dominant in $\langle 111 \rangle$ textured films of FCC metals^{4,11}.

Experiments on the Au/NaCl system presented evidence that twin GB's can also form during the growth of individual crystals. Twinning can result from growth accidents or substrates effects. The formation of small crystallites showing fivefold or sixfold symmetry can be attributed to this mechanism.



Fig.3

Surface morphology of Al films (300°C , $1.2\text{ }\mu\text{m}$, 10^{-4} Pa) shown on C-Pt replica. Films were deposited simultaneously onto glass (a), mica (b) and NaCl (c). The arrows mark the shadowing direction.

The formation of dislocations and their interaction with the GB

During their growth thin films are usually free from dislocations until coalescence starts. During the coalescence of slightly misoriented crystals, dislocation walls will be created while separate dislocations form during the filling of channels and holes¹³. Dislocations can also originate from the deformation of the film due to the differences in thermal expansion, between the film and substrate, and of misfit dislocation formation.

Dislocations moving in the film interact with the GB's and, in case of large grains, with one or both film surfaces. From slip trace analysis one can establish that most of the dislocations are generated at the GB and move from GB to GB¹⁴. GB's can emit and also capture dislocations, which can become an integral part of the appropriate GB structure by dissociating to internal GB dislocations^{14,15,16}.

There is a special kind of interaction between dislocations and GB's with a GB growth hill. In this case dislocations do not cut the hill but leave a dislocation segment under the hill when approaching the GB¹⁴. The segments under the hill are mobile and can slip. As dislocations from different slip systems leave segments under the hill, dislocation walls and networks can be formed. Consequently the hill will be separated from its host crystal by a small angle boundary. Similar dislocation movement can also be expected to result at curved internal surfaces and especially at faceted GB's.

Displacement of the GB

One can find in many cases that the surface growth morphology does not fit the actual position of the GB. A typical example of this is the displacement of a GB from its surface hill discussed in Ref.17. The usual displacement distance of a GB is $0.1 \mu\text{m}$, taking place after finishing the deposition and during the cooling of the specimen. Movements of larger distances though can take place during the deposition process.

SUMMARY

The GB plays an active role in film formation processes, defect structure formation and in the associated impurity effects.

The developing structure of the film and its stability depend on GB mobility which in turn is influenced by the structure and impurity content of the GB.

The interaction of the GB with dislocations and surface irregularities results in the appearance of new elements in the film structure. Dislocation and GB segments under the growth hills and impurities on grooved GB's lead to an increase in defect density near the GB's. The density of defects near to and in the GB's affect both the properties and the stability of GB's.

REFERENCES

1. R.B.Labibiwitz, A.N.Broers
in Treatise on Mat.Sci.and Technology, ed.by K.N.Tu and R.Rosenberg,
Vol.24 p.285 (1982)
2. A.Barna
in Proc.of 8th EUREM, Budapest, Vol.1. p.107 (1984)
3. M.Yose-Yacaman, T.Ocana
phys.stat.sol. (a) 42 571 (1977)
4. G.Radnóczy
in Proc.of 8th EUREM, Budapest, Vol.2 p.1229, (1984)
5. D.W.Pashley, M.J.Stowell
Phil.Mag 8 1605 (1963)
6. J.F.Pocza, A.Barna, P.B.Barna, I.Pozsgai, G.Radnóczy
Jap.J.of Appl.Phys. Suppl.2. Part 1. p.525 (1974)
7. C.R.M.Grovenor, H.T.Hentzell, D.A.Smith
Acta Met. 32 773 (1984)
8. P.B.Barna
in Proc.of 9th Vacuum Congr.Madrid, p.382 (1983)
9. F.M.Reicha, P.B.Barna
Acta Phys.Acad.Scient.Hung. 49 237 (1980)
10. P.B.Barna, G.Radnóczy, F.M.Reicha
Thin Solid Films (in press)
11. V.M.Ievlev, V.S.Postnikov, S.B.Kushev, K.S. Solovjov
FMM 42 915 (1967)
12. M.H.Jacobs, D.W.Pashley, M.J.Stowell
Phil.Mag. 13 29 (1966)
13. J.W.Matthews
Phil.Mag. 7 915 (1962)
14. G.Radnóczy, P.B.Barna
Journal de Physique 46 429 (1985)
15. P.H.Pumphrey, H.Gleiter
Phil.Mag. 30 593 (1974)
16. R.Z.Valiev, V.Zu. Gertsman, O.A.Kaibyshev, Sh.Kh.Khannanov
phys.stat.sol.(a) 77 97 (1983)
17. G.Radnóczy, P.B.Barna, A.Barna
in Proc.of 8th EUREM, Budapest, Vol.2. p.1241 (1984)

INVESTIGATION OF EBIC DISLOCATION CONTRAST AS A FUNCTION OF SEM PARAMETERS

A.L. Tóth

1. INTRODUCTION

From a simple imaging device the SEM became a complex instrument capable of making localized chemical and physical measurements on a nanometer scale. The need therefore of a quantitative understanding of its contrasting mechanisms became more and more important. In the signal forming process the localized electron beam together with the other non-localized parameters of the sample environment (temperature, electric field, etc.) , acts as a stimulus on the sample, generating the response signal, which is determined by them and the local properties of the sample. The usual method of measurement is to keep the excitation constant, and knowing the physical details of contrast formation, try to find out the unknown material properties from the quantitative evaluation of the response.

In our case the aim of a typical measurement was to establish a relationship between the EBIC contrast and the geometrical or physical properties of electrically active crystal defects. However, to clear the details of single defect characterization, we found it worthy to examine the influence of various experimental parameters on the EBIC dislocation contrast. In this type of measurements we vary the parameters of the stimulus on a given sample, and try to find out the details of signal formation. In this way we can set the limits of different measuring techniques, and obtain new information about the contrast forming process.

After measuring the effect of beam energy on dislocation contrast and resolution (Toth 1981), supporting the calculations of Donolato (1979), the next parameter to be investigated was the sample bias. This paper describes the change of EBIC dislocation contrast as a function of sample bias and beam current, and distinguishes its components of different origin.

2. EXPERIMENTAL

2.1. Samples and excitation

The samples were Schottky barrier diodes with Al metallization 0.3 mm in diameter and 100 nm in thickness on As doped Si substrate $N = 5 \times 10^{14}/\text{cm}^3$ with a dislocation density of $5000/\text{cm}^2$. The measurements were carried out in a JSM35 type SEM with 25 keV beam energy and 1-20 nA beam current (measured on Faraday cage). Accepting the Gruen range of Everhart and Hoff (1971) as a diameter of a uniformly generated sphere and substituting this value into Berz and Kuiken's expression (1976) for maximum generated minority carrier concentration, we obtain

$$P_{\text{max}} (25 \text{ keV}, 10 \text{ nA}) = 8.6 \times 10^{15}/\text{cm}^3$$

which shows high injection as compared to the doping level. The Debye length, the lower limit of plasma dimension, is $0.2 \mu\text{m}$; less than the typical depletion layer width $W(4V) = 3 \mu\text{m}$ and electron range $R(25 \text{ keV}) = 5 \mu\text{m}$. As the distribution of the electric field in barrier depletion layers always contains a weak field region, the occurrence of plasma effect can be expected (Leamy et al 1978).

2.2. Apparatus

To measure the dislocation contrast as a function of bias, a phase sensitive computer controlled data acquisition and reduction system was used (Labar et al 1983). (Fig.1).

The detector was a calibrated fast current amplifier (Keithley 427) used as a preamplifier of a phase sensitive (lock-in) amplifier (Keithley Autoloc, or Ortec Ortholoc with preamp. for high frequency measurement). The lock-in amplifier (PSD) separated the DC diode current due to the bias and the AC EBIC signal modulated by the chopped beam (generally 10 kc/s frequency, 50% duty cycle).

The EBIC signal was digitized by a voltage-to-frequency converter (VFC) and fed into the multichannel analyser (MCA) memory of an energy dispersive X-ray analyser system (Ortec EEDS-II), where it was treated as the pulses of the original X-ray detector.

The EDS system has been modified, both in hardware and software, to provide the possibility of stepwise digital line scan measurement with SEM

control commands between two steps. EBIC intensity measurements become possible as a function of the following computer controllable experimental parameters:

- beam X-Y position by digital scan generator (DSG),
- sample movement (SSD),
- sample bias,
- objective lens focus/defocus,

using digital-to-analog converters (DAC).

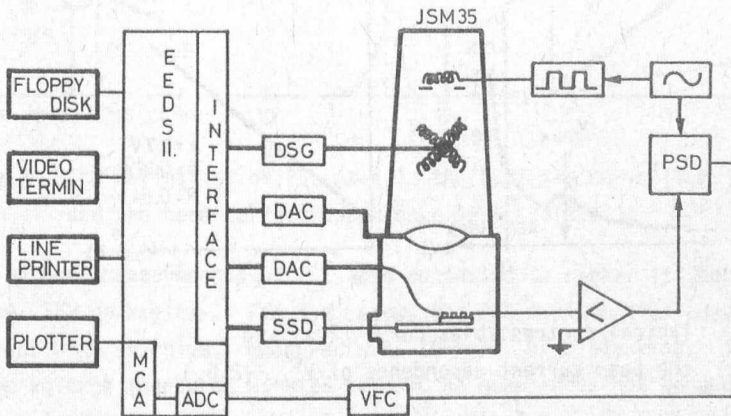


Fig.1 Block diagram of the system.

3. RESULTS

3.1. Dislocation contrast measurements

The dislocations to be measured were perpendicular to the surface, localized and checked on the conventional (unbiased DC) EBIC image.

The contrast was then measured as the relative difference of the EBIC intensity on the dislocation and on a reference area free of dislocations, $C = (I_{ref} - I_{disl}) / I_{ref}$ while the bias was changed from 9 V reverse to 1 V forward.

The contrast/bias curve has 3 components as shown in Fig.2 :

- A: a constant level observable at high reverse bias,
- B: an increasing part as approaching the forward bias,
- C: a maximum at V_{\max}^C

The V_{\max}^C bias is dependent on the beam current (i.e. on the generated excess charge carrier concentration) linearly, (Fig.2.b)

$$V_{\max}^C [\text{V}] = 0.7 + 0.16 \cdot i_0 [\text{nA}]$$

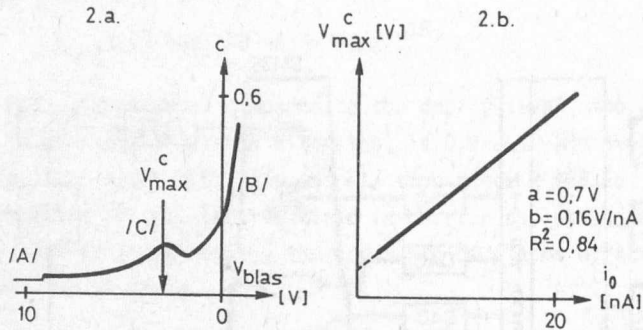


Fig.2 Typical contrast/bias curve (2.a) and the beam current dependence of V_{\max}^C (2.b.)

3.2. Plasma loss measurements

A possible hypothesis for the contrast maximum is the enhanced recombination inside an electron-hole plasma droplet free from a collecting electric field due to its polarisation at the edges.

To prove the plasma nature, the plasma loss (PLL) i.e. the relative difference of EBIC intensities generated by focused and defocused beam $PLL = (I_{DF} - I_F) / I_{DF}$, was measured simultaneously with the contrast measurement by computer controlled defocusing of the beam above the dislocation free area. (Fig.3.a).

As the plasma exists only under high current density, the enhanced bulk recombination measured with focused beam shows its presence. (Fig.3.b)

The linear relationship (Fig.3.c.) of the $V_{\text{max}}^{\text{PLL}}$ position of PLL maximum and the beam current is:

$$V_{\text{max}}^{\text{PLL}} [\text{V}] = 0.07 + 0.16 * i_0 [\text{nA}],$$

which shows a good agreement with the C component of the contrast/bias curve.

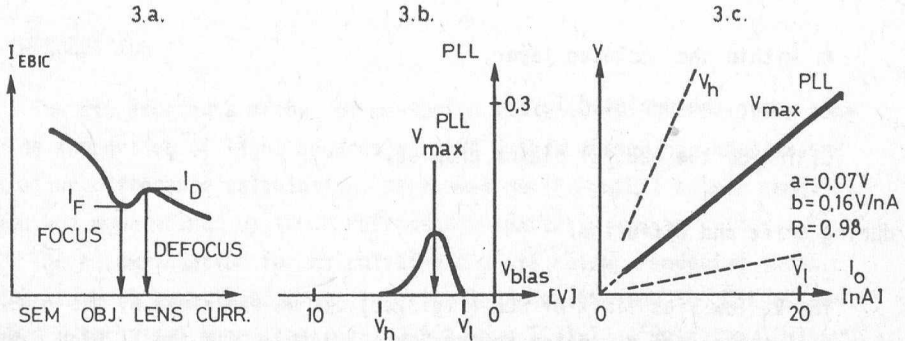


Fig.3 The definition of PLL (3.a.), the PLL/bias curve (3.b.) and the beam current dependence of $V_{\text{max}}^{\text{PLL}}$ (3.c.).

Further, measurements of PLL were conducted to clear its dependence on other SEM parameters. Fig.4.a. shows the PLL maximum/bias curves at 3 different beam energies, measured with 10 kc/s beam blanking. The PLL maximum voltage (measured with 25 keV, 10 nA beam) does not depend on beam blanking in the frequency range 1-100 kc/s (Fig.4.b.).

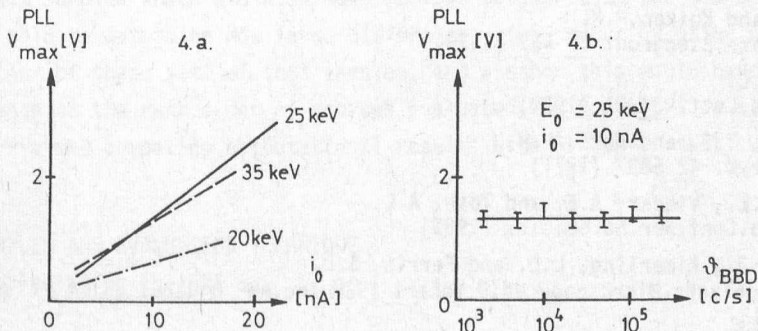


Fig.4 The beam energy (4.a.) and BBD frequency (4.b.) dependence of $V_{\text{max}}^{\text{PLL}}$.

4. CONCLUSION

As the plasma loss and the maximum in the dislocation contrast occur nearly at the same bias, and show the same beam current dependence, the components of the contrast/bias curve can be explained by recombination at the defect:

A: within the depleted layer,

B: under the depleted layer,

C: inside the neutral plasma droplet,

during drift and diffusion.

The V_l low bias limit of PLL (Fig.3.c.) can be explained by the approach of the plasma dimension to the Debye length, while the V_h high bias limit shows qualitative agreement with the predictions (i.e. linear dependence on beam current) of Tove & Seibt (1967) model for plasma erosion.

REFERENCES

- Berz, F. and Kuiken, H.K.
Solid State Electron. 19 437 (1976)
- Donolato, C.
Appl. Phys. Lett. 34 81 (1979)
- Everhart, T.E. and Hoff, P.H.
J. Appl. Phys. 42 5837 (1971)
- Labar, J.L., Vladar, A.E. and Toth, A.L.
Inst. Phys. Conf. Ser. No. 68. 181 (1983)
- Leamy, H.J., Kimerling, L.C. and Ferris, S.D.
Scanning Electr. Microscopy ed. O. Yohari (SEM Inc. AMF O'Hare) Vol. 1, 717 (1978)
- Toth, A.L.
Inst. Phys. Conf. Ser. No. 60, 221 (1981)
- Tove, P.A. and Seibt, W.
Nucl. Instr. and Meth. 51 261 (1967)

THE INFLUENCE OF THE TEST SAMPLES USED FOR CALCULATING COLOUR RENDERING INDICES

J. Schanda

1. INTRODUCTION

The CIE adopted a method of measuring and specifying the colour rendering properties of light sources in 1974¹. This method has been based on colour difference calculations performed on 14 Munsell colour samples, which are now defined by their reflectance spectra.

The recommendation for calculating the CIE colour rendering index (CRI) has been questioned ever since its introduction and the CIE established a technical committee (old TC-3.2, now TC 1-12, 'Relative Colour Rendering') to elaborate some revised suggestions^{2,3}. To be able to conduct visual experiments, test samples comparable to the original ones are needed.

However, the original Munsell samples are no longer available; some have been replaced by samples prepared with new pigments (these might be metameric) and some do not appear in the collection of samples presently distributed.

During the past years several institutions developed colour rendering test samples which are also more or less metameric to the CIE ones. To be able to determine how large differences could occur by using one or the other of these sets of test samples, and whether this would have an influence on the rank order of sources evaluated for their CRI, a study was performed comparing computational results with 5 sets of test samples.

2. SAMPLES AND EVALUATION TECHNIQUE

2.1. Calculating the CRI

The CIE test method for determining CRI has several drawbacks⁴: It is based on an outdated colour difference equation, uses a probably not too accurate formula for taking care of chromatic adaptation and is based on

reference illuminants of equal correlated colour temperature as that of the test source, a questionable concept.

Due to all these reasons, for the present study a modified CRI calculation method was used with only three reference illuminants: CIE Illuminant A, corresponding well to 'social lighting' requirements (incandescent lamps, warm white fluorescent tubes, etc.); a Planckian radiator with a colour temperature of 4300K (P 4300), which is felt to be an appropriate reference for lighting situations as needed in daylight supplementing; and CIE Illuminant D65, for artificial daylight simulating situations.

For only three reference illuminants larger differences in test and reference illuminant chromaticity have to be bridged, as for reference illuminants with equal correlated colour temperature. Therefore a nonlinear chromatic adaptation formula has been used⁵.

As the colour rendering calculation is based on the evaluation of surface colour differences, the CIELAB colour difference formula was incorporated into the present method.

Copies of the description of the recommended method are available from the author.

2.2. Test samples

Five sets of test samples were taken into consideration in this investigation:

- The CIE Test Samples as specified in CIE Publ.13.2.
- Test samples according to the DIN 6169 standard.
- Munsell samples with the same notation as presented in the CIE Recommendation, or samples most similar to these from a set received in 1980.
- The first 14 of the Japanese CRI samples*⁶.
- Colour samples selected from the Hungarian Coloroid colour order system, which are most similar in colour appearance to the CIE Test Samples.

*The author is indebted to Dr. Mori, who kindly supplied him with these samples.

For the first two sets reflectance spectra were taken from the literature^{1,7}, for the other three they were determined in $d/80^\circ$ measuring geometry, specular component excluded.

Colour differences were calculated for the four existing sets of test samples relative to the CIE Test Samples both for CIE Illuminant A and D65. Table 1 summarizes these results. As can be seen some of the samples deviate from the official test samples considerably. The deviations are not, however, prohibitively large for using the samples for CRI calculations (see e.g. Ref.8.).

2.3. Test illuminants

Three groups of fluorescent tubes were used in the present study, supplemented by a few high pressure discharge lamps:

- warm white fluorescent lamps of different colour rendering properties and a high pressure sodium lamp,
- medium colour temperature (neutral or cool white) fluorescent lamps and two high pressure discharge lamps (a mercury and a metal halide one),
- three high colour temperature (cool-daylight) fluorescent lamps.

Table 2 summarizes the correlated colour temperature and the traditional general colour rendering indices (R_a) of these lamps.

3. RESULTS

Table 3 presents the summary of our investigations. For every lamp the revised general colour rendering indices (R_a) are shown for the three reference illuminants and the five sets of test samples.

A general feature of all such calculations can be seen: A reference illuminant with higher correlated colour temperature then would correspond to the chromaticity of the test lamps provides a higher index. This changes only for lamps of good colour quality (this problem will be discussed in a later paper).

Analysing the results of the first group of lamps (warm colours), it is seen that for all lamps with the Japanese and the Munsell samples now available, higher R_a^* values are obtained than with the other sets of test

Table 1. Colour differences of the different sample sets related to the CIE Test Samples for Illuminant D65 and A.

Sample No	Illuminant	DIN	Munsell	Japanese	Coloroid
1	D 65	0,81	4,00	2,95	1,71
	CIE A	0,84	5,32	3,36	1,99
2	D 65	0,98	5,40	7,52	1,85
	CIE A	0,75	5,93	8,07	1,85
3	D 65	1,87	2,38	4,21	2,34
	CIE A	1,60	4,24	4,24	1,79
4	D 65	0,88	6,19	7,38	2,82
	CIE A	0,71	4,41	4,62	1,70
5	D 65	0,60	2,14	2,06	1,57
	CIE A	0,65	2,27	2,06	1,52
6	D65	1,15	2,98	5,00	1,90
	CIE A	1,38	2,98	5,22	1,87
7	D 65	0,53	4,53	2,78	2,65
	CIE A	0,59	3,73	2,62	2,18
8	D 65	0,74	1,53	0,99	2,11
	CIE A	0,69	2,54	0,86	2,83
9	D 65	5,46	10,75	12,18	7,22
	CIE A	5,48	11,47	11,31	6,58
10	D 65	1,11	7,57	16,5	3,17
	CIE A	1,36	6,44	16,1	2,40
11	D 65	2,56	7,11	8,58	2,62
	CIE A	3,39	4,37	3,76	0,80
12	D 65	7,64	13,11	15,75	18,59
	CIE A	10,63	16,66	23,95	26,89
13	D 65	1,01	2,13	4,80	1,72
	CIE A	1,09	2,79	5,26	1,79
14	D 65	5,42	8,77	4,65	2,73
	CIE A	4,57	7,94	4,67	2,84

Table 2. Correlated colour temperature and Ra of the illuminants used

Test ill.	Tc	Ra	Test ill.	Tc	Ra
Warm	2950	51,6	Natural	4070	83,0
Warm W	3070	51,0	Kolor R	4100	90,2
Warm Sp	2930	79,8	Kollux	4060	36,0
Warm Trib.	2990	81,8	TL 84	4050	81,3
HP-Sodium	1960	27,7	Cool Dayl.	6370	74,6
Neutral	4200	61,0	Art. Dayl.	6500	90,0
White	4170	65,0	TL 86	6160	80,0

Table 3. Ra* values with different test samples

Test ill.	Ref.ill.	CIE	DIN	Munsell	Japanese	Coloroid
Warm	CIE A	45.7	44.8	51.8	53.8	46.2
	P 4300	64.6	67.9	64.0	68.9	63.5
	D 65	57.9	62.0	54.8	61.4	55.1
Warm W	CIE A	49.3	49.8	55.9	56.9	50.9
	P 4300	66.1	63.4	63.1	67.5	62.0
	D 65	60.1	56.7	54.0	60.6	53.5
Warm Sp.	CIE A	66.3	67.5	70.7	72.4	67.4
	P 4300	75.4	75.2	70.2	76.4	72.9
	D 65	59.9	59.9	53.8	60.1	58.2
Warm Trib.	CIE A	70.9	69.9	74.5	76.0	74.0
	P 4300	73.1	71.6	66.0	71.5	71.2
	D 65	54.8	55.0	47.1	53.7	54.2
HP Sodium	CIE A	36.6	32.0	32.9	34.7	34.4
	P 4300	19.4	14.8	16.6	18.5	13.9
	D 65	11.3	6.8	9.1	11.4	3.8
Neutral	CIE A	27.1	28.8	34.6	35.7	28.8
	P 4300	64.8	64.5	69.2	69.1	65.2
	D 65	72.6	70.7	71.5	74.5	69.9
White	CIE A	31.7	33.2	38.4	39.6	33.5
	P 4300	69.2	68.7	79.2	72.8	69.6
	D 65	74.8	72.9	73.6	76.4	72.1
Natural	CIE A	35.8	37.9	41.3	44.0	36.6
	P 4300	80.6	80.4	82.4	83.7	80.6
	D 65	82.9	81.6	79.5	82.0	80.6
Kolorr.	CIE A	32.5	34.6	38.2	41.8	34.0
	P 4300	77.9	78.7	80.0	82.0	79.2
	D 65	76.7	76.8	75.4	78.0	77.3
Kollux	CIE A	5.4	8.7	17.8	18.7	8.0
	P 4300	41.5	42.1	48.0	48.6	41.4
	D 65	52.7	51.6	52.7	56.5	49.4
TL 84	CIE A	15.6	17.3	21.6	25.9	15.8
	P 4300	62.9	61.5	62.6	65.3	62.7
	D 65	68.1	66.8	64.6	66.4	67.3
F 7	CIE A	13.9	16.1	19.2	22.3	15.2
	P 4300	60.0	60.4	63.5	63.6	61.8
	D 65	78.1	77.9	80.8	80.5	78.6
Art.Dayl.	CIE A	20.1	22.3	23.8	27.6	19.5
	P 4300	72.3	73.0	73.6	74.6	72.3
	D 65	90.5	91.0	91.1	92.0	91.1
TL 86	CIE A	14.2	15.3	19.3	21.7	14.1
	P 4300	62.6	60.8	64.7	65.1	62.5
	D 65	79.6	76.3	77.9	78.5	77.8

samples. It is also interesting to note that for the CIE and DIN Test Samples the P 4300 reference illuminant provides higher R_a^* values than the CIE A illuminant. Not so for the Munsell and Japanese test samples for lamps of better colour quality. A difference produced mainly by a difference in the red samples.

For the medium colour temperature group the rank order of the CIE R_a and the present R_a^* (P 4300) is markedly different. This group would be well suited for testing the different formulae.

For the high colour temperature group the rank order based on R_a and $R_a^*(D65)$ calculated with the CIE Test Samples is the same, but changes for all the other test samples.

4. CONCLUSIONS

The model calculations have shown that the available sets of test samples do not produce the same results as the CIE Test Samples. The differences are low enough to permit the use of such samples in visual experiments. Caution is needed, however, with cases of samples where the colour difference produced by using the test lamp and the reference illuminant is large.

ACKNOWLEDGEMENT

The author is indebted to Mrs. A. Kovács for her kind help in determining the reflectance spectra of the three sets of material samples used in this experiment.

REFERENCES

1. CIE Publ. 13.2 (TC-3.2) Method of measuring and specifying colour rendering properties of light sources, (1974)
2. Halstead, M.B.
TC-3.2 Colour rendering report. Light and Lighting'83,
Proc. CIE 20th Session, Amsterdam, C3/14-15, (1983)
3. Bodmann, H.W.
Report on Division 1 Meeting, Vision and Colour, ibid C9/1-3.
4. Schanda, J.
Chromatic adaptation and colour rendering, CIE-Journal, 1/2, 30-37,
(1982)
5. Takahama, K., Sobagaki, H., Nayatani, Y.
Formulation of a nonlinear model of chromatic adaptation for a light-
gray background.
COLOR Res. & Appl., 9/2, 106-115, (1984)
6. Color charts for color rendering evaluation.
The Illuminating Engineering Institute of Japan, (1978)
7. Döring, G.
Aufsichtstestfarben zur meßtechn. Kennzeichnung der Farbwiedergabeeigen-
schaften von Farbproduktionsprozessen.
Farb-Info'84, Freiburg. (1984)
8. Opstelten, J.J.
The dependence of the general colour rendering index on the set of test
colours; the standard observer and the colour-difference formula.
Light Res. & Techn. 12/4, 186-194, (1980)

THERMAL DISSOCIATION OF InP COVERED WITH METALLIC CONTACT LAYERS

I. Mojzes , R. Veresegyházy , V. Malina**

1. INTRODUCTION

InP is one of the III-V compound semiconductors which is widely used for the fabrication of microwave and optoelectronic devices. This broad field of application requires the reliable contacting of both n- and p-type structures. To obtain reliable, low resistance ohmic contacts to InP devices mainly gold-based metallization systems, with suitable donors and acceptors, have been extensively studied. Technical practice has shown however, that the preparation of good ohmic contacts is still a great problem, especially when the requirements are high (for example, when the doping level of the material is low or when a device should work safely at high current densities).

Understanding of contact formation is impossible without taking into account the chemical and metallurgical reactions which take place at the semiconductor-metallization interface during the heat treatment of contacts. In the case of III-V compound semiconductors these reactions are usually accompanied by the evolution of volatile components (i.e. phosphorus for InP).

Various sophisticated analytical techniques, like the RBS^{1,2}, AES^{3,4}, SIMS⁵, ESCA^{6,7} and X-ray analysis^{8,9} have been used for the examination of these processes, the results obtained usually being completed with TEM, SEM and HVEM¹⁰ investigations to get some information about the surface morphology.

In this study the volatile component loss during the heat treatment of metallized InP samples has been examined. Such investigations were carried out previously for GaAs^{11,12,13,14,15,16,17}, GaP^{12,15} and GaAlAs¹³. Some

**Institute of Radio Engineering and Electronics
Czechoslovak Academy of Sciences,
Lumumbova 1, 182 51 Praha 8, Czechoslovakia

preliminary results obtained in our laboratory for Au-based InP systems were also published in short form^{18,19}. The interaction between zinc metallization and InP was also investigated using this technique²⁰. Application of this method - called Evolved Gas Analysis (EGA) technique²¹ - proved to be a very powerful tool for the investigation of contact formation leading to better understanding of processes taking place during the contact technology.

The differences between the EGA investigation and the classical studies concerning the thermal decomposition of compound semiconductors are that in the latter case most of the specimens were in powder form; the stationary processes and non-metallized semiconductors were studied in previous works²²⁻²⁷. In contrast to the classical studies the EGA technique uses single crystals or epitaxially layered structures covered with a thin metallic layer, the dynamic processes (similar to contact formation) with high heating and cooling rates being investigated in situ.

In the course of the present work, InP samples coated with gold, silver, nickel and the most widely used ohmic contact materials have been studied in non-equilibrium conditions. The thermal decomposition of the InP covered with these metallizations was found to be different for various metal systems and it depended also on their thickness. To obtain useful technological recommendations for the preparation of reliable ohmic contacts to InP, the dependence of observed phenomena on substrate orientation, conduction type and contact thickness was examined. An attempt has also been made to explain the processes leading to the volatile component loss.

2. EXPERIMENTAL

2.1. Experimental setup

The system used was capable of mass spectrometrically analyzing the volatile component loss by compound semiconductors heated in a vacuum in the temperature range of 100 to 700 °C. The constant heating rate of 150 °C/min was used in all experiments and measurements were made in the pressure range of 10^{-4} - 10^{-5} Pa. Fig.1 shows the block diagram of our apparatus. The sample holder and the measuring chamber were described in Ref.17. The oil-free vacuum was generated by an ion-getter pump with a relatively constant pumping rate. Note the liquid nitrogen cooling of the measuring chamber walls. The output of the mass spectrometer was connected to the

peak selector, so it was possible to monitor simultaneously the yields of various species. In the case of InP; P_1 , P_2 , P_3 , P_4 and In were measured and in some cases P_5 ; other constituents of the contact being also checked at the same time. The output signals of the peak selector were connected to the data collection system and were measured sequentially after amplification with a logarithmic amplifier. Through an A/D converter the data were transferred to the perforator for the subsequent computer analysis and plotting.

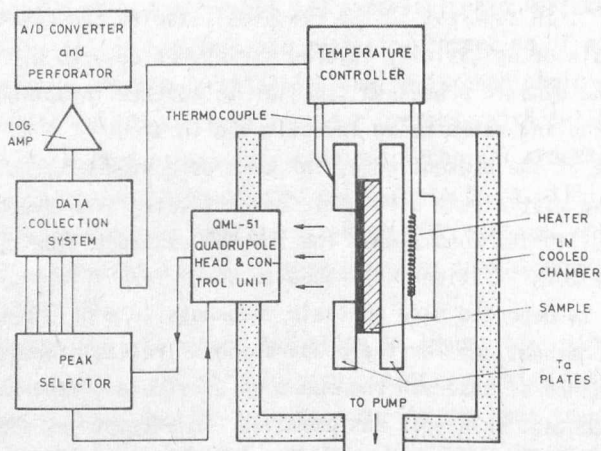


Fig.1 The experimental setup

2.2. Sample preparation

The material used for experiments was LEC pulled (100), (111) InP:Sn and (100), (111) InP:Zn with carrier concentrations of $8 \cdot 10^{16} \text{ cm}^{-3}$ and 10^{18} cm^{-3} , respectively. InP slices with a thickness of about $400 \mu\text{m}$ were mechanically and chemically polished and immediately prior to mounting into the evaporator they were cleaned using the "TAM technique" described in Ref.28.

Two kinds of samples were investigated in this work. So called Type 1 samples were evaporated a few months before the measurements ("old" samples); Type 2 samples were metallized a few days before the measurements

("new" samples). The metallization of InP slices was carried out in a liquid nitrogen trapped oil-diffusion pumped high vacuum coating unit with a normal base pressure of about 10^{-5} Pa. The metallizations investigated, such as Au, Ag, Ni, Au/In, Au/Ga, AuGe (Ge 12 wt.%), AuGe/Ni and AuBe (Be 1 wt.%) were deposited by thermal evaporation onto one side of the InP slices; a pressure of about 1×10^{-4} Pa and a substrate temperature of 170 °C were maintained during the evaporation.

3. RESULTS

It can be seen, from Fig.2, that different metallizations have drastically different effects on the decomposition of the InP substrate. In the case of uncovered InP samples, the decomposition at temperatures below 550 °C is very low and the phosphorus yield is lower than the background noise. Above 550 °C, the phosphorus yield increases rapidly, showing the increasing decomposition of InP. The In yield is still very low even at these temperatures, i.e. the evaporation is not congruent. The observed phosphorus yield vs temperature curve can be fitted with an $A \cdot \exp(-T_a/T)$ type of curve.

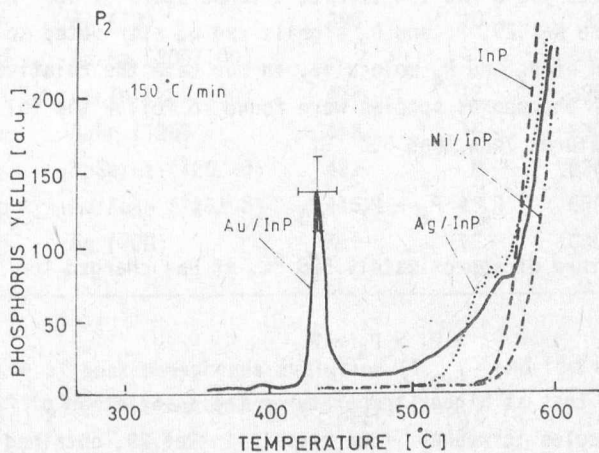


Fig.2 Phosphorus loss vs temperature curves for the various InP based compound semiconductor - metal systems: Au/200 nm/-n-InP (100), Ag/200 nm/-n-InP (100), Ni/80 nm/-n-InP (100). For comparison the thermal decomposition of pure, i.e. uncovered InP, is also depicted

When the surface of the InP is covered with a 200 nm layer of gold, a sharp peak appears at a temperature of about 430 °C. A few samples were quenched from the characteristic temperatures on the EGA curves. Observation of these samples proved that this sharp peak is accompanied by the melting of the metallization and by the transition of the metallization colour from gold to silver.

For further analysis it is useful to define a parameter which characterises the effect of metallization on the decomposition of the underlying InP. As the area under the phosphorus yield curve is proportional to the total phosphorus loss, a corresponding quantity is needed. In the case of gold metallization (above the temperatures of 550 °C) the curve can also be fitted with the exponential type function (with different constants). It allows us to define the metallization dependent integrated yield as the integration of the difference between the measured curve and the fitted exponential type curve (see insert in Fig.5).

Similarly, the 200 nm Ag/InP system shows a phosphorus evolution peak, i.e. silver also promotes the decomposition of InP. However, the quantity of evaporated phosphorus is less than in the case of gold coated samples (Table 1). No peaks were observed in the case of Ni metallization (Fig.2) and the phosphorus yield was low even at a temperature of 580 °C.

According to Ref.29, P_1 and P_3 signals can be attributed to dissociative ionization of P_2 and P_4 molecules. In our case the relative quantities of the four phosphorus species were found to follow the following order at temperatures less than 500 °C:

$$P_4 > P_2 > P_1 > P_3$$

Above a temperature of approximately 500 °C, it has changed to:

$$P_2 > P_1 > P_4 > P_3$$

which indicates that at higher temperatures the association of P_2 molecules to form P_4 molecules is weaker. (See results in Ref.29, obtained for free InP surface.)

Numerous measurements were carried out on (100) and (111) orientated p- and n-type InP samples with 200 nm Au. We found no differences in the shape of the phosphorus curves, in the position of the phosphorus yield peak or in the integrated phosphorus yield. The dependence of InP decompo-

sition on the thickness of the evaporated gold layer was then investigated. As Fig.3 shows, the shape of the EGA curve changes with decreasing gold layer thickness. During the measurements different sensitivities were used; these differences having already been taken into account, the intensities in different figures are directly comparable. The plot of peak temperature vs. gold layer thickness (Fig.4) shows that the peak temperature decreases almost linearly with decreasing gold layer thickness (in a logarithmic scale).

TABLE 1

	Type	Cond.	Metallization	T_{peak}	δT_{peak}	$\int YP_2$	$\delta \int YP_2$
		type	[nm]	[°C]	[°C]	[a.u.]	[a.u.]
1	1	n	Au (400)	441	16	1100	300
2	1	n	Au (200)	436	8	740	210
3	2	p	Au (200)	437	11	730	190
4	2	n	Au (50)	409	20	300	55
5	2	n	Au (30)	395	6	150	20
6	2	n	Au (13)	395	10	38	20
7	2	n	Au/Ga (200/100)	-	-	430	110
8	2	n	Au/In (200/100)	473	12	600	60
9	2	n	AuGe (120)	418	16	630	50
10	2	n	AuGe/Ni (120/30)	427	8	620	140
11	2	p	Au/AuBe (125/50)	415	13	650	120
12	2	n	Ag (200)	561	18	630	150

The temperature of peak phosphorus evolution (T_{peak}) and the integrated yield of P_2 ($\int YP_2$) with scatterings (δT_{peak} , $\delta \int YP_2$).

Type 1 - "old samples"

Type 2 - "new samples"

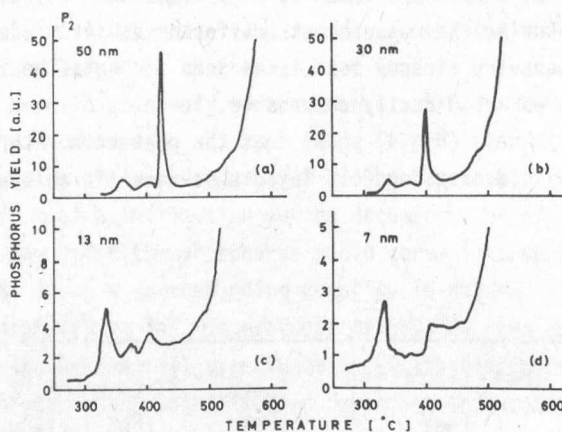


Fig.3

The effect of the gold layer thickness for the volatile component loss of Au-n-InP (100) contact system. Gold layer thicknesses are: 50 nm, 30 nm, 13 nm and 7 nm

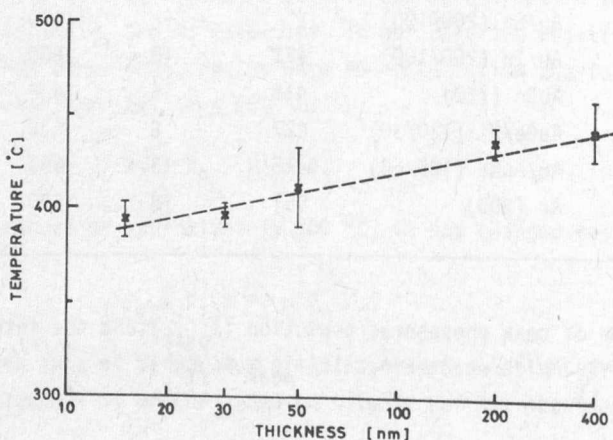


Fig.4

Peak phosphorus evolution temperature vs gold layer thickness (logarithmic scale) for the Au/InP system at the main peak

The integrated phosphorus yield also decreases as an inverse function of gold layer thickness (see Fig.5); the dependence being again roughly linear but this time on a linear gold layer thickness scale. Type 1 samples ("old" samples) show a moderate phosphorus loss in comparison with the Type 2 samples. Large scatterings can be attributed to the high heating rate applied and to the uncertainties in separating the metallization dependent integrated phosphorus yield from the total integrated phosphorus yield.

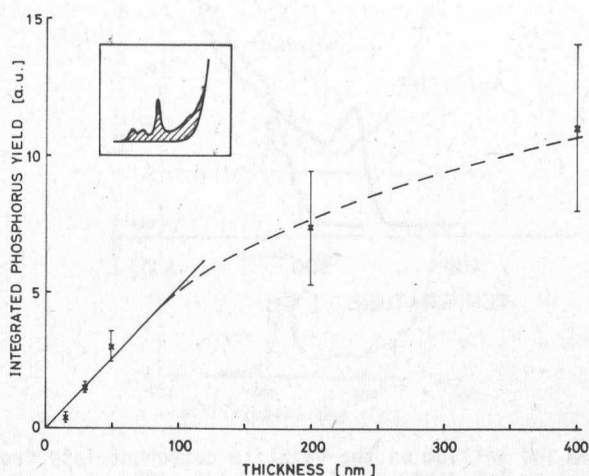


Fig.5

Integrated volatile component loss for the Au/InP structure. The insert shows the definition of integrated phosphorus loss.

Analysis of some 20 curves has proved that besides the main peak of phosphorus evolution there are also other peaks and shoulders (see Fig.3), which are believed to be connected with the metallurgical-thermodynamic processes taking place in the metal-semiconductor contact system. In the case of samples coated with relatively thin gold layer these peaks may even dominate the main peak.

To study the role of A_{III} metals in contact formation, (200 nm) Au/(100 nm) In/InP and (200 nm) Au/(100 nm) Ga/InP samples were investigated. Typical phosphorus evolution curves are shown in Fig.6. It can be clearly seen from this figure, that in both cases the integrated phosphorus loss

decreases in comparison with the Au-InP system. For both metallizations a suppression of the peaks can be observed, this effect being more marked for layers containing gallium.

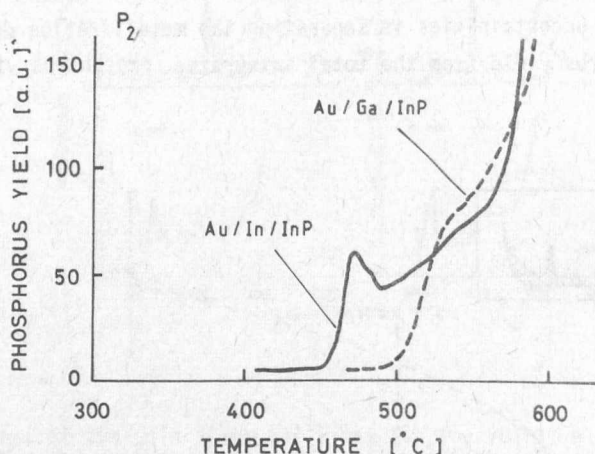


Fig.6

The effect of indium and gallium on the volatile component loss from the Au(200 nm)/In(100 nm) -n-InP (100) and Au(200 nm)/Ga(100 nm)-n-InP (100) contacts.

To obtain information about the processes taking place during the formation of real ohmic contacts, the annealing of Au/AuBe/p-type InP, AuGe/n-type InP and Ni/AuGe/n-type InP samples with various layer thicknesses was carried out. In these cases, the phosphorus loss vs. temperature curves seem to have two maxima, one of them sometimes appearing as a shoulder (Fig.7).

Because of its importance in the technology of optoelectronic devices, some preliminary measurements on the $\text{In}_{0.7}\text{Ga}_{0.3}\text{As}_{0.63}\text{P}_{0.37}$ material were also made. The main result being that the peak evolution temperature is the same for both arsenic and phosphorus. It shows that there is one dominating process, which leads to the transformation of the contact.

(See Fig.8)

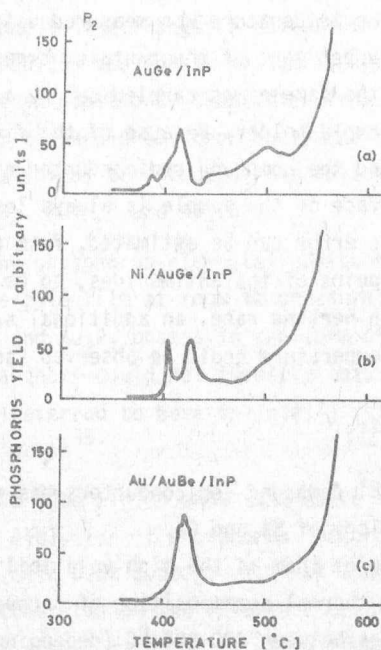


Fig.7

EGA curves of gold based ohmic contacts to InP

- a) AuGe/120 nm/-n-InP (100)
- b) Ni/30 nm/ /AuGe/120 nm/-n-InP (100)
- c) Au/125 nm/ / AuBe/50 nm/-p-InP (100)

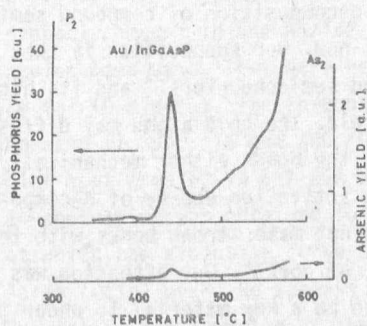


Fig.8

The arsenic and phosphorus evolution during the interaction of 400 nm gold with InGaAsP

4. DISCUSSION

4.1. Experimental conditions

In our sample holder the temperature was measured using a NiCr-Ni thermocouple welded to the upper part of the tantalum tweezer containing the sample. The heating of the sample was carried out by a tungsten filament from the rear of the sample holder. Because of the finite heat conductivity of the tweezers and the compound semiconductor sample, the measured temperature on the surface of the sample is always less than the real temperature. This systematic error can be estimated, from other measurements taken at the melting point of the antimonides, to be about 20-40 °C. As a consequence of the high heating rate, an additional scattering of the peak phosphorus evolution temperature could be observed (see Fig.2).

4.2. Discussion of the results

The technology of $A^{III}B^V$ compound semiconductors has raised new problems compared to the technology of Si and Ge.

The main reason of some of them is the high volatility of B^V elements. Because of this, the thermal decomposition of uncovered $A^{III}B^V$ compounds starts at temperatures between 400-600 °C (depending on the nature of the given compound). In the case of contact technology some of the elements, which are basic components of ohmic contacts (like Au and Ag) , or which are used as bonding materials or heat sinks (Au), do not suppress this decomposition, but on the contrary, promote it (see Fig.2). Alternatively, other metals like Ni on InP (Fig.2) or Pt and Al on GaAs¹⁵ do not induce large volatile component losses. The reason for this different effect of various metals on the decomposition of compound semiconductors has not been well understood until now. Our supposition is that the high diffusion rate of Au into compound semiconductors³¹ and its high electronegativity can play an essential role. The gold atoms may diffuse deeply into semiconductors and unstabilize the bonds either mechanically or electrically, i.e. they can lower the activation energy of decomposition. Another important fact is that Au does not make strong bonds with the volatile B^V component while, for example, Ni does³². Our attention was therefore focused mainly on Au, as it can be a key material to understand the mechanisms of metal-compound semiconductor interaction.

As mentioned earlier, the In out-evaporation was much lower than the evaporation of P, so an accumulation of In could be observed in the metallization. This accumulation lead to the gradual saturation of the gold film with indium and to the change in colour of the metallization. This effect was described for the InP-Au system as a transition from gold to pink². In our case an additional transition from pink to silver was also observed at higher temperatures. Upon analysing the reacted metallization (using various analytical techniques), the following phases were identified: α -Au, Au_4In , Au_9In_4 , AuIn_2 ⁹ and Au_3In ².

As regards the phosphorus, elemental phosphorus was found on and near the surface of the gold film at room temperature, with photoemission spectroscopy³³, AES³⁴ and Au_2P_3 phases in the form of clusters with X-ray diffraction². Other authors could not identify this phase⁹. However, our AES measurements (not referred to here in detail) supported the existence of a phosphorus-rich phase³⁵.

The EGA curves (see Fig.3) show that there are several mechanisms which lead to the evolution of phosphorus. According to our proposed mechanism, before the main peak appears (i.e. at lower temperatures), most of the phosphorus accumulates at the interface creating a phosphorus-rich formation. However some portion of it may diffuse to the surface where it evaporates. At higher temperatures, the dissociation of phosphorus-rich formation takes place and, in samples heated beyond the main peak, it is already absent (Fig.9).

A quasi-stable state, which the system can reach during the interaction, is another phenomenon which may lead to the development of peak evolution. As our AES measurements combined with depth profiling demonstrated³⁵ such a state probably occurs in the Au/InP systems. For these investigations, control samples were used. They were heat treated in forming gas in a standard furnace for 10 minutes. The In-content was found to be the same in the samples annealed at 350, 375 and 400 °C and it equaled 12 ± 3 atomic percents. Samples heat treated in our EGA setup were also analysed and the same indium concentration was obtained for the samples quenched from the temperature at which the evolution curve of phosphorus showed a minimum, before the large (main) peak. We suggest that this decrease of the reaction speed, leading to the lowering of the out-evaporation of the volatile component, is because the gold atoms cannot easily "etch" the InP

as they are bound to some extent in an Au-In (likely solid-solution) phase. During the main peak the contact melts and its colour changes from pink to silver, showing the increasing quantity of indium in the metallization.

As regards the mechanism leading to this large volatile component peak, it seems to be very probable that the saturation of the gold with In is continued in the solid phase, so its melting point is decreasing and at a given temperature, the metallization melts (perhaps first at the interface) and so promoting the decomposition of the phosphorus phase and accelerating the reaction.

The fact that the temperature of the main peak (and the other peaks and shoulders) decreases with the decreasing gold layer thickness is not surprising if we accept that the speed of the interaction depends only slightly on the thickness of the gold layer. In this case, when the gold layer is thinner, the saturation of the gold with indium in the different stages of interaction and the melting of the metallization may take place at slightly lower temperatures. Similarly, the thinner gold layer may take up proportionally less indium, so the total amount of evolved phosphorus (so-called integrated yield) will be less.

Moderate volatile component loss was observed for the so-called "old" samples, which corresponds with the results of Kinsbron et al¹³. The reason for it, however, is not yet clear because at room temperature the reaction speed should be so low that it is unreasonable to suppose that a considerable amount of phosphorus has out-evaporated before the EGA measurement.

As Fig.6 shows, the deposition of an additional layer of In or Ga between the Au metallization and the InP suppresses the phosphorus loss peak, the effect being more marked for gallium. The following is an explanation of this effect. In the case of an Au/In/InP system, the In layer will react first with the Au layer; In will diffuse into the Au and cause some saturation there. In this case only a small additional reaction between the Au and the InP surface takes place; a smaller phosphorus loss peak appears at temperatures higher than that for the Au-InP system.

Similarly in the case of the Au/Ga/InP system; at lower temperatures there will be a strong interaction between the Au and Ga layers and Ga will diffuse into the gold, while the surface of InP practically does not react with the gold. At higher temperatures, some interaction between Au, Ga and

also InP can take place, but Ga atoms will probably substitute most of the In atoms which escape from the InP surface, and will form Ga-P bonds which are stronger than the In-P bonds. It means that there will be only a small phosphorus loss at the temperature, which is sufficiently higher than that for Au/InP and Au/In/InP.

The ohmic metallizations also strongly interact with the underlaying semiconductor. As the integrated yields show, the gold is responsible for the large volatile component loss. The most significant changes occur in the EGA curve of Ni/AuGe contact. This is not surprising if we take into account the formation of several compounds³⁶. Even 1% Be may cause considerable changes to the evaporation vs temperature curve.

CONCLUSION

An evaporated Au film on the surface of the InP greatly enhances the decomposition of the semiconductor. The total quantity of evolved phosphorus is roughly proportional to the quantity of gold. It shows that the dominating process is the saturation of gold with indium. The fact that additional In decreases the out-evaporation, also refers to this phenomenon. The sharp peak, which appears on the EGA curve of InP covered with a thick gold layer, shifts to a lower temperature when the gold metallization is thinner. Taking into account that the appearance of the peak is connected with the melting of the contact, we can explain this phenomenon as follows. While the reaction is taking place at the interface the liberated In is spreading in the whole contact metallization, so a higher temperature (and a longer time) is required to reach the melting point corresponding to the In content in the alloy. On the other hand, products of the reactions which take place in the solid phase (at lower temperature), could only be detected if the gold film was thin. In conclusion, the following effects are assumed to be responsible for the observed peak structure; reactions which take place in the solid phase, formation and decomposition of a phosphorus rich phase and the acceleration of reactions when the contact melts. Gold in ohmic contacts promotes the decomposition of InP, so the appearance of Au-In alloys with relatively low melting points is natural. To avoid the melting and "balling up" of the contact, low temperature annealing, the reduction of the relative quantity of gold or the use of diffusion barrier layers to prevent gold diffusion from the outer region is required.

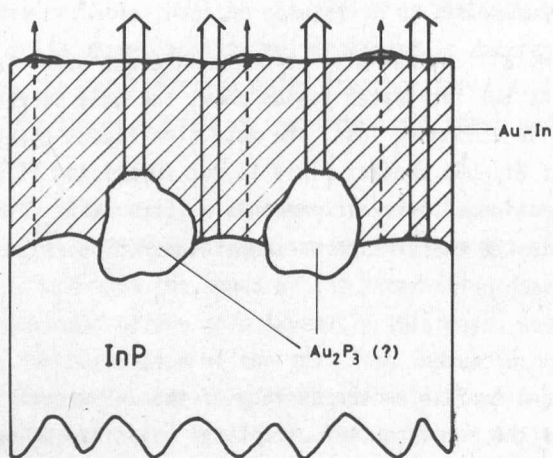


Fig.9

Sources of observed phosphorus out-evaporation from the Au/InP contact system.

ACKNOWLEDGEMENTS

The authors thank the authorities of the Czechoslovak and Hungarian Academies of Sciences for the opportunity to cooperate. The authors are also indebted to Prof.E.Nagy and Dr.I.C.Szép for their interest, support and helpful discussion on this topic. The technical assistance of Cs.Farkas is gratefully acknowledged.

REFERENCES

1. Barnes, P.A., Williams, R.S.
Solid-State Electronics, 24 907 (1981)
2. Piotrowska, A., Auvray, P., Guivarc'h, A., Pelous, G.
J.Appl.Phys., 52 5112 (1981)
3. Szydlo, N., Olivier, J.
J.Appl.Phys., 50 1445 (1979)
4. Christou, A., Anderson, W.T., Jr.
Solid-State Electronics, 22 857 (1979)
5. Tuck, B., Ip, K.T., Eastman, L.F.
Thin Solid Films, 55 41 (1978)
6. Bayliss, C.R., Kirk, D.L.
J.Phys.D.: Appl.Phys., 9 233 (1976)
7. Williams, R.H., McKinley, A., Hughes, G.J., Montgomery, V.,
McGovern, I.T.
J.Vac.Sci. Technol., 21 594 (1982)
8. Vandenberg, J.M., Temkin, H., Hamm, R.A., DiGiuseppe, M.A.
J.Appl.Phys., 53 7385 (1982)
9. Vandenberg, J., Temkin, H., Hamm, R.A., DiGiuseppe, M.A.
Thin Solid Films, 104 419 (1983)
10. Steeds, J.W., Rackham, G.M., Merton-Lyn, D.
Institute of Physics Conf.Ser. No.60, pp.387-396, (1981)
11. Sebestyen, T., Menyhard, M., Szigethy, D.
Electron.Lett., 12 96 (1976)
12. Szigethy, D., Sebestyen, T., Mojzes, I., Gergely, G.
in Proc. 7th International Vacuum Congress and 3rd International
Conference on Solid Surfaces (Vienna),
Vol.3 1959-1961 (1977)
13. Kinsbron, E., Gallagher, P.K., English, A.T.
Solid-State Electronics, 22 517 (1979)
14. Chung, D.D.L., Wong, L.K.
in Proc.10th NATAS Conf. (Boston), pp.149-151 (1980)
15. Mojzes, I., Sebestyen, T., Szigethy, D.
Solid-State Electronics, 25 449 (1982)
16. Leung, S., Wong, L.K., Chung, D.D.L., Milnes, A.G.
J.Electrochem.Soc., 130 462 (1983)
17. Szigethy, D., Mojzes, I., Sebestyen, T.
Int.J.Mass Spectrom.Ion Phys., Vol.52 pp.117-129 (1983)

18. Mojzes, I., Szigethy, D., Veresegyhazy, R.
Electron.Lett., 19 117 (1983)
19. Mojzes, I., Malina, V., Veresegyhazy, R.
Proc.of Surface Analysis'83 Bratislava, pp.88-91 (1983)
20. Nakahara, S., Gallagher, P.K., Felder, E.C., Lawry, R.B.
Solid-State Electron., 27 557 (1984)
21. Gallagher, P.K.
Thermochimica Acta, 26 175 (1978)
22. Folberth, O.G.
J.Phys.Chem.Solids, 7 295 (1958)
23. Drowart, J., Goldfinger, P.
J.Chim.Phys.55 721 (1958)
24. Gutbier, H.B.
Z.Naturforschung, 14A 32 (1959)
25. Gutbier, H.B.
Z.Naturforschung, 16A 268 (1961)
26. Lou, C.Y., Somorjai, G.A.
J.Chem.Phys., 55 4554 (1971)
27. Arthur, J.R.
Surf.Sci., 43 449 (1974)
28. Tuck, B., Hayes-Gill, B.R.
phys.stat.sol. (a) 60 215 (1980)
29. Farrow, R.F.C.
J.Phys.D.: Appl.Phys., 7 2436 (1974)
30. Mojzes, I., Veresegyhazy, R.
J.Electrochem.Soc., 132 1255 (1985)
31. Rembeza, S.I.
Fiz.Tech.Polup., 3 613 (1969) (in Russian)
32. Williams, R.H., Montgomery, V., Varma, R.R.
J.Phys.C.: Solid State Phys., 11 L735 (1978)
33. Lindau, I., Spicer, W.E., Kendelewicz, T., Petro, W.G.
Proc. IX IVC-V ICSS, Madrid, p.146 (1983)
34. Hiraki, A., Shuto, K., Kim, S., Kannmura, W., Iwami, M.
Appl. Phys.Lett., 31 611 (1977)
35. Veresegyhazy, R. et al, to be published
36. Veresegyhazy, R., Kovács, B., Mojzes I.
Proc.Symp. on Electronics Technology, Budapest, Vol.I. 465 (1985)



REPORTS ON ACTIVITIES

In this section a brief account is given of the activities of our institute. There was no significant change in the number of permanent staff, which is given here according to the scheme of organization:

Scientific Staff	93
Technical Assistants	92
Administration	72
Services	54
	<hr/>
	311

THE PERSONNEL OF SCIENTIFIC DIVISIONS

N a m e	Scientific	Technical
Semiconductor Research	25 (3)*	20
Metal Research	26 (5)*	20
Structure Research	16 (2)*	17
Optics and Electronics	9	21
Microwave Devices	17	14
	<hr/>	<hr/>
	93	92

*on leave of absence

MEMBERS WITH ACADEMIC DEGREES

Members of HAS:	2
Academic Doctors of Science:	3
Candidates of Science:	26
University doctors:	12

Members of the scientific staff are active in many commissions of Academy and in various engineering societies both at home and abroad; a number of them are lecturing at universities. We are therefore positive that our people are not living in isolated ivory towers but are working together for the scientific and economic progress of the country.

SEMICONDUCTOR RESEARCH DIVISION

E. Lendvay

In this brief survey we report only some essential results of our current research activities. In the Semiconductor Research Division of the MTA MFKI the period of 1984-1985 is characterized by investigations increasingly concerned with research and development in optoelectronics. Remarkable results have been achieved in different fields:

- the growth of single crystals and epitaxial layers of the well known III-V semiconductors such as GaAs, InP, their ternary (GaAlAs) and quaternary alloys (GaInAsP) as well as on the LPE growth of new quaternaries, the pseudo-ternary antimonides.
- Continuing our laser-diode programmes, efforts in developing GaAs based laserdiodes have been directed towards the production of pigtailed modules for optical telecommunication and for the development of LD-s for laser xerography (printers). Besides GaAs/GaAlAs LD research, we have also been concerned with the development of InP/InGaAsP DH systems and with the application of quaternary AlGaInSb as a detector material for the second optical window.
- We completed the development of our new deep level spectrometer (DLS 82). As with the previous version a continuous, deep interest is shown in our new fully digitalized deep level spectrometer, which is suitable not only for GaAs but also for Si wafers. Applying our DLS-82 we realized the first operating contactless wafer-scanner using a mercury contact and a frequency-scanned DLTS method. (See in G.Ferenczi's paper in this volume)

- The superlattice research programme has started the development of a special LPE technique. Most recently we have been able to grow GaAs and GaAlAs layers as thin as 10 nm up to the layer number 80-100.

Reviewing the progress in the fields mentioned the main task of the single crystal growth was to establish a material (substrate) basis of our device development. This work led to the LEC growth of [100] orientated GaAs crystals with low dislocation density (common project with the Italian CNR-MASPEC institute) as well as to the growth of InAs and GaSb crystals. Wafers cut from these crystals serve as a substrate or active material for device development. Using GaSb substrates interesting results have been achieved preparing GaSb/AlGaInSb heterojunctions. These systems are promising ones for optoelectronics, and we will give data about them elsewhere in this volume.

In GaAs/GaAlAs laserdiode research, contact stripe lasers have been developed. The construction and installation of a microcomputer controlled LPE system (joint work with the Technical University of Budapest) and the installation of some new LPE systems with semi-transparent walls and/or with new temperature programmers made it possible to considerable increase our efforts to produce reliable, high-power GaAs/GaAlAs laserdiodes and InP/GaInAsP LD-s. The GaAs/GaAlAs laserdiode development is described elsewhere, so we will not go into details. However, we mention here some results with respect to the laserdiode program. To facilitate the stability (reliability) and diode parameters a complex laser-tester has been developed and built which is able to test 60 LD-s in a temperature range of 10-100°C simultaneously. The tester consists of 4 independent units; each contains 15 LD-s with the output power being adjusted by dial between 0.05-5 mW, regulating the driving current electronically. There is an option for pulsed mode (30 kHz, 300 ns) and the system has a central controlling unit which reads and digitalizes the data before transmitting them to a computer. This equipment has already aroused wide interest among specialists at home as well as abroad.

The progress in fiberoptic technology has been promoted not only by the production of ultra-low-loss fibers and laserdiodes, but also by the development of detectors. During the last two years progress has also

been made in developing photodiodes at the MFKI. Our previous investigations showed that the quaternary AlGaInSb, suits for the first and second optical windows in optical telecommunication. This material indicates a complete coverage of the 0.7 - 1.7 μm region is possible. Photodiodes operating in both the 0.75 - 0.95 μm and 1.30 - 1.55 μm spectral ranges have been prepared from the GaSb/AlGaInSb heterosystem, allowing a single detector to replace both Si and Ge detectors.

Our activities in the last two years have also been influenced to a considerable extent by the growth and application of quantum-well structures. The utilization of these systems enabled several records to be achieved in both optoelectronics and superfast IC-s. Multiple quantum-well structures (superlattices) are usually grown by high-technologies; by MBE or MO-CVD. In this Institute we have developed a relatively simple and fast LPE technique for multilayer growth. This growth is performed in a vertical reactor with a rotary graphite boat. Superlattices, with layer thickness of 10-50 nm and layer number 20-100 were grown in the GaAs/GaAlAs system. Laserstructures made from the superlattice wafers show light emission at the visible-infrared border. We have real hope in the near future of producing and measuring quantum-size effects on these samples. They can be used for many applications. Phase-locked monolithic arrays of gain-guided superlattice laserdiodes are an approach to high power output at relatively low power densities and long life times. Superfast transistors (HEMT-s) also contain a quantum-well which - in principle - can also be grown using our technology. Prospects for further development and application include such areas as detectors, high power lasers and new superlattice structures containing pseudo-ternary antimonides and binary III-V compounds.

METAL RESEARCH DIVISION

L.Bartha

The scope of our activity in metal research in the period 1984-85 was fairly wide. We dealt with special problems concerning statistical physics, with some fundamental aspects of powder metallurgy and have also done R+D work within the chemical and mechanical technology fields. Additionally a few on-line inspection systems have been developed and produced by us.

In order to describe the properties and evolution of microstructures, our theoretical group have studied various statistical physical models, including the percolation model of disordered systems, the aggregation phenomena and dendritic growth of crystals. In this volume, the papers of Kertész and Vicsek report on the progress in these fields.

With respect to the basic phenomena in powder metallurgy field, we have made efforts in the following topics. We clarified the nature of bonding between the primary particles in hard agglomerates in undoped tungsten powders produced by hydrogen reduction of oxides. The stabilising factors of the residual porosity and chemically driven cavitation have been studied. Beside soluble and insoluble gases, incompatibility stresses connected with diffusion fluxes have been taken into account, and the evolution of the pore structure has been followed up with computer simulation. Another major topic was the study of the high temperature degradation processes in composites. A serious obstacle to be overcome in the development of nickel based superalloys with reinforced tungsten fibres, is the diffusion induced grain boundary migration in tungsten and the embrittlement connected with it. To this end the grain boundary diffusion induced recrystallisation has been followed up in various dilute tungsten alloys in order to test the current theoretical models of the process. Further, the

relaxation of the thermal stresses was measured by means of a high temperature microdilatometer in order to gain an insight into the validity of the various continuum approaches applied for the theoretical prediction of the evolution of thermal stresses in two phase ceramics.

Within chemistry, the majority of work was carried out in research of separation methods. In following the national efforts for utilising secondary raw-material sources, processes were investigated which can help reprocessing and separation of valuable metallic components of scraps in both an economical and environmental way. Besides the necessary chemical investigations, equipments were constructed for the realization of processes both on laboratory and also on production scale forming complete technologies.

In order to study electrodialysis and ion separation through ion-exchange membranes, several single- or multicell units were built in the 100-5000 cm² membrane area size-range. Properties of construction materials, efficiency and economy of steps and several chemical side-effects, like precipitation, change in permeability, etc. were investigated. The method proved to be very advantageous to the recovery of alkaline ions from solutions of ores leached by alkaline hydroxides. Beside that the metallic component of the ore can be prepared for further processing. The recovery of the alkaline hydroxide is not only an economic advantage but also decreases the salt-contamination of the environment. The electrodialysis had a large-scale use in the Na₂WO₄ solution case, when a stable, dissolved isopolyacid was formed with excellent properties, to be transformed to ammonium paratungstate (APT) - a usual intermediate product in tungsten metallurgy.

One of the most up to date separation methods is the liquid ion-exchange extraction technique based on specific formation of metallorganic compounds which can be extracted by an organic solvent. It has several advantages:

- the active organic reagent and the organic solvent recycle, without considerable loss, and can be used separately. In this way small amounts are able to carry great amounts of metal to be extracted;
- reactor vessels can be switched in cascade and a number of metallic components can be separated at the same time;
- because of the intensity of the material-contact, relatively small vessels are needed;

- the possibilities of continuous operation mode and of process control.

We have built mixer-settler units of 200 ml and of 20 l (the latter having a separation capacity of 5 kg W/hour) for laboratory tests and semi-industrial purposes.

In the course of chemical investigation a reaction was found for the extraction of the above mentioned tungstic-isopolyacid, which helped us to transform it to a high-purity APT.

Both processes, coupled together, perform a new, efficient method for APT production.

The extraction method was successfully used for the separation of the components of mixed metals like Co-Ni, Ta-Nb etc.

The separation of valuable metal components always requires dissolution as the first step. Very often, by applying nitric acid, oxidation occurs, and from which noxious nitrous gases evolve. In case of several metal-mixtures H_2O_2 was successfully used as an oxidation agent. The advantage of H_2O_2 , that its oxidation potential can be influenced by homogeneous catalysts, was used in some cases, such as the specific dissolution of Mo beside W. Only O_2 develops as a by-product. Another example is the dissolution of the binder phase of sintered, polycrystalline diamond tools in order to recover diamond grains. For practical applications an automatic, dissolving unit of industrial size was constructed. The costs of recovery are a small fraction of the costs of synthesis.

The specific dissolution of a galvanically bound abrasive diamond layer was achieved by electrochemical means, recovering high-value tool bodies for repeated use.

The chemical activity described above has a necessary analytical background based mainly on AAS, ASP, NAA but also on some further classical methods.

In the field of mechanical metallurgy doped tungsten has been used as a model for many years. Research aims have been to understand the relationship between tungsten processing and wire properties and also the relationship between these wire properties and the quality of incandescent lamp filaments.

The so called fine wire in the diameter range 10-200 μm is processed under fairly extreme circumstances. Because of the high temperature deformation (drawing) and the oxidation-sensitivity W needs appropriate protection as the thin wire has a high specific surface area. The interaction between the metal and its environment is not negligible and can cause many different internal transformations inside the metal. The high specific surface area results in a great wear force comparable with the deformation force itself. The optimization of wire drawing needs coordination between optimum values of several parameters. For this purpose, the investigation intends to discover and coordinate these optimum values for reaching higher deformation rates and better wire quality. For the realization of this aim the development of fast sensors, like wire-temperature sensors, dynamometers and fast acting devices are proceeding.

Dies are of basic importance in wire drawing. Earlier dies made of hard metal and (in the small diameter range) single crystal diamonds were used. Nowadays synthetic, polycrystalline diamond dies have taken over certain diameter ranges not only for quality reasons but for their long lifetime as well.

The lifetime of a die and the quality of a wire drawn by it is determined partly by the profile and inner surface of the hole and partly on the casing of the die. The casing is supposed to fix the die steadily in a wide temperature range. We have studied the casing using powder metallurgical methods. Several dispersion strengthened materials were investigated and applied. Dies made by such means are presently undergoing industrial tests.

Trends show that the use of ceramic materials - as tools and as parts in high temperature constructions - is growing rapidly. Recently we have started to study alumina-silicon nitride based ceramics, first of all as a cutting tool. This area of work should widen in the future.

In contact with industry, we traditionally worked on developing on-line inspection systems for use under industrial conditions - not always favourable. Such equipments are used either for process or quality control. In recent years a group of magnetic and magneto-inductive non-destructive testing devices were developed to control the quality of metallic (mainly ferromagnetic) products. The work is still going on though some units already successfully work in several production plants.

Under the extreme conditions of steel making, correct temperature measurement is sometimes difficult. We are working now on a temperature measuring system for controlling continuous casting, based on eddy current loss depending on the temperature of the material.

It was worked out and is still successfully used a non-radioactive tracer method to determine sources of extrinsic inclusions in the course of steel processing.

A three-dimensional computer-model of the material flow in the crystallizer of a continuous casting device has been constructed. It describes material currents and inclusion movement under different conditions and helps to find optimum parameters for minimal inclusion content in the steel.

We cooperate in different fields with universities, with research institutes and with industrial companies, not only in Hungary but also abroad. The details about our partners are described in the section 'International relations' of this volume. Several of our scientists give regularly lectures on universities. As a part of our activity, diploma theses and doctor theses are prepared under the supervision of our senior scientists.

STRUCTURE RESEARCH DIVISION

L. Zsoldos

Structure Research in our terminology covers a rather wide field of activity from, for example, the study of surface morphology or measurement of lattice parameter changes to analytical electronmicroscopy. Generally speaking we are interested in all kinds of deviation from the idealized periodic structure of solids which considerably influences the physical or technological properties. All studies are, of course, connected to the research projects of the institute.

The activities can be classified into three groups:

- a) Development of new methods or devices and the improvement of already existing equipment.
- b) The application of our knowledge (and methods) to solve various distinct problems.
- c) The research of phenomena related to diffraction effects, thin film properties, surface effects, and to the behaviour of lattice defects.

In this volume paper by J.Lábár and I.Pozsgai, G.Radnóczy and B.P.Barna, A.L.Tóth, and G. Gergely respectively are presenting new results in group a) and c). Here, in addition, we give a very brief summary of other work.

The development of new devices and the improvement of the existing ones has become important in recent years.

Within this programmes, computer controlled systems were developed for our microdensitometer (for the measurement of diffraction patterns), for the Auger-electron spectrometer and for the double crystal topographic

goniometer. The system for the JSM-25 scanning microscope is near to completion.¹

From among the new devices the ion beam thinning attachment for TEM specimen preparation should be mentioned². This attachment with its new powerful and long life ion sources is able to produce an excellent smooth surface over a rather large area and with reasonable thinning rates (30-40 $\mu\text{m}/\text{h}$ for Si, Al and GaAs at high angle incidence, and 6-10 $\mu\text{m}/\text{h}$ at an incidence of 1-4 degrees). The performance of the device is illustrated by an electronmicrograph of a mica sample in Fig.1.

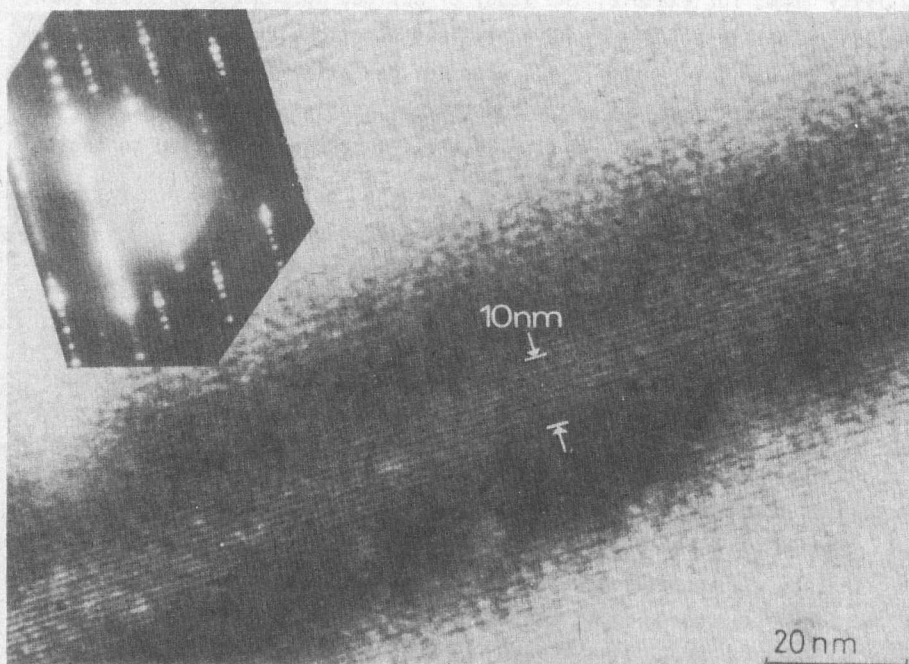


Fig.1 A lattice resolution TEM image taken by a JEOL 100U microscope from mica perpendicular to the cleavage plane. The diameter of the whole image area showing lattice resolution is 100 μm . (Photograph by A. Barna). The sample was mechanically polished down to 60 μm followed by the ion beam thinning at 30° for 2.5 hours.

Utilizing the role of internal total reflection in cathode luminescence (CL) detection, a new CL collecting and detecting system, the total reflection cathode luminescence, (TRCL) has been developed³. Its use improves the image quality and is especially useful for small samples.

The study of Au growth on Al revealed information of two kinds of Au_2Al crystal.⁴ One of them forms tetrahedra with their apices growing into the Al layer, whereas the other one grows in thin layer and is strongly influenced by the oxidation of the Al surface. (Holes and channels are formed.)

SiO_{1+x} layers prepared by inclined evaporation were studied by TEM in cross section and, depending on growth conditions, deviations from the 'tangent rule' were traced.^{5,6}

The x-ray diffraction study of solid state phase transformation of materials containing excess 'fixed' species like water or NH_3 , showed that an anisotropic lattice deformation already had taken place below the transformation and that the deviation from the stoichiometry influences the physical and/or chemical behaviour of the materials, even if their room temperature diffraction patterns are similar.⁷

The x-ray topographic contrast of dislocation in elastically bent crystals proved that the white dynamic image (in slightly absorbing crystals), may appear independently of the sign of the strain gradient parameter.⁸

A considerable amount of our results were realised through cooperation with other laboratories abroad, which is presented in this volume elsewhere, together with the main topics of cooperation.

REFERENCES

1. Tóth A.L., Lábár, J.L. Vladár, A.E.
Computer controlled measurement of charge collection signals in the SEM
Proc. of EUREM'84 Vol.1. p.307, Budapest, 1984.
2. Barna, A.
A new type ion milling equipment for sample preparation.
Proc.8. Eur.Congr. EM., p.107 Budapest, 1984.
3. Tóth, A.L.
Total reflected cathodluminescence (TRCL) in the SEM.
Hungarian-Austrian Conf. on Electron Microscopy, Balatonaliga, 1985.
4. Radnóczy, G., Barna, P.
The growth of Al₂Au crystallites on Al(111) films.
Thin Solid Films 116 1-2-3 143 (1984)
Paper presented at the 2nd International Summer School on Thin Film
Formation, Hajduszoboszló, Hungary, 18-24 September, 1983.
5. Geszti, O., Gosztola, L. Seyfried, E.,
Cross sectional transmission electron microscopy study of obliquely
evaporated silicon oxide thin films.
Thin Solid Films (to be published)
6. Barna, A., Geszti, O., Gosztola, L. Seyfried, E.
Cross sectional transmission electron microscopy study of obliquely
evaporated silicon oxide thin films.
To be published in 'Defect in Glasses' Conference Series of the
Material Research Society edited by F.L. Galeener, D.L. Griscom,
M.J.Weber
7. Farkas-Jahnke, M., Somogyi, M., Tekula-Buxbaum, P., Petrás, L.
Deviation from stoichiometry and lattice flexibility.
Acta Cryst. A 40S 103 (1984)
8. Zsoldos L.
Unusual dislocation contrast on the x-ray transmission topographs of
elastically bent crystals.
Acta Cryst. A 40S 329 (1984)

DIVISION OF OPTICS AND ELECTRONICS

J. Schanda

The main task of the Division of Optics and Electronics is the establishment of new methods of radiometric, photometric and colorimetric measurements, the development of new measuring techniques and the study of effects coupled to these areas of optics.

Building on the results of the co-operation with the National Bureau of Standards, Washington, USA, a radiometric scale has been developed based on the so-called 'self-calibration technique' of measuring the external quantum efficiency of Si photocells. At present this endeavour continues for the derivation of a photometric scale directly from the radiometric one.¹ To achieve this goal further emphasis was given to the production of $V(\lambda)$ -filters for the investigation of residual errors related to filter-photocell combinations² and to increase the sensitivity of optoelectronic devices³.

A new series of investigations along this line dealt with components of optical communication networks - mainly measuring fibre parameters, developing instrumentation for power measurement on emitters, cables and fibres.

In the main line of activity the results achieved in the above mentioned fundamental investigations were used practically in developing illuminance and luminance meters⁴. One of these instruments features a very fine $V(\lambda)$ -filter correction (Class A according to DIN 5032) in a pocket size instrument. Fig.1 shows the $V(\lambda)$ -curve, the spectral responsivity curve produced by full-filtering a Si-photovoltaic cell ($s(\lambda)$), and the so-called error curve ($\sigma(\lambda)$) showing the residual spectral mismatch. The $F1'$ value represents the average error according to DIN 5032.

Besides optical power measurement much effort was made to reach better characterization of materials. The new LED-Glossmeter⁵ is the results of

one of these endeavours. It uses three LEDs as light sources for the ISO standard measuring geometries of 20° , 60° and 85° . The detectors are Si-photocells. The use of a.c. techniques and of modern i.c. technology enabled the production of the robust, compact and versatile instrument seen in Fig.2. Further, the properties of reflectance standards have been investigated and the possibilities of measuring diffuse and total reflectance transmittance have been extended to measure colour characteristics as well⁶.

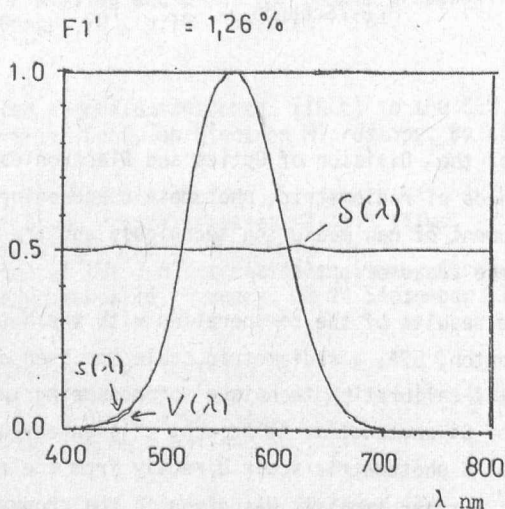


Fig.1 $V(\lambda)$, spectral responsivity curve ($s(\lambda)$) and error curve ($\sigma(\lambda)$) of a filtered Si-photocell

These colour determinations were used in the continuing effort to establish a better description of the colour rendering properties of light sources. In this field of activities emphasis was placed on three questions: The possibility to ameliorate the present international recommendation on colour rendering (CIE Publ.13.2)⁷. The main idea in the recommendation put forward by our Division is that the colour rendering should be referred to the application area, i.e. 'social-lighting' (e.g. lodgings, theatres, foyers, dining rooms), day-light supplementing lighting (most office and working environments) and critical colour evaluation lighting.

According to this the use of three reference illuminants is recommended (CIE Standard Illuminant A and D65 and P4300, i.e. a Planckian radiator of 4300K colour temperature). The colour difference should be evaluated

using CIELAB space. To reach a General Colour Rendering Index, quadratic averaging over all the test colour samples has been suggested. This is a stricter prescription than used at the moment, but is alleviated by incorporating an exponential function to couple the colour rendering indices to colour differences. This leads for sources of the highest colour rendering class to figures comparable to those received using the traditional calculations.

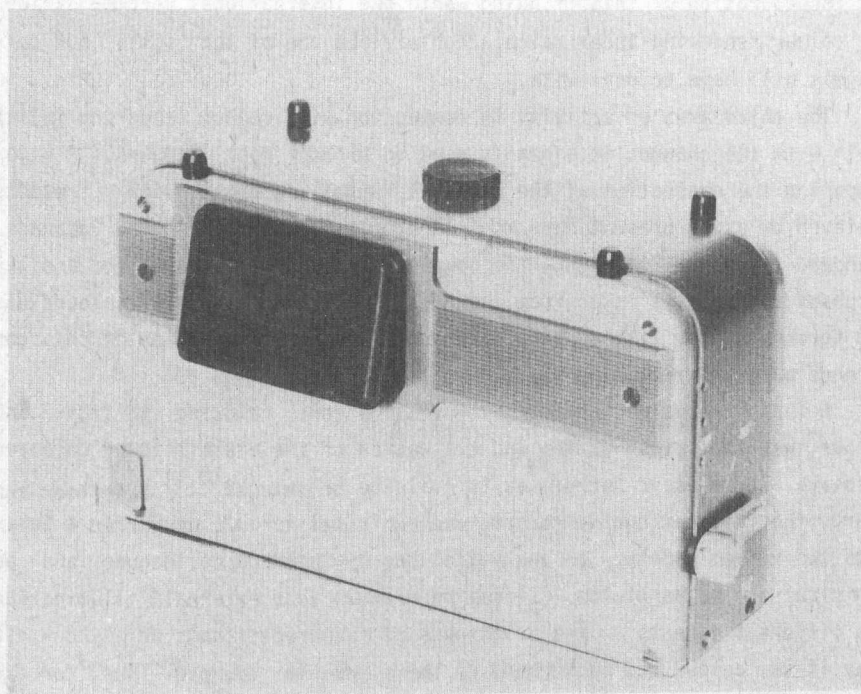


Fig.2 MFKI LED-Glossmeter

A second area of activities was a better evaluation of skin-tones. Here two series of investigations were carried out: Based on the investigation of human complexion reproduction it can be shown that a distortion towards more reddish hue and/or higher saturation is acceptable

but the distortion is rejected if it is towards greenish hues or lower saturation. Founded on the above considerations a combined colour rendering-colour preference index has been elaborated⁸.

The second point in this series of investigations was the establishment of better test samples for the evaluation of skin-tones. Comparing the results achieved by calculating colour rendering indices using the BBC skin-tones, it was established that complexion colours showed reflectance spectra as illustrated in Fig.3 and can be used to establish colour rendering indices for the Caucasian, Oriental and Negroid complexion colours. The incorporation of this finding into the international recommendation for colour rendering index calculation will be one of the tasks our colleagues will have to deal with.

The third area of activity in connection with colour rendering indices dealt with the changes in pigments used to produce test samples. A paper comparing the evaluation of the original Munsell-samples with results achieved by using present day Munsell-samples, samples from the Japanese Standard on Colour Rendering, the samples produced by the BAM for similar purposes and samples taken from the Hungarian Coloroid book of colours was put forward at the last session of the AIC⁹ (the reproduction of this conference paper is reprinted in the present volume on page 77).

A further area of fundamental investigation, relating to light and colour, was the investigation and evaluation of the visibility of coloured displays. Three basic techniques to evaluate brightness^{10,11} have been compared; the internationally recommended empirical formula by Warren & Covan, plus two vision models, an analytical one by Guth and colleagues and an empirical one by Bartleson. It has been shown that external illumination has different effects on the brightness of coloured signals on a VDU - display if the colour and background of the signal is changed. Thus, for example, yellowish, greenish and whiteish hues are strongly effected by external illumination. If balanced brightness is requested the external adaptation illumination has also to be taken into consideration.

As can be seen from the very short overview presented in this section of the Yearbook, the task of the Division of Optics and Electronics is manifold; starting from the fundamental investigation of the radiometric scale it extends as far as visibility and colour rendering. A number of research areas have not been tackled in this section, their results being enumerated, however, in the attached bibliography.

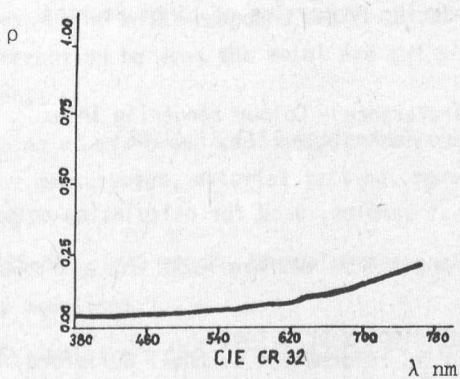
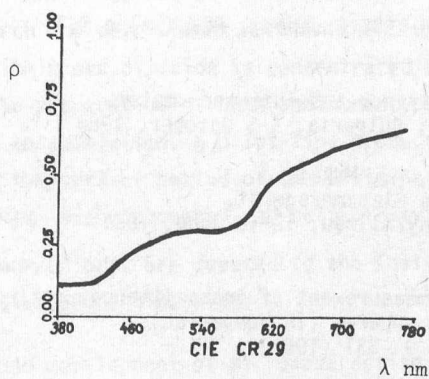
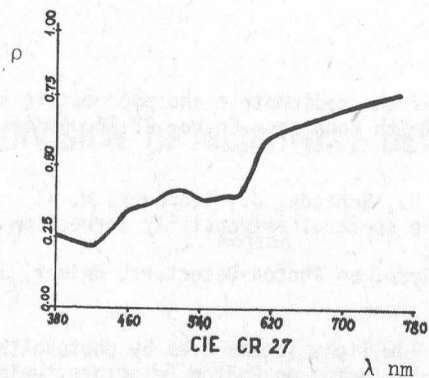


Fig.3 Reflectance spectra of skin-tones
a) Caucasian; b) Oriental and c) Negroid

REFERENCES

1. Eppeldauer, G.
Simple realization of the radiometric and photometric scales.
Lecture of the IMEKO Xth Congress, Praha, 22-26, April, 1985.
Proc. Vol.4. p.208.
2. Makai, J., Czibula, G., Schanda, J., Schröder, W.
The importance of the spectral responsivity correction in case of opto-electrical elements.
11th International Symp. on Photon-Detectors, Weimar, 11-13 Sept. 1984.
3. Eppeldauer, G.
Measurement of very low light intensities by photovoltaic cells.
Lecture of the 11th Int.Symp. on Photon Detectors, Weimar, 11-13 Sept. 1984.
Proc. (IMEKO Secr. H-1371 Budapest, POB 457) p.182
4. Makai, J.
A new compact illuminance and luminance meter.
Licht'84 Conference, Bulgaria, 4-6 October, 1984
5. Schanda, J., Kántor, K., Makai, J.
Ein neues, kompaktes Glanzmessgerät.
DGaO Conference, Isny/Allgäu, 12-16 June, 1984.
6. Rácz, M.
Instrument for the measurement of transmittance, reflectance and colour within a photometer sphere. (in Hungarian)
Mérés és Automatika 9 331 (1984)
7. Draft Technical Report on an Interim
Method of Measuring and Specifying
Relative Colour Rendering Properties of Light Sources
3rd Edition
8. Schanda, J.
A combined colour preference - Colour rendering index
Lighting Research and Technology 17/1 31 (1985)
9. Schanda, J.
The influence of test samples, used for calculating colour rendering indices.
AIC International Congress Colour 85, Monte Carlo, 16-22 June, 1985.
10. Schanda, J.
On the evaluation of display brightness.
Conference on Colour in Information Technol. Guildford, U.K.
26-29 March, 1985.
11. Schanda, J.
Brightness Evaluation of Colored VDU signals.
International Display Res.Conf. San Diego, Calif,USA 15-17 Oct. 1985.

DIVISION OF MICROWAVE DEVICES

I. Mojzes

Our division was organised at the beginning of 1984, with the task to perform research and development work in the field of microwave devices and phenomena. Within our division is concentrated the complete technological line for the preparation of GaAs semiconductor devices - from epitaxial growth to encapsulation. A pilot-line production for the devices was developed in the earlier period of the division's activity and was organized including high frequency and reliability testing of devices.

Presently, our efforts are devoted to the following major fields within technical physics and engineering:

1. The research and development of microwave active semiconductor devices including the construction, the technology, measurement and testing;
2. The investigation of metal-compound semiconductor junctions and especially the interaction between the metal and the semiconductor during heat treatment;
3. The application of microwave semiconductor devices and the microwave technique for measurement, material testing, remote sensing, and controlling purposes.

In these areas we are also involved in basic problems, especially of measurement and modelling.

Accordingly, we give a short review of our latest achievements in these major fields of research. All the results, however, are not included.

The first step in the research and development of a device is the production of a suitable layer structure. For this purpose the well-established

lished AsCl_3 VPE method was used. Layer structures of different thicknesses and concentration profiles on the conductive or semiinsulating substrates were prepared for Gunn, Schottky and varactor diodes and MESFET's. Detailed analysis carried out in the last year has allowed us to produce structures with contact and buffer layers of a given carrier concentration and homogeneity with high yield. The application of a new profile plotter and the traditional galvanomagnetic measurements were the most important tools for wafer testing.

The most important result achieved in the microwave diode field was the development of GaAs tuning varactors for the X-band. Low loss and high linearity are the most important features of these devices.

An improvement in the Gunn and Schottky technologies was carried out to improve the reliability and productivity of the pilot-line production for these devices.

The main activity was focused on the development of MESFET's. This project is now in progress. Both classical and self-aligned structures were examined. Using GaAs as substrate some passive elements of the monolithic microwave IC's were also realized and investigated this year.

Further, some ellipsometric investigations were carried out for dielectric-compound systems like SiO_2 -InSb and SiO_2 -GaAs. These structures were also investigated for electrical breakdown.

For device testing a computer controlled microwave test set was developed and widely used.

Investigation of the metal-compound semiconductor junction was focused on interaction during the heat treatment applied in the ohmic contact formation. GaAs, InP, InAs, GaSb and InSb coated with gold-based metallization were deeply analysed. Ternary and quaternary structures were also examined to obtain information on the processes taking place during the heat treatment of sophisticated semiconductor devices. A wide and very fruitful collaboration was arranged and the work was divided up among the teams in order to synthesize and achieve results. New general methods for the modelling and measurement of specific contact resistivity were proposed, which allowed comparison with results and methods published in literature. The application of various analytical techniques like back-scattering, Auger and X-ray analysis, and microprobes supported the re-

search activity with a very useful contribution.

The application of the microwave semiconductor devices and the microwave technique for measurement, material testing, remote sensing and control purposes is still in its infancy. Our energies have been directed towards the development of the microwave head for distance measuring equipment, the development of vehicle sensors, for coal-mining and urban transport. In the field of material testing, a measuring arrangement for microwave absorber testing was developed.

These are the most important results of the past two years research. Some of these results were published and presented to international and national conferences and workshops. Four patents have been granted to our colleagues during this period, which stresses the importance of this research activity.

THE OFFICE OF THE ATTORNEY GENERAL

WASHINGTON, D. C.

DEPARTMENT OF JUSTICE

OFFICE OF THE ATTORNEY GENERAL

WASHINGTON, D. C.

DEPARTMENT OF JUSTICE

OFFICE OF THE ATTORNEY GENERAL

WASHINGTON, D. C.

DEPARTMENT OF JUSTICE

OFFICE OF THE ATTORNEY GENERAL

WASHINGTON, D. C.

DEPARTMENT OF JUSTICE

OFFICE OF THE ATTORNEY GENERAL

WASHINGTON, D. C.

DEPARTMENT OF JUSTICE

OFFICE OF THE ATTORNEY GENERAL

WASHINGTON, D. C.

DEPARTMENT OF JUSTICE

OFFICE OF THE ATTORNEY GENERAL

WASHINGTON, D. C.

DEPARTMENT OF JUSTICE

OFFICE OF THE ATTORNEY GENERAL

WASHINGTON, D. C.

DEPARTMENT OF JUSTICE

OFFICE OF THE ATTORNEY GENERAL

WASHINGTON, D. C.

INTERNATIONAL RELATIONS

The management of RITPh has always been aware of the importance of scientific ties with institutions of other countries and has made great efforts to establish scientific co-operation with them. During 1984-85 we had regular contacts based on written agreements, with the institutions listed in Table 1.

Common work was carried out during stays by delegated staff-members within exchange schemes involving institutions of other countries. Papers were published and lectures held on results of such co-operation.

The scientific achievements of our institute have also been demonstrated in talks delivered by colleagues at international conferences. In addition, most of them were published in outstanding scientific journals.

A list of international conferences where our staff members appeared as invited speakers during 1984-85, is presented in Table 2.

The intensity of co-operation and interest in our work may be appreciated by observing the number of foreign scientists visiting our institute during these past two years. A partial list of the visitors connected with various co-operation projects is presented in Table 3.

Within this framework of co-operation with foreign institutions leave of absence was afforded to a number of our staff-members in order to study new developments abroad within the field of activities of our institute. Foreign scholarships awarded to our members serve the same purpose but it is unfortunate to note, the rate of their incidence is rather low.

It is only to be hoped that with the international political atmosphere becoming milder scientific contacts will thrive for the mutual benefit of science and human community.

TABLE 1.

AUSTRIA

J. Kepler Universität, Linz
Institut für Experimental Physik

Technische Universität, Wien
Institut für Angew. u. Techn. Physik

Institut für Chem. Techn. anorg. Stoffe,
Wien

CZECHOSLOVAKIA

Institute of Radioelectronics,
Czechoslovak Academy of Sciences
Prague

Electrotechnical Institute of the
Slovak Academy of Sciences
Bratislava

GERMAN DEMOCRATIC REPUBLIC

Zentral Institut für Elektronenphysik der AdW,
Berlin

Institut für Festkörperphysik and Elektronen-
mikroskopie, Halle

Werk für Fernsehelektronik,
Berlin

Institut für Halbleiterphysik,
Frankfurt/O

FEDERAL REPUBLIC OF GERMANY

Physikalisch-Technische Bundesanstalt
Braunschweig

Max Planck Institut
Institut für Werkstoffwissenschaft
Stuttgart

FRANCE

Institute of Optics,
University of Orsay,

Institute for Electron diffraction and
Microscopy,
University of Marseille

ITALY

MASPEC Laboratories of CNR,
Parma

POLAND

Institute for Electron Technology,
Warsaw

Institute for the Technology of Electronic
Materials,
Warsaw

Institute of Physics,
Polish Academy of Sciences,
Warsaw

cont. TABLE 1.

SOVIET UNION

Institute for Superhard Materials,
Ukrainian Academy of Sciences, Kiev

Baikov Institute for Metallurgy,
Moscow

Institute for Technical Physics,
Academy of USSR,
Leningrad

Institute for Semiconductor Physics
of the Academy of USSR, Siberian Branch,
Novosibirsk

Institute of Crystallography,
Academy of Sciences of USSR
Moscow

Institut for Semiconductors,
Ukrainian Academy of Sciences,
Kiev

UNITED STATES OF AMERICA

National Bureau of Standards,
Washington

YUGOSLAVIA

Institute for Electronics and Vacuum Physics,
Ljubljana

TABLE 2.

P.Barna	Int.Thin Film Conference Stockholm, Sweden	August, 1984.
L.Bartha	Int.Conference on Hard Metals Rhodos, Greece	September, 1984.
G.Czibula	Photondetector Symposium Weimar	September, 1984.
G.Eppeldauer	Photondetector Symposium Weimar, GDR	September, 1984.
Mrs.M.Farkas	Int.Conf. on Crystallography Hamburg, FRG	August, 1984.
G.Ferenczi	Int.Conference of Semiconductor Physics San Francisco, USA	August, 1984.
K.Kazi	9th Workshop on Active Micro- wave Devices Eindhoven, Netherland	October, 1984.
E.Lendvay	Physics and Technology of GaAs Reinhardsbrunn, GDR	November, 1984.
M.Menyhard	Eur.Conference of Surface Spectroscopy York, England	April, 1984.
J.Schanda	Svetotechnika'84 Hradec Kralove, Czechoslovakia	May, 1984.
	Licht'84 Weimar, GDR	May, 1984.
	Int.Photondetector Symposium Weimar	September, 1984.
	29th Int.Scientific Colloquium Illmenau, GDR	October, 1984.
L.Zsoldos	Int.Conf. on Crystallography Hamburg, FRG	August, 1984.

P.Barna	6th Int.Symp.on High Purity Materials in Science and Technology, Dresden, GDR	May, 1985.
G.Eppeldauer	X. IMECO Congress Prague, Czechoslovakia	April, 1985.
G.Ferenczi	5th Lund International Conference on Deep Level Impurities in Semi- conductors St.Andrews, GB	June, 1985.
I.Gadl	VI. World Conference on Sintering Herceg-novi, Yugoslavia	August, 1985.
J.Kertész	12th Int. Sem. on Phase Transitions and Crit. Phen. Aussois, France	March, 1985.
E.Lendvay	Int.Conf. Phys.Tech. of Compensated Semiconductors Madras, India	February, 1985.
I.Mojzes	4th Int.School Phys.Probl. in Microelectronics Varna, Bulgaria	May, 1985.
I.Pozsgai	EMAG'85 Newcastle, England	August, 1985.
J.Schanda	Conf.on Colour in Information Technology Guildford, England	March, 1985.
A.Tóth	4th Conference on Microscopy of Semiconductors Oxford, England	March, 1985.

1984

D.Aas	University of Linz	Austria
G.Beistel	Zentralinst.für Elektronenphysik, Berlin	GDR
J.Betko	Electrotechnical Institute, Bratislava	Czechoslovakia
E.Bugiel	Institute for Semiconductur Physics, Frankfurt/O	GDR
Ja.Carenkov	Ioffe Institute for Technical Physics, Leningrad	Soviet Union
R.Fremunt	Institute for Radioelectronics Prague,	Czechoslovakia
C.Frigeri	CNR-MASPEC, Parma	Italy
J.Gerasimenko	Institute for Semiconductor Physics, Novosibirsk,	Soviet Union
H.Grimmeiss	University of Lund	Sweden
R.Haubner	Institute of Chemical Technology of Inorganic Materials Technical University of Vienna	Austria
J.Heidenreich	Institute for Solid State Physics, Halle	GDR
K.Heinrich	National Bureau of Standards Washington	USA
L.Kolesnik	Institute of Rare Metals Moscow	Soviet Union
P.Krispin	Zentralinstitut für Elektro- nenphysik, Berlin	GDR
A.Kuhar	Institute of Radioelectronics, Prague	Czechoslovakia
V.Kuzmiak	Institute of Radioelectronics, Prague	Czechoslovakia
B.Lux	Institute of Chemical Technology of Inorganic Materials Technical University of Vienna	Austria

cont. TABLE 3

V.Malina	Institute of Radioelectronics Prague	Czechoslovakia
J.Mertens	Humboldt University, Berlin	GDR
K.Mielenz	National Bureau of Standards Washington	USA
P.Mrozek	Institute for Physical Chem- istry, Warsaw	Poland
F.Osvald	Institute of Radioelectronics Prague	Czechoslovakia
G.Petzow	Max-Planck Institute for Powder Metallurgy, Stuttgart	FRG
A.Renou	University of Marseille	France
J.Rentsch	Institute for Electronics Berlin	GDR
G.Salviati	CNR-MASPEC, Parma	Italy
R.Sitter	J.Kepler University Linz	Austria
W.Smid	Institute of Physics Prague	Czechoslovakia
N.Stelian	Institute for Semiconductor Physics, Bucharest	Romania

1985

C.A.Ambroziak	UNITRA-ITE, Warsaw	Poland
V.Antipov	Bajkov Institute, Moscow	Soviet Union
H.J.Anklam	IHP AdW GDR, Frankfurt/O	GDR,
P.Balk	Technical University, Aachen	FRD
E.Bugiel	IHP, AdW, GDR, Frankfurt/O	GDR,
A.Caucatelli	Institute for Metrology, Torino	Italy
J.S.Colligen	University of Salford	England

P.C. Euthymiou	University of Athen	Greece
M.Gillet	University of Marseille,	France
B.Gruzza	Univ.Clermont Ferand.	France
J.Hova	Institute of Radioelectronics Prague	Czechoslovakia
A.Jablonski	Institute of Physical Chemistry Warsawa	Poland
M.Kaminski	Argonne National Laboratory, Chicago	USA
I.Klamka	UNITRA-ITE, Warsawa	Poland
J.Kodl	Institute of Radioelectronics Prague	Czechoslovakia
D.V.Korbutjak	Institute of Semiconductors, Kiev	Soviet Union
P.Kordos	Electrotechnical Institute Bratislava	Czechoslovakia
V.Malina	Institute of Radioelectronics Prague	Czechoslovakia
R.Mattheis	IHP AdW GDR, Frankfurt/O	GDR
B.Mroziewicz	UNITRA-ITE, Warsawa	Poland
G.I.Papaioannou	University of Athene	Greece
G.Sauter	Phys.Techn.Budesanstalt Braunschweig	FRG
R.Schaefer	National Brueau of Standards Washington	USA
T.Thieme	Zentralinstitut für Electronen- physik, Berlin	GDR
S.Thomson	Glasgow University	England

LIST OF PUBLICATIONS

1984-1985

1984

- Andor, L., Lőrinczi, A., Siemion, J. Smith, D.D., Rice, S.A.
Shot-noise-limited detection scheme for two-beam laser spectroscopies.
Review of Scientific Instruments 55 1 64 (1984)
- Baltes, H.P., Andor, L., Nathan, A., Schmidt-Weinmar, H.G.
Two-dimensional numerical analysis of a silicon magnetic field sensor.
IEEE Trans.on Electron Devices 31 7 996 (1984)
- Ennen, H., Pomrenke, G., Aszódi, G., Kaufmann, U., Windscheif J,
Schneider, J.
Luminescenz Seltener Erden in III-V Halbleitern und Si.
48.Physikertagung des D.P.G. 12-17 März, 1984. Münster, BRD
- Balázs, J., Túttő, P., Serényi, M.
Calorimeter for quality assessment of optical fibres. (in Hungarian)
Finommechanika-Mikrotechnika 23 8 225 (1984)
- Barna, A.
A new type ion milling equipment for sample preparation.
Proc.8. Eur.Congr. EM., p.107 Budapest, 1984.
- Barna, A., Barna P., Radnóczy, G.
Formation processes of vapour deposited thin films (16 mm movie with text)
Proc.8.Eur.Cong., EM., p.1273 Budapest, 1984.
- Barna, A., Barna, P., Radnóczy, G., Tóth, L.
UHV in-situ TEM study of two dimensional island growth on Al₂Au phase by
depositing Au.
Proc.8.Eur.Congr. EM., p.1247 Budapest, 1984.
- Barna, A., Barna, P., Radnóczy, G., Sáfrán, G.
In-situ UHV TEM study of the two-dimensional growth of Al₂Au phase on
Al(111) surface.
Ultramicroscopy, 15 1-2 101 (1984)
- Barna, A., Sáfrán, G., Tóth, L.
In situ electron microscopy study of structural and electrical changes in
Ni-Cr thin films.
Thin Solid Films 116 229 (1984)
Abstract of a paper presented at the 2nd International Summer School on
Thin Film Formation, Hajduszoboszló, Hungary, 18-24 September, 1983.
- Barna, P., Richter U., Barna A., Paal, Z., Zimmer, H.
Dispersity and crystal changes of Pt-black catalysts under various
treatments.
Proc. 8.Eur.Congr.EM., p.1171 Budapest, 1984.
- Luby, S., Roman, P., Barna P.
Elektromigracna odolnost Al-Cu-Si tenkovrstovych spojov zhotovenych mag-
netronovym naprasovaním.
Elektrotechnicky Casopis 35 c.4 298 (1984)

Barna, P., Bodó, Z., Gergely, G., Croce, P., Adam, J., Jakab, P.
Ellipsometric and X-ray specular reflection studies on naturally grown
overlayers on aluminium thin films.
Thin Solid Films 120 4 249 (1984)

Papp, G., Beleznyay, F.
Special points and ideal-vacancy-induced deep level in Si and some III-V
semiconductors.
Acta Physica et Chemica. Acta Universitatis Szegediensis
Nova series. 30 fas.3-4 121 (1984)

Beleznyay, F.
Localized lattice instability in zinc-blende semiconductors: Microscopic
model for large lattice relaxation and for high-temperature anomalous
diamagnetism.
Physical Review B-29 8 4602 (1984)

Eppeldauer, G.
Measurement of very low light intensities by photovoltaic cells.
Lecture of the 11th Int.Symp.on Photon Detectors, Weimar, 11-13 Sept.1984.
Proc. (IMEKO Secr.H-1371 Budapest, POB 457) p.182

Gál, I.
Effect of dislocation distribution on the X-ray scattering.
Proc.of the 5th Risø International Symposium on Metallurgy and Materials
Science, Roskilde, 3-7 September, 1984.
Roskilde, p.249 (1984)

Ranganathan, R., Gál, M., Taylor, P.C.
Temperature dependence of photoluminescence in $a:\text{Si}_{1-x}\text{Ge}_x:\text{H}$ alloys
Bull.Am.Phys.Soc. 30 307 (1984)

Zhang, X.C., Gál, M., Nurmikko, A.V.
Transient photomodulation spectroscopy of bound excitons in doped GaSe
Bull.Am.Phys.Soc. 29 477 (1984)

Zhang, S.X., Gál, M., Nurmikko, A.V.
Exciton confinement by layers in GaSe: Direct evidence from subnanosecond
time-resolved spectroscopy.
Phys.Rev.B. Rapid Comm. 30 6214 (1984)

Zhang, X.C., Hefetz, Y., Gál, M., Nurmikko, A.V.
Kinetics of bound and free excitons at low densities in semiconductors.
Presented at Fourth International Conf. of Ultrafast Phenomena
Monterey, Ca, June 1984.

Jablonski, A., Mrozek, P., Gergely, G., Menyhárd, M., Sulyok, A.
The inelastic mean free path of electrons in some semiconductors and metals.
Surf.Interface Anal. 6 291 (1984)

Gergely, G.
New developments in elastic peak electron spectroscopy.(abstract)
Acta Universitatis Wratislaviensis No.782 (Matematyka, Fizyka, Astronomia)
45 (1984)
Surface Research.Proc.of the 7th Seminar on Surface Physics,
Wrocław-Karpacz p.27 1983.

- Czermann, M., Vágó, Gy., Geszti, O., Menyhár, M.
Correlations between the structural and physical properties of indium tin oxide thin films and their preparation parameters.
Thin Solid Films 116 1-2-3 202 (1984)
Abstract of a paper presented at the 2nd International Summer School on Thin Film Formation
Hajduszoboszló, Hungary, 18-24 September, 1983.
- Bessenyei, G., Zsoldos, B., Geszti, O.
Preparation of Ni thin films resistors by chemical reduction. (In Hungarian)
Hiradástechnika XXXV/8 353 (1984)
- Koltai, M., Geszti, O., Menyhár, M.
The effect of nitrogen doping on properties of thin 50% Ni - 50% Cr films.
Thin Solid Films 116 221 (1984)
Paper presented at the 2nd International Summer School on Thin Film Formation, Hajduszoboszló, Hungary, 18-24 September, 1983.
- Geszti, T.
Nonideal Frenkel-Kontorova model of two-level systems in glasses.
Physical Review B., Condensed Matter 3rd ser. 30, 4 1811 (1984)
- Gyuró, I., Lendvay, E., Hársy, M., Pozsgai, I., Somogyi K. et al.
Crystal growth of GaSb under microgravity conditions.
Acta Astronautica 11 7-8 361 (1984)
- Tóbiás, F., Ivanov, P., Gaal, I.
Sensitivity and linearity of Förster-Probes.
Journal of Magnetism and Magnetic Materials 41 431 (1984)
- Szabó, J., Ivanov, P., Bartha, L., Gaal, I.
A static zeroing method for determination of magnetic anisotropy in large ferromagnetic sheets.
Journal of Magnetism and Magnetic Materials 41 250 (1984)
- Kazi, K., Mojzes, I., Angelov, I., Urshev, L.K.
Determination of the microwave equivalent-circuit parameters of metal-ceramic encapsulation for microwave two-terminal devices.
Proc. of Conference Microwave and Radiolocation'84
Varna, Bulgaria, p.111 October, 1984.
- Metzger, J., Kertész, J.
Effective medium theory for diffusion with further neighbour hopping.
J.Phys.C: Solid State Physics 17 5153 (1984)
- Kertész, J., Metzger, J.
Region of validity in theories of diffusion near to the percolation threshold.
Journal of Physics - A: Mathematical and General 17 9 L501 (1984)
- Beregi, E., Hartmann, E., Lábár, J.L.
The dissolution forms of gadolinium gallium garnet single crystal spheres.
EUREM p.1003 Budapest, 1984.

Lendvay, E.

Thermal etching of ZnS.

Journal of Physics D Applied Physics 17 7 1083 (1984)

Lendvay, E.

Ternary $A_{III}B_V$ antimonides

Progress in Crystal Growth and Characterization 8 4 371 (1984)

Lendvay, E.

New semiconductors and their possible applications

Czechoslovak Journal of Physics B-34 5 479 (1984)

Invited paper on the International Conference of Radiative Recombination and Related Phenomena in III-V Compound Semiconductors
Prague, 4-7 October, 1983.

Lendvay, E., Görög, T., Rakovics, V.

GaAs/GaAlAs superlattice structures grown by LPE.

Tagungsberichte der Konf. 'Phys. and Technology of GaAs'
Reinhardtsbrunn, 1984.

Lendvay, E.

New trends in the application of III-V semiconductors.

Tagungsberichte der Konf. 'Phys. and Technology of GaAs'
Reinhardtsbrunn, 1984.

Lendvay, E.

Ternary $A_{III}B_V$ antimonides.

Progr. Crystal Growth and Charact. Pergamon Press, Vol.8.p.371 (1984)

Lendvay, E.

GaAs and its application in the microelectronics

Magyar Aluminium (International number) Nos.3-4 139 (1984)

Yagi, E., Flik, G., Fürderer, K., Haas, N., Herlach, D., Major, J.,

Seeger, A., Jacobs, W., Krause, M., Krauth, M., Munding, H-J., Orth, H.

Quantum diffusion of positive muons in iron.

Phys.Rev. B30 441 (1984)

Makai, J., Czibula, G., Schanda, J., Schröder, W.

The importance of the spectral responsivity correction in case of optoelectronic elements.

11th Int.Symp. on Photon-detectors, Weimar, 11-13 September 1984.

Makai, J.

A new compact illuminance and luminance meter.

Licht'84 Conference, Bulgaria, 4-6 October, 1984.

Szilvásy, Cs., Menyhárd, M., Gergely, G.

Auger electron spectroscopy studies of impurity effects on the hot deformability of AISI M2 high speed steel.

Crystal Research and Technology 19 2 187 (1984)

Mrozek, P., Menyhárd, M., Wernisch, J., Jablonski, A.

Surface composition of the ordered Al50-Co50 alloy.

physica status solidi A/84 1 39 (1984)

Menyhárd, M., Sulyok, A.

Electron spectrometer-computer system.

Proc. 5th Seminar on Electron Spectroscopy of Socialist Countries.

Dresden, 26-29 August, 1984.

Ed: Technical University, Dresden p.85 (1984)

Menyhárd, M., Gergely, G., Sulyok, A., Bertóti, I.

Electron spectroscopy study of carbides in AISI M2 high speed steel.

Proc. 5th. Seminar on Electron Spectroscopy of Socialist Countries.

Dresden, 26-29 August, 1984.

Ed: Technical University, Dresden, p.83 (1984)

Mojzes, I., Oláh, A., Veresegyházy, R., Zsebe, L.

Equipment for reliability testing of high power Gunn diodes.

Proc. of the CONSTRONIC'84 Conf. Budapest, 9-11 October, 1984. p.237

Mojzes, I.

Fast alloying technique for improved ohmic contacts to n-GaAs.

Solid-State Electronics 27 10 925 (1984)

Neugebauer, J., Gerey, G.

Ammonium molybdates used in powder metallurgy.

International J. of Refractory and Hard Metals 3 2 96 (1984)

Pozsgai, I.

Detection limits of energy dispersive X-ray fluorescence analysis in the scanning electron microscope.

Proc. 8th European Conf. on Electron Microscopy 1 453 (1984)

Radnóczy, G.

Grain boundary structure of thin films.

Thin Solid Films 116 1-2-3 111 (1984)

Abstract of a paper presented at the 2nd International Summer School on

Thin Film Formation, Hajduszoboszló, Hungary, 18-24 September, 1983.

Radnóczy, G., Barna P.

The growth of Al_2Au crystallites on Al (111) films.

Thin Solid Films 116 1-2-3 143 (1984)

Paper presented at the 2nd International Summer School on Thin Film Formation, Hajduszoboszló, Hungary, 18-24 September, 1983.

Radnóczy, G., Barna P., Barna, A.

Detection of grain boundary displacements in Al films.

Proc. 8th European Congr. EM.: Budapest, p.1241, 1984.

Katzer, D., Sáfrán, G.

Scanning electron microscopy of the microtopography of a (111) silicon surface.

Ultramicroscopy, 15 1-2 135 (1984)

Schanda, J.

Comments about the measurement of whiteness. (In Hungarian)

Mérés és Automatika, 9 327 (1984)

Somogyi, K.

Preparation and characterization of VPE in III-V compounds.

Conference on Physics and Technology,

GaAs and other III-V Semiconductors, Reinhardtbrunn, 19-24 November 1984.

Fried, M., Lohner, T., J  r  li, E., Vizkeleti, G., Mezey, G., Gyulai, J.

Somogyi, M., Keskors, H.

Investigation of ion implanted semiconductors by ellipsometry and back-scattering spectrometry.

Thin Solid Films 116 191 (1984)

Sz  kefalvi-Nagy,   ., Fromm, E., Jehn, H.

Reaction model of high-temperature oxidation of refractory-metal carbides at low oxygen pressures.

Zeitschrift f  r Metallkunde 75 4 287 (1984)

T  th, A.L., L  b  r, J.L. Vlad  r, A.E.

Computer controlled measurement of charge collection signals in the SEM

Proc. of EUREM'84 Vol.1. p.307, Budapest 1984.

T  th, A.L.

EBIC dislocation contrast as a function of SEM parameters

Proc. of EUREM'84 Vol.2. p.975, Budapest 1984.

Uray, L.

The effect of void size on the resistivity of sintered tungsten.

physica status solidi (a) 82 2 545 (1984)

Uray, L., Meny  rd, M.

The segregation of iron in tungsten.

physica status solidi (a) 84 1 65 (1984)

R  cz, Z., Vicsek, T.

Cluster statistics and scaling in a regular model of diffusion controlled deposition.

in Kinetics of Aggregation and Gelation, edited by F.Family and D.P.Landau (North-Holland, Amsterdam,) p.255 (1984)

Vicsek T., Family, F.

Critical dynamics in cluster-cluster aggregation.

in Kinetics of Aggregation and Gelation, edited by F.Family and D.P.Landau (North-Holland, Amsterdam) p.111 (1984)

Vicsek, T., Family F.

Dynamic scaling for aggregation of clusters.

Phys.Rev.Lett. 52 1669 (1984)

Vicsek, T.

Pattern formation in diffusion-limited aggregation.

Phys.Rev.Lett. 53 2281 (1984)

Zsoldos, L.

Comment on the paper 'Some remarks on the origin of X-ray diffraction phenomena' (In Hungarian)

Acta Phys.Hung. 56 185 (1984)

1985

Andor, L., Barta, E., Csontos, Z. (Mrs), Koltai, F., Pfeifer J., Püspöki, S., Radácsi, J. (Mrs), Serényi, M.

Development of semiconductor lasers in RITPh (in Hungarian).

Finommechanika és Mikrotechnika (in press) (1985)

Gangli, P., Arató, P.

'Texture Simulation'

Proceedings of the XII. Hungarian Diffraction Conference, p.9, Sopron, 1985.

Aszódi, G., Weber, J., Uihlein, Ch., Pu-lin, L., Ennen, H., Kaufmann, U.,

Schneider, J., Windscheif, J.

Zeeman analysis of the ytterbium luminescence in indium phosphide.

Phys. Rev. B., 31 12 7776 (1985)

Barta, E., Hoffmann, G., Pfeifer, J., Ponomarenko, J., Püspöki, Zs.,

Radácsi, E., Somogyi, K.

Shallow Zn diffusion GaAs.

Symposium on Electron-Technology, Budapest, 16-19 April, 1985.

Eppeldauer, G.

Simple realization of the radiometric and photometric scales.

Lecture of the IMEKO Xth Congress, Praha, 22-26, April, 1985.

Proc. Vol. 4 p.208

Ferenczi, G.

Identification of deep levels by junction spectroscopy.

Acta Physica Polonica A67 143 (1985)

Ferenczi, G.

Identification of deep levels in semiconductor devices.

Proc. of the Swedish-Hungarian Seminar on Solid State Physics, p.175.

Budapest, 1985.

Ferenczi, G., Pavelka, T., Somogyi M.

Measurement of the depth distribution of implantation induced defects in Si.

Proc. of the Symposium on Electron-Technology, Vol.1 p.97, Budapest, 1985.

Ferenczi, G., Boda, J., Biricz, P.

Method and apparatus to detect deep levels in a non-destructive way in semiconductors especially in single-crystal wafers.

Hungarian Patent application No. 3401/85., Budapest (1985)

Gaal, I., Horáček, O.

Chemisch bedingte Porenvergrößerung.

Proceedings of the 11th International Plansee Seminar, Reutte, Austria

Vol.II, p.99, (1985)

Gaal, I., Makarov, P.V., Povarova, K.B.

Some characteristics of technically pure tungsten powders.

Proceedings of the 11th Plansee Seminar, Reutte, Austria,

Vol.III p.105 (1985)

Gaal, I.
Beziehung zwischen der Mikrostruktur und den oberen und unteren Leitfähigkeitsgrenzwerten bei Zweiphasensystemen.
Proceedings of the VIII. International Conference on Powder Metallurgy, Dresden, p.15 (1985)

Gaal, I., Lipták, L.
Chemisch bedingte Porenvergrößerung.
Proceedings of the VIII. International Conference on Powder Metallurgy, Dresden, p.73 (1985)

Gál, M. Yuan, K.C., Taylor, P.C., Stringfellow, G.
Doping superlattices in organometallic VPE InP.
Appl. Phys.Lett. 47 405 (1985)

Gal, M., Viner, J., Taylor, P.C., Kuo, C.P., Stringfellow, G.B.
Photoluminescence study of confined electron-hole plasma in $\text{Ga}_x\text{In}_{1-x}\text{As}$ heterostructures.
J.Appl. Phys. 58 948 (1985)

Gal, M., Viner, J., Taylor, P.C.
The existence of a universal low-energy tail in the photoluminescence of $\text{a-Si}_{1-x}\text{Ge}_x\text{:H}$ alloys.
Phys.Rev.B. Rapid Comm. 31 4060 (1985)

Gal, M., Viner, J., Taylor, P.C.
Alternative method for measuring optical absorption below the band edge in thin a-Si:H .
Bull. Am.Phys.Soc. 30 259 (1985)

Gal, M., Taylor, P.C.
Temperature dependence of the absorption in a-Si and related alloys.
11th International Conference on Amorphous and Liquid Semiconductors, Rome, 2-6 September, (1985)

Gergely, G., Jablonski, A., Menyhård, M., Mrozek, P., Sulyok, A.
Determination of the inelastic mean free path of electrons by elastic peak electron spectroscopy.
Acta Univ. Wratislaviensis No.847
Proc. 8th Sem.Surface Physics, 46 17 (1985)

Gergely, G., Menyhård, M.
Some problems of in-depth profiling of layer structures. New ways, possibilities.
Proc. Symp. on Electron-Technology, 16-19 April, 1985. Budapest
Ed: Optical, Acoustical and Filmtechnical Society, Budapest
1 111 (1985)

Gergely, G., Menyhård, M., Sulyok, A., Jablonski, A., Mrozek, P.
Determination of the mean free path of electron in solids from the elastic peak. II. Experimental results.
Acta Phys.Hung. 57, 139 (1985)

Jablonski, A., Mrozek, P., Gergely, G., Menyh rd, M., Sulyok, A.
Determination of the mean free path of electrons in solids from the elastic peak. I. Simplified theoretical approach.
Acta Phys.Hung. 57 131 (1985)

Kolonits, V.P., Czermann, M., Geszti, O., Menyh rd, M.
The oxidation of tantalum-based thin films.
Thin Solid Films, 123 45 (1985)

Horacsek, O., Gaal, I.
Influence of gaseous impurities on the densification characteristics of sintered refractory metals.
Proceedings of the 11th International Plansee Seminar, Reutte, Austria, Vol.II.p.181 (1985)

Kert sz, J. , Cserti, J., Sz p, J.
Monte Carlo simulation programs for microcomputers.
Eur. J. Phys. p.723 (1985)

Kert sz, J., Sz p, J., Cserti, J.
Dendritic growth by Monte Carlo in growth and form. - A modern view .
Proceedings of the Cargese Sommer School. E.: H.E.Stanley and N.Ostrowsky, p.67 (1985)

Sz p, J., Cserti, J., Kert sz, J.
Monte-Carlo approach to dendritic growth.
J.Phys. A. 18, L413 (1985)

Lalinski, T., Kordos, P., Kov cs, B., Mojzes, I., Szentp li, B. ,
Tichy-R cs, A.
Optimization of the heat treatment for forming AuGe based contacts to n-GaAs.
phys.stat.sol. (a) 88 1 K87 (1985)

Jaroli, E., Mezey, G., Zsoldos, E., Kov cs, B., Mojzes, I., Lohner, T.
Kotai, E., Manuaba, A., Fried, M., Gyulai, J.
Intermetallic compound formation of Ge-Ni and Ge.Al.Ni systems by furnace annealing and ion beam intermixing.
Presented at the 7th Int.Conf. on Ion Beam Analysis, Berlin, FRG, 7-12 July, 1985.
Published in Nuclear Methods in Phys. Res.B.

Kozma, L., Warren, R., Henig, E.Th.
Kriechverhalten von wolframfasern in Diffusionskontakt mit Nickel und Eisen.
Verbundwerkstoffe: Technologie und Pr fung (Ed.: G. Ondracek)
Deutsche Gesellschaft f r Metalkunde, Oberursel, p.295 (1985)

Beregi, E., L b r, J., Hartmann, E., Hild, E., Tanos, F.
The dissolution forms of $Y_3Fe_{4.2-x}Sc_xGa_{0.8}O_{12}$ single crystal spheres.
Hungarian-Austrian Joint Conference on Electron Microscopy, A5-7 Balaton-
aliga, Hungary, (1985)

Sterk, E., Sári, K., Balla, M., Lábár, J.
Investigation of garnet materials by scanning electron microscopy.
Hungarian-Austrian Joint Conference on Electron Microscopy, A5-8,
Balatonaliga, Hungary, (1985)

Hartmann, E., Beregi, E., Lábár, J.
Dissolution of GGG single crystal spheres in acids.
J.of Crystal Growth 71 191 (1985)

Lendvay, E.
Principles and applications of CVD and PE CVD methods.
Proc. High Purity Mater. and their Application. Dresden,
Vol.1. p.150 (1985)

Lendvay, E., Petrás, L., Geborkyan, V.A.
Selective LPE of AlGaInSb onto GaSb substrates.
J.Cryst. Growth 71 317 (1985)

Lendvay, E., Görög, T., Rakovics, V.
Growth of GaAs/GaAlAs superlattices and their application in optoelectronics.
Mater. Electron Technol. 105 280 Budapest (1985)

Lendvay, E., Petrás, L., Gevorkyan, V.A.
Selective epitaxial growth of AlGaInSb
Acta Phys.Hung. 57 319 (1985)

Lendvay, E., Gevorkyan, V.A., Petrás, L., Pozsgai, I., Görög, T.
Liquid Phase Epitaxy of AlGaInSb.
J.Cryst. Growth 71 (in press) (1985)

Lendvay, E., Görög, T., Rakovics, T.
LPE growth of GaAs-GaAlAs superlattices.
J.Cryst.Growth 71 (in press) (1985)

Lendvay, E., Hársy, M., Görög, T., Gyuró, I., Pozsgai, I., Koltai, F.
et al.
The growth of GaSb under microgravity conditions.
J.Cryst. Growth 71 538 (1985)

Lendvay, E.
Quaternary A^{III}B^V antimonides in physics and technology of compensated
semiconductors.
Ed.V.S.Gopalam, Tata Publ. New Delhi, 1985.

Lendvay, E., Görög, T., Rakovics, T.
Growth of GaAs/GaAlAs superlattices and their applications in opto-
electronics.
in 'Physics and Technology of Compensated Semiconductors'
Ed. V.S.Gopalam, Tata Publ. Inc. New Delhi, 1985.

Major, J., Fürderer, K., Herlach, D.
Furnace for high-temperature Muon-Spin-Rotation measurements.
Rev.Sci.Instr. 56 7 1428 (1985)

Menyhárd, M., Sulyok, A.
 Ionization loss spectroscopy.
 Acta Univ. Wratislaviensis, No.847
 Proc. 8th Sem.Surface Physics 46 57 (1985)

Mojzes, I., Veresegyházy, R., Kovács, B., Gurbán, S., Pécz, B., Radnóczy, G.
 Thermal dissociation of III-V compounds - Physicochemical effects influencing the contact parameters.
 Invited paper at the 4th International School on Physical Problems in Microelectronics ISPPME'85, Varna, Bulgaria, 11-19 May, (1985)

Mojzes, I., Vaulin, Ju., Gerasimenko, N., Obodnikov, V., Kovács, B., Veresegyházy, R.
 Spatial distribution of the components in Au/GaAs system after scanning laser annealing.
 phys.stat.sol. (a) 87 K127 (1985)

Mojzes, I., Veresegyházy, R.
 Comments on the 'Physicochemical effects of heating gold thin films on gallium arsenide'.
 J.of the Electrochemical Soc. 132 5 1255 (1985)

Nagy, E., Kertész, J.
 Application oriented fundamental research. Percolation Theory and its applications.
 in 'The Days of Swedish Science' Ed.: N.Kroo, KFKI, p.115 (1985)

Pozsgai, I.
 On the atomic number dependence of the X-ray fluorescence analysis in the electron microscope.
 Lecture presented at EMAG'85 in Newcastle-upon-Tyne, Sept. 1985.
 (to be published in the Electron Microscopy and Microanalysis (1985))

Schanda, J.
 On the evaluation of display brightness.
 Conf. on Colour in Information Technol. Guildford, U.K., 26-29 March, 1985.

Schanda, J.
 A combined colour preference - Colour rendering index.
 Lighting Research and Technology, 17 1 31 (1985)

Schanda, J.
 The influence of test samples, used for calculating colour rendering indices.
 AIC International Congress Colour 85, Monte-Carlo, 16-22 June, 1985.

Schanda, J.
 Brightness evaluation of colored VDU signals.
 International Display Research Conference, San Diego, Calif., USA
 15-17, October, 1985.

Lohner, T., Mezey, G., Fried, M., Ghita, L., Ghita, C., Merlens, A., Kerkow, H., Kótai, E., Pászti, F., Bakay, F., Vizkeleti, Gy., Járóli, E., Gyulai, J., Somogyi, M.
 Analysis of high dose implanted Si by high depth resolution RBS spectroscopic ellipsometry and TEM.
 Mat.Res.Soc. Symp.Proc. Vol.35 p.523 (1985)

Sulyok, A.
 Intensity of core level electron energy loss peaks of Ti.
 ECOSS 7. 1-4 April, 1985, Aix-en-Provence
 (Europhysics Conf. Abstracts 9C 211, Ed.: University Aix-Marseille, (1985)

Kirchheim, R., Szőkefalvi-Nagy, A., Stolz, U., Speitling, A.
 Hydrogen in deformed and amorphous $\text{Pd}_{80}\text{Si}_{20}$ compared to hydrogen in deformed and crystalline palladium.
 Script.Met. 19 843 (1985)

Tóth, A.L.
 Investigation of plasma effect on EBIC dislocation contrast in Si.
 Inst.Phys.Conf.Ser. (Oxford, 1985) (in press)

Vadasdi, K., Oláh, R., Szilassy, I., Jeszenszky, A.
 Preparation of APT by means of electrodialysis and solvent extraction.
 Proceedings of the 11th International Plansee Seminar, Reutte, Austria,
Vol.I. p.77 (1985)

Vadasdi, K., Mikéta, Gy., Mészáros, M., Szilassy, I.
 Hydrometallurgical recovery of valuable metals from cemented carbide scraps.
 Proceedings of the 11th International Plansee Seminar, Reutte, Austria,
Vol.I. p.939 (1985)

Veresegyházy, R., Kovács, B., Mojzes, I.
 Mass spectrometric investigations of Au-Ge-Ni contacts to $\text{A}^{\text{III}}\text{B}^{\text{V}}$ compounds.
 Proc. of Symposium on Electron-Technology, 16-19 April, 1985. Budapest, Hungary,
Vol.I., p.464 (1985)

Meakin, P., Vicsek, T., Family, F.
 Dynamic cluster size distribution in cluster-cluster aggregation: effects of cluster diffusivity.
 Phys.Rev. B31 564 (1985)

Meakin, P., Vicsek, T.
 Internal structure of diffusion-limited aggregates.
 Phys.Rev. A32 685 (1985)

Meakin, P., Vicsek, T.
 Internal anisotropy of diffusion-limited aggregates.
 in Fractals in Physics, ed. by L. Pietronero and E. Tosatti, North Holland, Amsterdam, p.87 (1985)

Family, F., Vicsek, T.
 Scaling of the active zone in the Eden process on percolation networks and the ballistic deposition model.
 J.Phys. A18 L75 (1985)

Family, F., Vicsek, T., Meakin, P.
Are the random fractal clusters isotropic?
Phys.Rev.Lett. 55 641 (1985)

Family, F., Vicsek, T.
Dynamic scaling in aggregation phenomena.
in Physics of Finely Divided Matter, ed. by M.Daoud,
Springer Verlag p.57 (1985)

Family, F., Meakin, P., Vicsek, T.
Cluster size distribution in chemically controlled cluster-cluster
aggregation.
J.Chem.Phys. (in press) (1985)

Vicsek, T.
Formation of solidification patterns in aggregation models.
in 'Fractals in Physics' edited by L.Pietronero and E.Tosatti, North
Holland, Amsterdam, p.211 (1985)

Montag, L.M., Family, F., Vicsek, T., Nakanishi, H.
An optimized phenomeno-logical renormalization group for geometrical
models: Applications to diffusion-limited aggregation.
Phys.Rev. A32 2632 (1985)

Vicsek, T., Meakin, P., Family, F.
Scaling in steady-state cluster-cluster aggregation.
Phys.Rev. A32 1122 (1985)

Vicsek, T.
Formation of solidification patterns in aggregation models.
Phys. Rev. A 2841 (1985)



85.1.

1 x. 16.